Investigation of the mechanism of action of a synthetic cyclic antimicrobial peptide

Inaugural-Dissertation

to obtain the academic degree

Doctor rerum naturalium (Dr. rer. nat.)

submitted to the Department of Biology, Chemistry and Pharmacy

of Freie Universität Berlin

by

Kathi Scheinpflug

from Berlin

2015

The present study was conducted from September 2010 until August 2014 under the supervision of Dr. Margitta Dathe and Prof. Dr. Volker Haucke at the Leibniz-Institut für Molekulare Pharmakologie (FMP), Berlin and during a research stay at the Centre For Bacterial Cell Biology (CBCB), Newcastle University, Newcastle (UK) from September until December 2014.

1. Reviewer: Prof. Dr. Volker Haucke

   Leibniz-Institut für Molekulare Pharmakologie (FMP)

2. Reviewer: Prof. Dr. Matthias F. Melzig

   Institut für Pharmazie, Freie Universität Berlin

Date of defence: 24 November 2015

Affidavit

I hereby declare that I have written my doctoral thesis entitled “Investigation of the mechanism of action of a synthetic cyclic antimicrobial peptide” independently and I have used no other means than those quoted within this study.

Berlin, June 2015 Kathi Scheinpflug

Für meine Eltern

Der Beginn aller Wissenschaften ist das Erstaunen,

dass die Dinge so sind, wie sie sind.

- Aristoteles -

1 Abstract

Antimicrobial peptides represent an ancient class of molecules which is found throughout the animal and plant kingdom. In higher organisms they are part of the innate immune system and serve as first line defence against infectious pathogens. In contrast to conventional antibiotics, resistance development against antimicrobial peptides is rather low which has attracted a great deal of attention in the field of antibiotic research. Precise knowledge of the mechanism of antimicrobial action provides the basis for the development of novel, highly efficient antibiotic agents which selectively kill microbial pathogens.

This study is focused on elucidating the antimicrobial mechanism of action of the synthetic cyclic hexapeptide cWFW. Unlike the majority of antimicrobial peptides, this small molecule does not kill bacteria by permeabilisation of the membrane. In order to analyse alternative mechanisms of action, i.e. peptide translocation into the cytoplasm and demixing of membrane lipids, different peptide derivatives were synthesised to fulfil the technical requirements for the spectrum of methods applied. Peptide modification involved labelling with different fluorescent reporter groups as well as amino acid substitution. Minor changes in the primary structure were found not only to reduce the antimicrobial activity but also to change the non-permeabilising mechanism of action of the parent peptide. However, two derivatives could be identified which conserved the properties of cWFW. Using HPLC analysis and fluorescence microscopy, the bacterial cytoplasmic membrane could be confirmed as target structure. Moreover, we observed pronounced accumulation of the antimicrobial peptide at distinct sites of the lipid matrix. Peptide translocation into the cells, however, could not be detected. In order to characterise peptide interactions with different membrane phospholipids, we performed live cell imaging and isothermal titration calorimetry. We found that cWFW preferentially integrates into membrane regions with high curvature strain such as the division septum and the cell poles. In addition, the cyclic hexapeptide strongly reduced the fluidity of the bacterial membrane and induced a demixing of phospholipids into large domains. The immense impact of peptide-induced phase separation was manifested in the delocalisation of membrane-associated proteins which is suggested to influence vital processes such as cell growth and division.

The results obtained in the present study point to a novel mechanism of antimicrobial killing for the cyclic hexapeptide cWFW which is considered of low risk to induce the development of bacterial resistance.

2 Zusammenfassung

Antimikrobielle Peptide gehören evolutionär betrachtet zu einer sehr alten Klasse von Molekülen und kommen in zahlreichen Tier- und Pflanzenarten vor. In höher entwickelten Organismen stellen sie einen Teil des Immunsystems dar und erfüllen eine essentielle Funktion bei der unspezifischen Abwehr von pathogenen Mikroorganismen. Im Gegensatz zu konventionellen Antibiotika ist die Gefahr der Resistenzentwicklung gegen antimikrobielle Peptide relativ gering, was ihnen eine zentrale Bedeutung für die Erforschung neuartiger Substanzklassen verleiht. Die Untersuchung des antimikrobiellen Wirkmechanismus trägt dabei entscheidend zur Entwicklung innovativer, hoch-spezifischer Antibiotika bei.

Ziel der vorliegenden Arbeit ist die Aufklärung des antimikrobiellen Wirkmechanismus des synthetischen, zyklischen Hexapeptids cWFW. Es besitzt eine sehr hohe Aktivität gegen Gram positive und Gram negative Bakterienspezies, allerdings beruht die Wirkung des kleinen Moleküls nicht auf Membran-Permeabilisierung, wie es für die meisten anderen antimikrobiellen Peptide gezeigt wurde. Alternative Wirkmechanismen basieren entweder auf der Translokation von Peptiden ins Zytoplasma der Zellen oder auf direkter Interaktion mit bestimmten Membrankomponenten. Für die Untersuchung dieser Prozesse wurden verschiedene Derivate des Zyklopeptids synthetisiert. Wir konnten zeigen, dass minimale strukturelle Veränderungen, wie der Einbau von Fluorophoren oder Aminosäuresubstitution, generell zu einer Verringerung der antimikrobiellen Aktivität führen und zum Teil eine Permeabilisierung der bakteriellen Membran bewirkten. Dennoch konnten zwei Peptid-Derivate identifiziert werden, bei denen die nativen Eigenschaften von cWFW erhalten waren und die für weitergehende Versuche verwendet wurden. Mittels Fluoreszenzmikroskopie und HPLC-Analyse konnten wir starke Wechselwirkungen des Zyklopeptids mit der bakteriellen Membran und Akkumulation in bestimmten Bereichen der Lipid-Matrix beobachten. Eine Translokation ins Zytoplasma hingegen wurde nicht festgestellt. Um die Interaktion mit bestimmten Phospholipiden genauer zu charakterisieren, wurden Bindungsstudien an lebenden Zellen und, unter Anwendung von isothermaler Titrationskalorimetrie, auf Model-Membran-Level durchgeführt. Es konnte gezeigt werde, dass sich das Zyklopeptid bevorzugt in Lipidbereiche einlagert, die eine hohe Krümmungsspannung

aufweisen, wie an den Polen und der Zellteilungsebene. Darüber hinaus reduziert cWFW erheblich die Fluidität der Bakterienmembran und bewirkt eine starke Entmischung von Phospholipiden, was durch die Bildung großflächiger Membrandomänen nachgewiesen werden konnte. Diese Phasenseparation hatte große Auswirkungen auf die Lokalisation und Funktionalität membran-ständiger Proteine, die eine wesentliche Rolle während des Zellwachstums und der Teilung spielen.

Die Ergebnisse unserer Untersuchungen deuten darauf hin, dass die hohe bakterizide Aktivität des synthetischen Zyklopeptids cWFW auf einem neuartigen, bisher unbeschriebenen antimikrobiellen Wirkmechanismus beruht, welcher kaum Risiken für eine Resistenzentwicklung birgt.

3 Introduction

Antimicrobial peptides represent an ancient class of molecules that is found in myriad species throughout the animal and plant kingdom. In higher organisms they are part of the innate immune system and serve as first line defence against pathogenic microorganisms. Against the background of increased resistance of bacteria towards conventional antibiotic treatment there is a pressing need for the development of alternative therapies. The application of antimicrobial peptides bears a high potential to combat microbial infections. Due to their mechanism of action these compounds possess a broad-spectrum activity and there is only a low risk to induce bacterial resistance.

Structural and mechanistic studies provide the basis to elucidate crucial parameters for the design of new, optimised drug candidates and minimise toxic side effects. The investigation of antimicrobial peptides is considered a turning point in the challenge to combat global antimicrobial resistance and paves the way to a new antibiotic research era.

3.1 Antimicrobial therapy

3.1.1 The antibiotic era

The first systematic approaches to identify antimicrobial agents were carried out at the end of the nineteenth century when the "germ theory of disease" was becoming accepted. Ground-breaking screenings of small molecules led to the discovery of *Salvarsan* by Paul Ehrlich in 1907, an arsenic compound to treat syphilis and trypanosomal infections and heralded the era of chemotherapeutic therapy (1). During the following years further investigations were expanded to include natural compounds derived from environmental bacteria and fungi which were marked by high activity and relatively low toxicity. The application of drugs of the penicillin family is considered a milestone in the treatment of infectious diseases and paved the way for the "golden era" of antibiotic research (1940s-1960s) where most of today's clinically relevant antibiotics were discovered (Figure 1), (2).

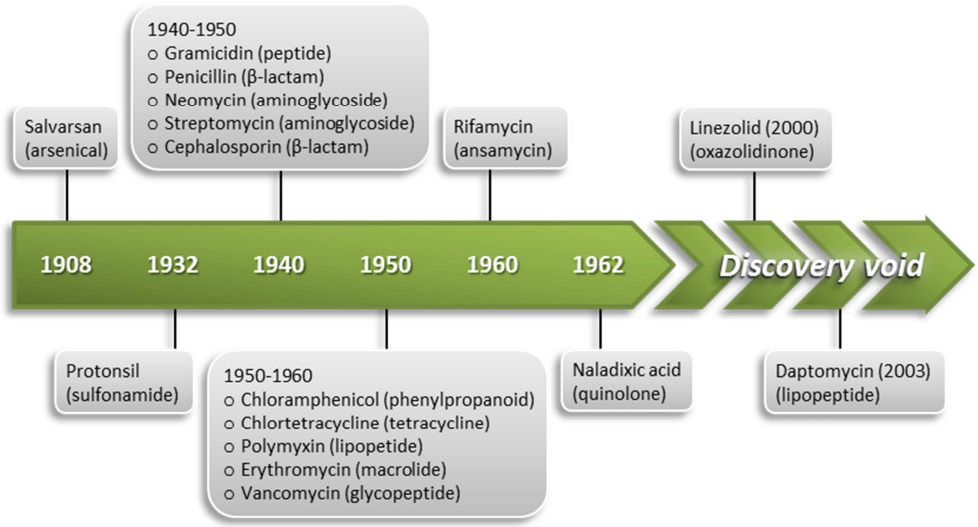

Figure 1 Timeline of antibiotic drug discovery. The antibiotics linezolid and daptomycin were first discovered in 1955 and 1986, respectively, and only revived at the beginning of the 21st century due to the lack of new compounds (modified from Wright, 2007 (2)).

The latest compound to be approved for clinical use in 2003, the lipopeptide daptomycin, was already extensively studied in the 1980, and ever since that time no new class of broad-spectrum antibiotic compounds has reached clinical application (3, 4) [1]. The following discovery void that still continues today, together with the fast-paced emergence of multi-drug resistant microorganisms, poses a global health threat. In 2014 the *World Health Organization* (WHO) proclaimed a "post-antibiotic era" where common infections and minor injuries might yet again lead to fatal outcome and emphasised the urgent need for the development of alternative antimicrobial agents (5).

3.1.2 Bacterial physiology and antibiotic targets

With increasing knowledge of the physiology and metabolism of microorganisms the research on antimicrobial agents became more targeted, from broad-spectrum to highly selective molecules. Most bacteria can be divided into Gram positive and Gram negative species depending on the composition of their cell wall (Figure 2).

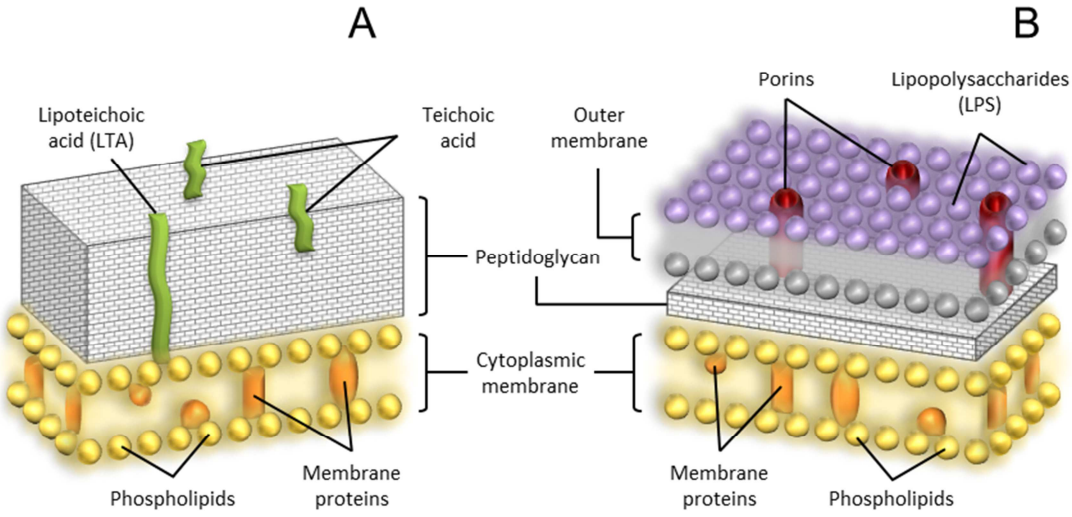

Figure 2 Bacterial membrane compositions. (A) Gram positive cell wall with thick peptidoglycan layer and (B) Gram negative cells with an additional outer membrane and thin peptidoglycan layer.

[1] In 2011 and 2012 the narrow-spectrum antibiotics fidaxomicin and bedaquiline were introduced which target *Clostridium difficile* and *Mycobacterium tuberculosis*. Further approvals are related to specific application against hospital-acquired MRSA in single or combination therapy.

Gram positive cells are surrounded by a thick layer of peptidoglycan. This tight meshwork composed of the sugar derivatives N-acetylglucosamine and N-acetylmuramic acid is cross-linked by a small number of different L- and D-amino acids. In addition, these cells contain long lipoteichoic acids (LTA) which span through the entire cell wall and are embedded in the cytoplasmic membrane. Peptidoglycan is also present in Gram negative bacteria, albeit with a significant thinner diameter. To withstand turgor pressure, these cells possess an additional outer membrane which mainly consists of lipopolysaccharides (LPS) and conveys much of the toxicity associated with Gram negative pathogens. Furthermore, the phospholipid composition of the cytoplasmic membrane also varies widely between different bacteria species (Figure 3) (6). The most abundant lipids are the zwitterionic phosphatidylethanolamine (PE) and the anionic phosphatidylglycerol (PG) and cardiolipin (CL). In general, PE is found to a higher extent in Gram negative cells while PG constitutes the majority of the bilayer of Gram positive bacteria species. Compared to most eukaryotic membranes, bacterial cells contain at least 15% of negatively charged phospholipids which, together with the exposure of LPS and LTA, renders the surface highly negative and attribute for the strong selectivity of cationic antimicrobial agents.

A

Bacterial Species	Total Lipid Content [%]		
	PG	PE	CL
Gram negative cells			
E. coli	15	80	5
Y. kristensenii	20	60	20
P. aeruginosa	21	60	11
Gram positive cells			
B. subtilis	70	12	4
S. aureus	58	0	42
B. cereus	40	43	17

B

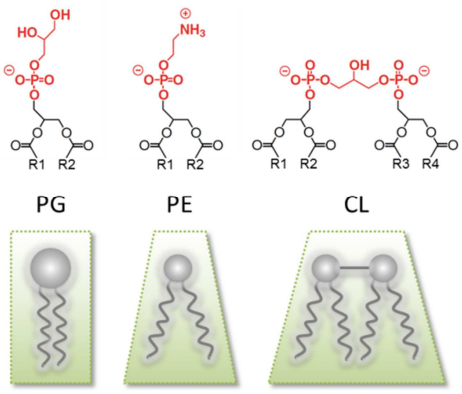

Figure 3 Overview of the most abundant bacterial phospholipids. (A) Table of lipid distribution in different bacterial species (adapted from Epand and Epand, 2009 (7). (B) Structure of phospholipid head groups of phosphatidylglycerol (PG), phosphatidylethanolamine (PE) and cardiolipin (CL) with schematic representation of respective spatial demands (chemical structures modified from Oliver et al., 2014 (8)).

These differences in membrane composition contribute to variations in susceptibility of bacteria towards certain antibiotics, termed *intrinsic resistance*. The additional outer membrane of Gram negative cells represents an effective physical barrier for many antimicrobial compounds, e.g. vancomycin which cannot penetrate the LPS layer and therefore is mainly active against Gram positive cells (9). Other compounds, such as β-lactam antibiotics, rapidly kill growing cells by interfering with peptidoglycan synthesis, but are, however, ineffective against non-dividing, persistent bacteria. Despite the large amount of antibiotics, the number of main targets is very low and can be summarised by (*i*) inhibition of cell wall synthesis, (*ii*) nucleic acid and (*iii*) protein synthesis (Figure 4).

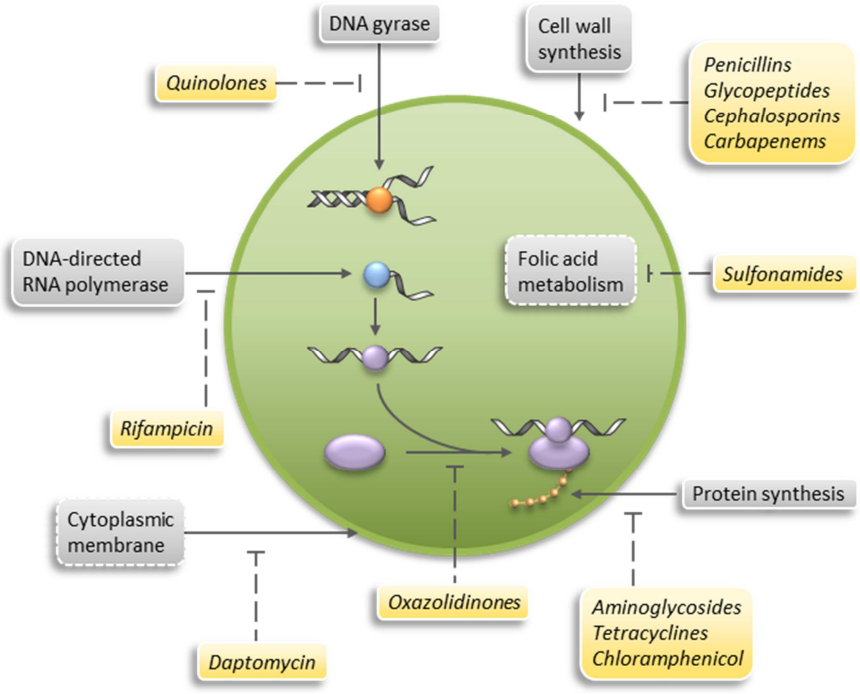

Figure 4 Antibiotic target structures in bacterial cells. A selection of antibiotic drugs/classes are presented in yellow boxes with respective target structures shown in grey (modified from Lewis, 2013 (3)).

In the first case, interference with peptidoglycan turnover results in growth arrest and/or loss of mechanical stability and the high internal osmotic pressure will eventually lead to bursting of cells. Few antibiotic agents also target the cytoplasmic membrane such as

daptomycin which depolarises and disrupts the cytoplasmic bilayer (10). Inhibition of nucleic acids and protein biosynthesis require antibiotic substances to translocate over the cytoplasmic membrane. Subsequent effects are only bacteriostatic and can lead to growth recovery of cells once the drug is removed (11). Another bacteriostatic mechanism of action has been demonstrated for the antibiotic class of sulfonamides which selectively inhibit the initial step in folate synthesis. However, strong resistance development has restricted systemic treatment and reduced the application, e.g. to uncomplicated urinary tract infections (12).

Although many of the conventional antibiotic drugs have proven high initial efficacy, the specific interaction with a particular cellular structure, however, is prone to induce the development of resistance, i.e. through mutations in chromosomal genes or horizontal gene transfer between individual bacteria cells.

3.1.3 Resistance development

The evolution of bacterial mutant strains which have acquired resistance to a particular environmental stress is a natural process favoured by selection pressure. Nevertheless, the excessive and often inappropriate use of antibiotics over many years has largely contributed to the increased number of infections with multidrug-resistant microbes which are estimated to kill 25.000 people annually in Europe (5).

Different bacterial mechanisms have been described to counter the attack of antimicrobial agents. They can be classified into three major strategies: (*i*) reduction of the intracellular antibiotic concentration, (*ii*) modification of the antibiotic target and (*iii*) inactivation of the antibiotic substance itself (Figure 5) (3, 13). Considering the first strategy, the bacterial cell envelope constitutes an effective barrier. Fernández and Hancock investigated how the overexpression of porins and efflux pumps enhances antibiotic export, thereby decreasing the permeability of the outer membrane (14). Multiple studies on the Gram positive pathogenic strain *S. aureus* demonstrated how thickening of the cell wall conveys resistance to antibiotics such as vancomycin (15, 16). Furthermore, changes in surface charge achieved for example by alterations in LPS and LTA molecules, but also phospholipid head groups, have been proven an efficient

measure to repel polar substances and to minimise initial contact with bacterial cells (17, 18). A decrease in the intracellular antibiotic concentration is also achieved by rigidification of the cytoplasmic membrane which is based on changes in phospholipid composition and fatty acid synthesis and has been reported to be involved, e.g. in daptomycin resistance (19).

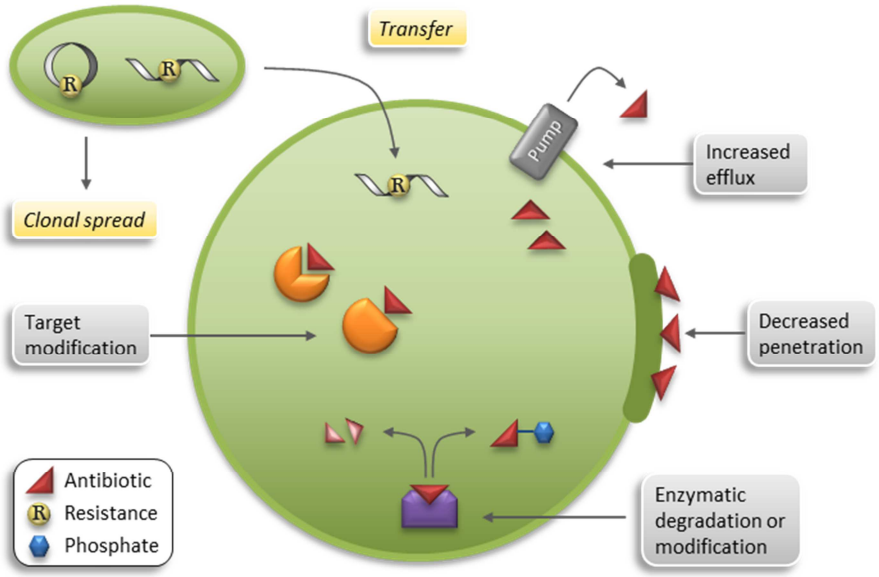

Figure 5 Mechanisms of acquired bacterial resistance against conventional antibiotics. The major resistance strategies include decreased accessibility to the target structure and modification of the target or the antibiotic substance (modified from Lewis, 2013 (3)).

If, however, antibiotic substances have succeeded in crossing the bacterial envelope they are confronted with intracellular challenges (Figure 5). These include lowered binding affinities between the antibiotic and its target which can be based on a single point mutation in the chromosome or uptake of homologous genes by transformation (9). Post-translational modifications, e.g. methylation, mask the drug-binding site of the target molecule and have been reported to be involved in resistance to chloramphenicol and linezolid (20). Moreover, thousands of bacterial enzymes have been elucidated which are able to either hydrolyse antibiotic substances, as in the case of penicillin degradation by β-lactamases, or transfer chemical groups onto the drug which creates steric hindrance and blocks interaction with the target substance (9, 21).

These mechanisms, which also include overproduction of the target structure, have evolved as potent methods to reduce the effective concentration of the antibiotic agent.

Thorough understanding of bacterial resistance is required to aid future development of novel therapeutic compounds which kill microorganisms by different molecular mechanisms. In this context, increasing efforts have been made to study the potential application of antimicrobial peptides as alternative antibiotic agents (22).

3.2 Antimicrobial peptides

3.2.1 Role in innate immunity

Owing to their broad-spectrum activity, which includes Gram positive and Gram negative bacteria, fungi, enveloped viruses and parasites, antimicrobial peptides have extensively been studied as novel therapeutic agents (23). Cationic antimicrobial peptides from higher eukaryotic organisms are often referred to as *Host Defense Peptides* (HDPs) as they fulfil a major role in the immediate and non-specific immune response against infectious pathogens. They can be either constitutively expressed or induced upon an immune stimulus, as in the case of lysozyme and defensins, respectively (24). In addition to direct interaction with microorganisms these peptides possess strong immunological properties (Figure 6), (25, 26). HDPs have been demonstrated to balance the induction of pro- and antiinflammatory stimuli, e.g. by modulating Toll-like receptor (TLR)-signalling in response to bacterial LPS and LTA exposure (27). Natural and also synthetic peptides have the ability to recruit leukocytes to sites of infection by chemotaxis (28, 29). In addition, direct attraction of immune cells has been observed which is proposed to be based on similar functions between HDPs and chemokines due to the cationic and amphipathic nature of both species (30, 31). Davidson et al. could further demonstrate peptide-induced differentiation and activation of macrophages and neutrophils, thereby elucidating a potential link between innate and adaptive immune response (32). In this context, also a direct interaction of

Host Defense Peptides with B and T cells was shown to provide long-lasting and efficient immune responses (33-35). Recently, bacterial infections were observed to trigger the formation of neutrophil-derived extracellular traps (NETs). This meshwork is expelled from the cells like a net to catch invading pathogens and consists of nuclear material and antimicrobial peptides, including the human cathelicidin LL-37 (36, 37). Cellular clearance of bacteria is also facilitated by the non-inflammatory programmed cell death (apoptosis). Here, LL-37 was shown to play an ambiguous role. While the peptide triggers death of epithelial cells by caspase activation, apoptosis is inhibited in neutrophils which is thought to counteract the short half-life of these cells, thus supporting general innate host defence (38).

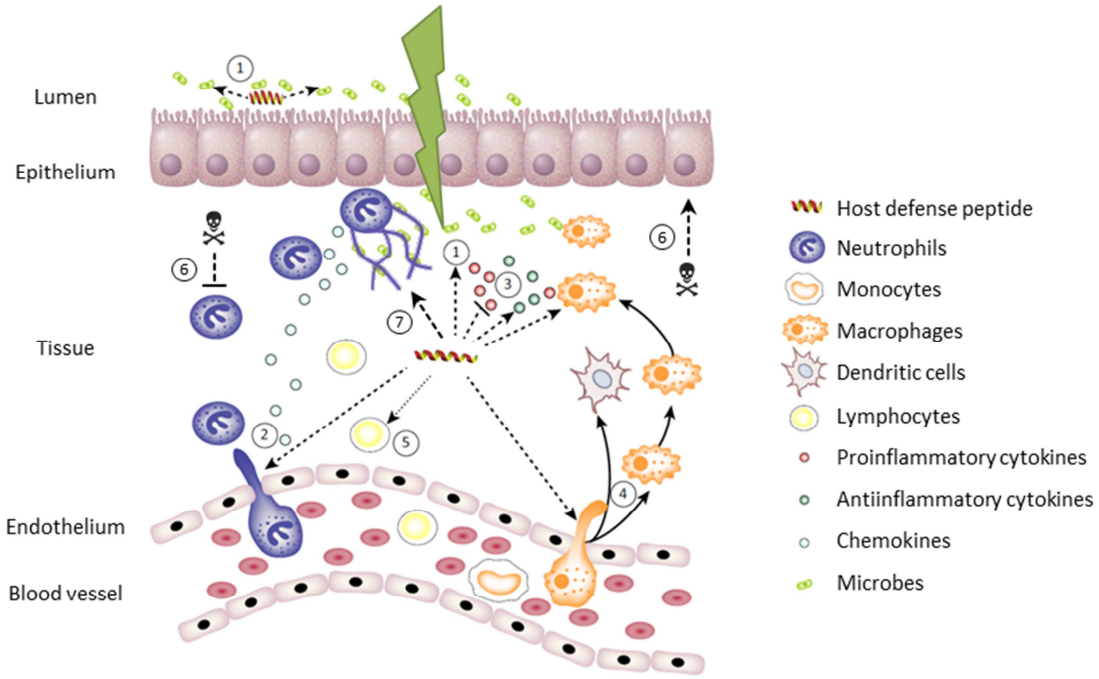

Figure 6 Role of antimicrobial peptides in innate immunity. Schematic presentation of the various immunological functions of cationic peptides, also called Host Defense Peptides (HDPs). (1) Direct interaction with invading bacteria; (2) recruitment of immune cells such as neutrophils and monocytes; (3) reduction of proinflammatory cytokines (e.g. TNFα) and enhanced production of antiinflammatory mediators (e.g. IL-10); (4) induction of macrophage and dendritic cell differentiation and activation; (5) modulation of adaptive immunity by interaction with lymphocytes; (6) cell-specific regulation of apoptosis; (7) components of neutrophil-derived extracellular traps (NETs) (modified from Mansour et al., 2006 (25)).

3.2.2 Antibiotics vs. antimicrobial peptides

Apart from their wide range of activity, antimicrobial peptides (AMPs) possess multiple properties which make them superior to conventional antibiotics. First of all, most peptides specifically target the membrane of microorganisms. The high selectivity is favoured by electrostatic interactions between the negative bacterial envelope and the cationic charge of the peptides (see 3.2.4 Antimicrobial mechanisms of action). Binding to the pathogen surface is independent of receptor-mediated interactions and antimicrobial targets are often non-proteinaceous. Moreover, some peptides also attack multiple microbial structures which effectively dampens bacterial defence and has been described in a concentration-dependent manner for the peptides nisin and magainin (39, 40). As mentioned above, in addition to their direct antimicrobial activity, AMPs show endotoxin-neutralising and immune-stimulatory effects (41). Furthermore, they are effective as single agents or can be released as cocktails of different peptides, each one acting by a distinct mechanism (42). Synergistic effects were also observed with traditional antibiotics and are proposed to be related to strong peptide-membrane interactions which render the bacterial surface more permeable and increase the uptake of intracellular drugs (43). Thus, individual concentrations of the involved antimicrobial agents can be minimised which is thought to reduce cytotoxicity and the emergence of resistance.

One of the most important features that distinguishes antimicrobial peptides from conventional antibiotics is the comparably low risk to select for bacterial resistance (40). This observation is discussed to be related to the co-evolution of peptides and microorganisms for millions of years accompanied by a step-wise adaptation to putative resistance strategies. This in turn has led to a balanced host-pathogen interaction and created the inventory of today's antimicrobial peptides. Furthermore, the diverse and often non-specific target structures usually do not involve protein binding sites. Hence, in contrast to conventional antibiotic treatment, there is only little selection pressure giving rise to mutants which have acquired superior defence mechanisms (44, 45).

Nevertheless, microorganisms have found ways to reduce the effectiveness of antimicrobial peptides (46). These countermeasures in most cases affect the bacterial membrane and are supposed to reduce initial interaction sites. Examples include cell

wall modifications, reduction of surface charge, decrease in membrane fluidity or increase of bilayer thickness and enhanced efflux of peptides by bacterial pumps (47-49).

Although there are many advantages of antimicrobial peptides over conventional antibiotics, there are also major drawbacks which currently still restrict their medical application (43). Due to their small size, the peptides are subject to proteolytic degradation. This influences pharmacodynamics parameters, such as bioavailability, target delivery and effective concentration. In addition, at higher dosage, which is required for systemic application, some peptides were observed to induce haemolysis in red blood cells (50).

Currently, the antimicrobial peptides gramicidin S and polymyxin B, which are both of bacterial origin, are approved by the FDA for medical treatment of bacterial infections. However, their use is limited to topical applications as both substances show toxic side effects in systemic therapy (22, 51). The lantibiotic nisin, which was first isolated from *Lactococcus lactis*, efficiently kills Gram-positive bacteria species and has been employed as preservative in many different food products since the late 1960s (52).

To date, a particular clinical significance is attributed to the cyclic lipopeptide daptomycin from *Streptomyces roseosporus* which has a strong bactericidal effect and is used for a variety of serious Gram positive infections (53). The high antibiotic potency becomes evident considering its therapeutic application against vancomycin-resistant enterococci (VRE) and also methicillin-resistant *Staphylococcus aureus* (MRSA). However, it is alarming that already a couple of years after introduction on the market, daptomycin non-susceptible strains have evolved (17).

3.2.3 Peptide structure and activity

The class of antimicrobial peptides is characterised by a broad structural diversity regarding size, amino acid composition and secondary structure (41). Natural representatives are processed from larger precursor molecules and can be post-translationally modified, e.g. by glycosylation or C-terminal amidation. Some peptides are produced after proteolytic cleavage of proteins, such as in the case of the amphibian buforin II which was first isolated from the stomach tissue of the toad *Bufo bufo gargarizans* and is derived from histone H2A (54). Also, enzymatic cleavage of the mammalian protein lactoferrin gives rise to lactoferricin which was reported to have strong antimicrobial and antiviral activity (55).

The more than 2500 agents that are listed to date in the *Antimicrobial Peptide Database* (APD, (56)) differ widely in their secondary structure (Figure 7). In nature, numerous linear peptides with α-helical and β-sheet arrangement or mixed secondary structure elements have been observed. However, in most cases these are random coil peptides which only adopt their antimicrobially active form upon interaction with bacterial membranes and lipid vesicles (57, 58).

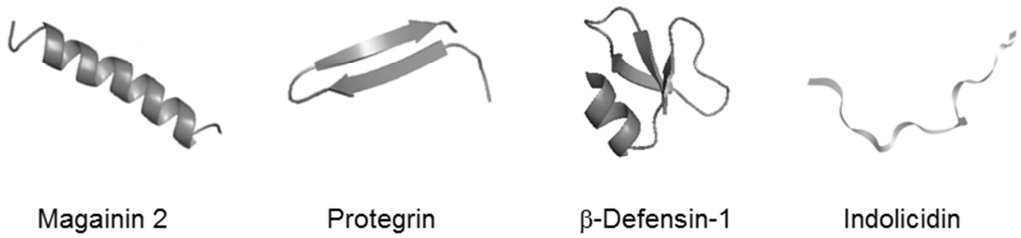

Figure 7 Secondary structures of selected antimicrobial peptides. Peptide structures were obtained from PDB: amphibian magainin 2 (2MAG) (59), porcine protegrin (1PG1) (60), human β-defensin-1 (1IJU) (61) and bovine indolicidin (IG89) (62).

In addition, many cyclic antimicrobial peptides have been found in bacteria, plants and animals (63). For example, the class of *lantibiotics* are gene-encoded peptides produced by many Gram positive bacteria species. Their unique intramolecular rings are formed by the non-proteinogenic thioether amino acids lanthionine or methyl-lanthionine which

strongly impact their three dimensional structure (64). Furthermore, the plant peptide family of *cyclotides* comprises many thousand members which have a seamless circular backbone that is additionally cross-linked by disulphide knots (65). The first cyclic mammalian peptide was isolated from leukocytes of rhesus macaques, named rhesus θ-defensin-1. In contrast to the bacterial and plant representatives, this antimicrobial peptide is produced from two genes each encoding a short linear peptide. These precursors are subsequently ligated in a double head-to-tail fashion and further cross-linked by disulphide bonds (66, 67). In general, backbone ligation and intramolecular side chain interactions render cyclic peptides highly stable. They can be exposed to high temperatures, extreme pH values and proteolytic cleavage, however, they were shown to still retain their strong antimicrobial activity (68).

Antimicrobial peptides are highly diverse even among closely related species which accounts for an adaptation of the organism to a particular ecological niche with its unique microbial environment. Nevertheless, most peptides exhibit a large number of cationic residues, and show a predominance of one or two amino acids throughout the whole molecule. In this context, the class of R- and W-rich peptides has been extensively studied (69-73). The significance of arginine and tryptophan side chains within peptides and also larger proteins is related to their complementary properties which energetically favour interaction and insertion into bacterial membranes (72). While tryptophan has a strong preference for interfacial regions of lipid bilayers, the guanidinium group of arginine gives cationic charge and a unique geometry of hydrogen bonding which are the basis for selective interaction with anionic components of bacterial membranes (74). With regard to the underlying conformational principles, all of these peptides adopt an amphipathic structure upon interaction with bacterial membranes, i.e. in the antimicrobially active form cationic regions are spatially separated from hydrophobic parts of the molecule. The polar residues establish strong interactions with the negatively charged head groups of bacterial phospholipids. Subsequently, hydrophobic side chains facilitate insertion of the peptide into the acyl chain region of the bilayer (75).

3.2.4 Antimicrobial mechanisms of action

Electrostatic attraction is suggested as basis for the initial contact between peptides and microorganisms independent of the different mechanisms of action. Although it has been demonstrated that peptides readily insert into model membrane vesicles with acidic phospholipids, first interactions are supposed to be established with anionic compounds of the outer membrane (LPS) and the cell wall (LTA) (39). Subsequently, peptides transverse the peptidoglycan layer and make contact with cytoplasmic membrane lipids.

Permeabilisation of the microorganism's membrane is reported to be the most dominant mode of action and is often induced by α-helical peptides which are able to span the entire thickness of the bilayer (41). In this regard, many different models have been described to disrupt the integrity of the cytoplasmic bilayer (Figure 8). In the *barrel-stave model* peptide helices form tight bundles with a central lumen which leads to the formation of transmembrane pores. Hydrophobic regions of the peptides interact with the core of the bilayer while polar residues line the interior of the channel. This mechanism, however, is rather unique and has only been shown for the fungal peptide alamethicin (76). For membrane permeabilisation induced by the *carpet model*, antimicrobial peptides first accumulate tightly side by side on the surface in a parallel fashion (77). This alignment already affects the mobility and curvature of the membrane. With increasing concentrations peptides act as detergents which eventually break down the integrity of the bilayer under the formation of lipid micelles. In addition, many α-helical peptides, such as magainin 2, protegrin or LL-37, have been described to act by the *toroidal-pore model*. Here, the polar side chains bind strongly to the acidic phospholipid head groups which forces the lipids to bend towards the inner lining of the pore (78). Recent investigations to determine the number of involved molecules have elucidated the appearance of "disordered toroidal pores" which are characterised by smaller numbers of peptides sufficient to induce lipid bending (79). In general, pore formation represents a very efficient method of cell killing as it directly impairs the barrier function of the membrane.

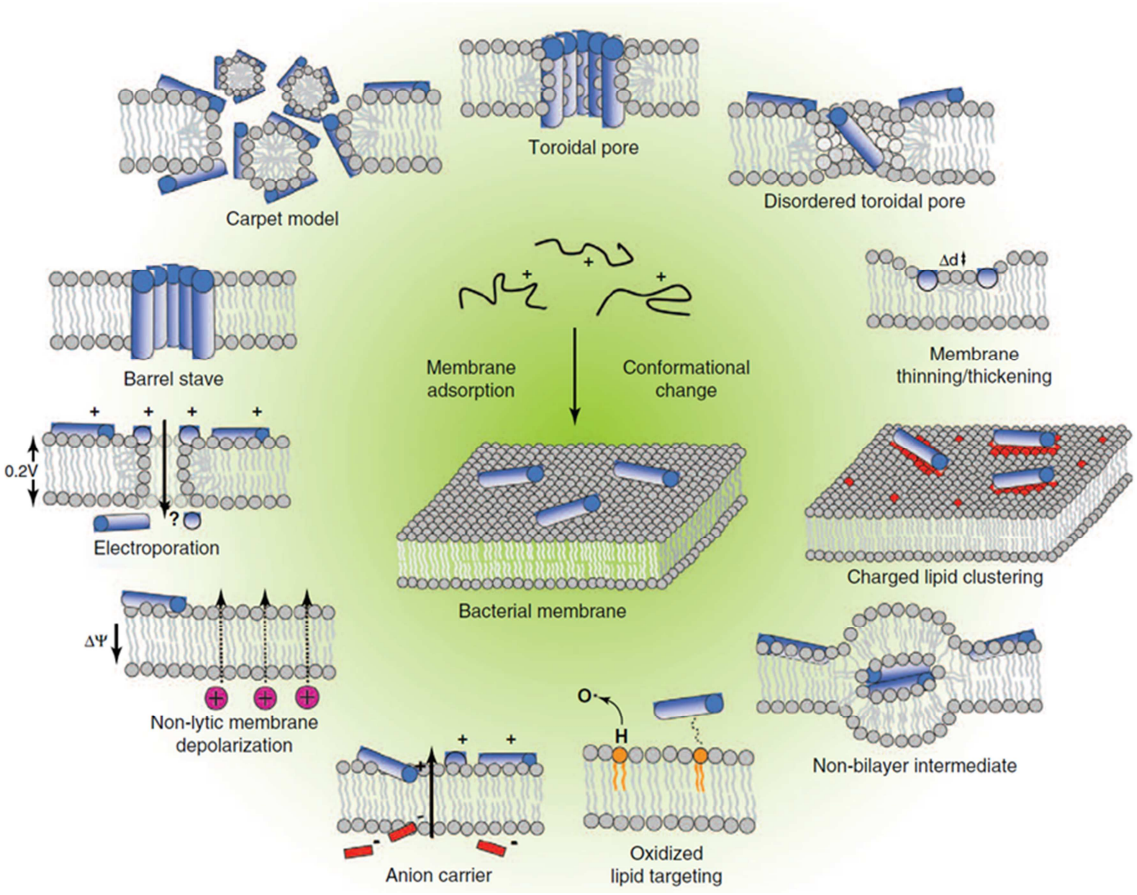

Figure 8 Antimicrobial peptide-induced effects on the bacterial cytoplasmic membrane. Different models have been described for pore formation and also non-lytic mechanisms which reduce the barrier function of the membrane or destroy the pH gradient. See text for details (adapted from Nguyen et al., 2011 (80)).

However, other membrane-targeting mechanisms have been described which have only little or no impact on the integrity of the lipid bilayer. Some of them are rather specific and include for example peptide-induced electroporation. This phenomenon is based on an increase in membrane potential above a threshold of 0.2 V due to accumulation of cationic peptides at the cell surface which renders the bilayer transiently permeable for small molecules (81, 82). On the contrary, the cyclic peptide antibiotics valinomycin, a potassium-selective ion carrier, and daptomycin have been reported to dissipate membrane potential which in turn is connected to delocalisation and impaired functionality of membrane proteins (83, 84). Depolarisation of the membrane potential has further been described for bovine lactoferricin which eventually impedes the proton-

motive-force and inhibits ATP-dependent multi-drug efflux pumps (55). Similarly, it has also been suggested that the linear peptide indolicidin can function as inherent ion carrier as it is able to couple with small anions across the bilayer and facilitates their efflux (85). Furthermore, Mattila et al. could demonstrate that oxidised lipid head groups which are formed after release of reactive oxygen species (ROS) during phagocytosis might play a role in the targeting of bacterial membranes by antimicrobial peptides (86).

Besides the antimicrobial mechanisms mentioned above, several peptides have been described which *target intracellular structures* (39). For instance, the amphibian peptide buforin II is able to translocate over the cytoplasmic membrane without permeabilisation and is suggested to interact with nucleic acids (87, 88). In other cases, translocated peptides were observed to interfere with vital physiological processes, such as septum formation during division, peptidoglycan synthesis or protein biosynthesis. Although intracellular peptide targets can be very efficient with regard to cell killing, they are often observed in synergistic activity with membrane disruption. Yet again, this demonstrates how multiple mechanisms render antimicrobial peptides superior over conventional antibiotic agents.

A third mechanism of action which has only recently been discovered *in vitro* is based on peptide-induced *lipid demixing*. Cationic antimicrobial agents were shown to have the ability to cluster anionic phospholipids head groups which is thought to interfere with pre-existing lipid phases in the bilayer and subsequently impairs functional microdomains (89). Furthermore, linear and cyclic R-,W-rich peptides induce lipid phase separation also in PE and PG model bilayer systems (90). It has been demonstrated before that lateral, mobile lipid domains exist naturally in bacterial membranes. These include changes in lipid distribution and composition during the cell cycle which are required for bacterial division (91, 92). Hence, the impact of antimicrobial peptides on bacterial lipid raft formation and disturbance of protein function is subject to intensive investigations (93). However, although phase boundary effects are proposed to occur also under physiological conditions, those that arise from peptide-induced lipid clustering are presumed to happen too swiftly for the cells to be able to compensate for this lipid re-arrangement (6). This mechanism of action has

raised increased awareness as it is suggested that peptide specificity for a particular bacterial species can be predicted based on the ability to cluster anionic lipids which might be of great benefit in the design of novel antibiotic agents.

The mechanism of action and activity of an antimicrobial peptide are influenced by biophysical parameters, such as hydrophobicity, hydrophobic moment and hydrophilic face, as well as molecular size and charge (94, 95). Hence, modulation of these features during peptide synthesis is used to study variations in peptide-lipid interactions and to improve the antimicrobial activity spectrum.

3.3 cWFW - A synthetic cyclic hexapeptide with high antimicrobial potential

In the 1990s, Blondelle and colleagues established a synthetic combinatorial library screen to identify new lead structures for the development of antimicrobial agents based on the active motif of lactoferrin (96, 97). With the aid of this new technology, the high abundance of arginine and tryptophan residues was confirmed as crucial structural parameter that enhances antimicrobial activity which is especially pronounced for linear hexapeptides. Earlier investigations of helical peptides with high amphipathicity revealed that the antimicrobial activity and selectivity for microorganisms are rather determined by global structure parameters and membrane composition than amino acid composition (98, 99). Based on the linear sequence Ac-RRWWRF-NH_2, different sets of synthetic hexapeptides were analysed with regard to their antimicrobial activity. To this end, the position of the individual amino acid residues was changed in order to elucidate the role of peptide sequence. Furthermore, the impact of the secondary structure was investigated with conformationally restrained cyclic hexapeptide analogues (70).

Dathe et al. found that cyclisation results in a pronounced increase in antimicrobial activity compared to the linear sequences (100). Moreover, clustering of hydrophobic

and cationic regions was observed to enhance the amphipathic nature of these small hexapeptides which accounts for the strong membrane activity. Further studies were conducted to investigate the influence of the peptide ring size on the interaction with *E. coli* membranes and also haemolytic activity (101). In this connection, best results were obtained for a cyclic hexapeptide with the sequence cyclo(RRRWFW), termed cWFW (Figure 9).

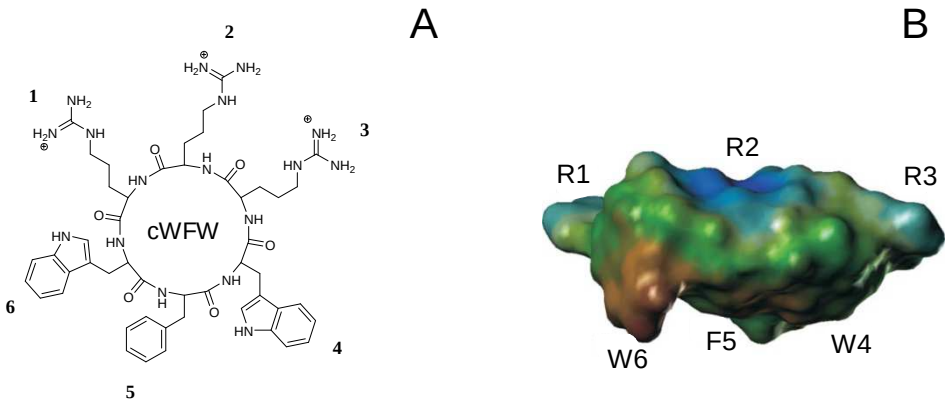

Figure 9 Structure of the synthetic antimicrobial hexapeptide cWFW. (A) The primary structure of cWFW (cyclo(RRRWFW)) shows backbone cyclisation and clustering of cationic and hydrophobic regions. (B) The strong amphipathic alignment of the six amino acid residues is demonstrated by the hydrophobicity profile of the secondary structure (modified from Appelt et al., 2008 (102)).

The cyclic hexapeptide is characterised by a clustered arrangement of three arginine residues opposed to the hydrophobic side chains of tryptophan and phenylalanine. This alignment renders the molecule highly amphipathic. NMR studies revealed that cWFW adopts a secondary structure with two regular β-turns in membrane-mimicking environments (102). In interaction with detergent micelles, all aromatic side chains are orientated in the same direction establishing a pronounced hydrophobic peptide face which integrates into the micellar core while the arginine residues interact with the outer anionic head groups. cWFW was shown to have a high antimicrobial activity against Gram positive and Gram negative bacteria and is bactericidal even at low concentrations (103). Although the small hexapeptide fulfils all the structural requirements for strong interaction with bacterial membranes, there is considerable evidence that the peptide does not act by membrane permeabilisation.

4 Aim of the study

The aim of the present study is to elucidate the antimicrobial mechanism of action of the small synthetic peptide cWFW. It selectively kills bacteria at very low concentrations, however, the underlying principles of cell killing differ from those described for other antimicrobial peptides. As cWFW does not appear to induce bacterial resistance, characterisation of the antimicrobial mechanism provides highly useful information for the design of novel antibiotic compounds. Investigation of the structural determinants of peptide activity is pursued with a combination of biological and biophysical techniques, including microbial cell culture, fluorescence live cell imaging, isothermal titration calorimetry and HPLC.

5 Materials and methods

5.1 Materials

5.1.1 Chemicals and consumables

If not stated otherwise, all chemicals and consumables used in this study were purchased from Acros Organics (Belgium), Becton Dickinson (Heidelberg), Life technologies (Darmstadt), Merck (Darmstadt), Roth (Karlsruhe), Sarstedt (Nümbrecht), Schott (Mainz), Sigma-Aldrich (USA), Thermo Scientific (Schwerte), TPP (Switzerland) and VWR Chemicals (Darmstadt).

Substances	**Working Solution**	**Source**
Benzyl alcohol (BA)	5 M in DMSO	Sigma-Aldrich
Casamino acids	20% in ddH_2O	BD Biosciences
Laurdan	1 mM in DMF	Sigma-Aldrich
$DiSC_3(5)$	15 µM in LB/15% DMSO	Life technologies
Isobutyrate (IB)	10 mM in ddH_2O	Sigma-Aldrich
Isovalerate (IV)	10 mM in ddH_2O	Sigma-Aldrich
Methylbutyrate (MB)	10 mM in ddH_2O	Sigma-Aldrich
NAO	10 µM in DMSO	Sigma-Aldrich
Nile Red	1 µg/ml in DMSO	Life technologies
Propidium iodide (PI)	10 µg/ml in ddH_2O	Sigma-Aldrich
MTT reagent	5 mg/ml in DPBS	Sigma-Aldrich

5.1.2 Media and buffers

Solution	Composition
Nutrient broth	LB broth - Lennox's version 10 g/l tryptone 5 g/l yeast extract 5 g/l NaCl
Nutrient agar	LB broth with agar - Lennox's version 15 g/l agar 10 g/l tryptone 5 g/l yeast extract 5 g/l NaCl
BHI	Brain heart infusion 6 g/l infusion from brain heart (solids) 6 g/l peptic digest of animal tissue 5 g/l sodium chloride 3 g/l dextrose 14.5 g/l pancreatic digest of gelatin 2.5 g/l disodium phosphate
SMM	Supplemented minimal medium 12 µl/ml glucose (40 % stock) 10 µl/ml tryptophan (2mg/ml stock) 6 µl/ml MgSO4 (1M stock) 1 µl/ml casamino acids (20%) 0.5 µl/ml Fe-citrate (2.2mg/ml stock)
BMM (104)	Belitzky minimal medium (used for proteomic profiling, (105))
Cell culture medium	DMEM (Dulbecco's modified Eagle's medium, Gibco) 4.5 g/l glucose 10% (v/v) heat inactivated foetal calf serum (FCS) 50 units/ml penicillin, 50 µg/ml streptomycin
Washing buffer	DPBS(G) - Dulbecco's phosphate buffered saline (+1 g/l glucose)
Trypsin/EDTA	0.25% trypsin, 380 mg/l Na-EDTA
Phosphate buffer	10 mM NaH_2PO_4 /Na_2HPO_4, 154 mM NaCl, 0.1 mM Na-EDTA, pH 7.4
HPLC buffer	80% (v/v) acetonitrile 0.1% (v/v) trifluoroacetic acid (TFA) in ddH_2O
CD buffer	10 mM NaH_2PO_4 /Na_2HPO_4, 154 mM NaF, 0.1 mM Na-EDTA, pH 7.4

5.1.3 Peptides and lipids

Peptides used in this study were either synthesised at the Leibniz-Institut für Molekulare Pharmakologie (FMP), department of Chemical Biology (Beyermann group) or purchased from Biosyntan GmbH, Berlin.

Peptide	Sequence	Mass [g/mol]
cWFW	c-RRRWFW	989.2
cRKR	c-RKRWFW	960.5
cRKK	c-RKKWFW	931.5
cKRK	c-KRKWFW	931.5
cKKR	c-KKRWFW	931.5
cKKK	c-KKKWFW	903.5
cW_2[Fluos]	c-RRRWWK[Fluos]	1327.5
cW_3[Fluos]	c-RRWWWK[Fluos]	1357.5
cW[Cu]W	c-RRRW[Ala-Cu]W	1086.3
cW[NBD]W	c-RRRW[Dap-NBD]W	1090.9
cR2[Cu]	c-KRKW[Ala-Cu]W	1030.3
cR2[NBD]	c-KRKW[Dap-NBD]W	1033.9
KLA-1 (99)	KLALKLALKAWKAALKLA-NH_2	1949.5
Polymyxin B (103)	cyclic decapeptide with variable acyl chain	1385.6
Fluos-buforin	Fluos-TRSSR AGLQF PVGRV HRLLR K-NH_2	2790.7
Fluos-penetratin	Fluos-RQIKI WFQNR RMKWK K-NH_2	2601.6

Cu-coumarin; Dap-diaminopropionic acid; Fluos-carboxyfluorescein; NBD-nitrobenzoxadiazole.

All lipids used in this study were purchased from Avanti Polar Lipids, Inc., USA.

Lipid	Description
POPC (PC)	1-hexadecanoyl-2-(9Z-octadecenoyl)-sn-glycero-3-phosphocholine
POPE (PE)	1-hexadecanoyl-2-(9Z-octadecenoyl)-sn-glycero-3-phosphoethanolamine
POPG (PG)	1-hexadecanoyl-2-(9Z-octadecenoyl)-sn-glycero-3-phospho-(1'-rac-glycerol)
Cardiolipin (CL)	Heart, bovine (predominant species CL(18:2))
E. coli extract	Polar lipid extract from *E. coli* (71.4% PE, 23.4% PG, 5.2% CL (mol%))

5.1.4 Bacteria strains and mammalian cell lines

E. coli K12 DH5α and *B. subtilis* DSM 347 were purchased from DSMZ (German Collection of Microorganisms and Cell Culture). *B. subtilis* 168 CA/ED wild type were obtained from the Centre For Bacterial Cell Biology (CBCB), Newcastle University, UK.

Wild type strains	**Description**	**Genotype**	**Culture medium**
E. coli K12 DH5α	Plasmid host for cloning	(106)	LB
B. subtilis 168 CA	Wild type	*trpC2*	LB
B. subtilis 168 ED	Wild type (strain background of Mre-mutants)	*trpC2*, *walRmut*	LB + 20 mM MgSO4
B. subtilis DSM 347	Quality control strain according to DIN 58959-7 and Ph. Eur., assay of antibiotics	(106)	LB

L-form bacteria *E. coli* W1655 F+ (LWF+) and *B. subtilis* L-170 (L-170) were kindly provided by Dr Christian Hoischen, Leibniz Institute for Age Research, Germany.

L-form strains	**Description**	**Genotype**	**Culture medium**
E. coli W1655 F+ (LWF+)	*E. coli* L-form (cell wall-deficient)	(107)	BHI + 70 mg/ml penicillin
B. subtilis L-170 (L-170)	*B. subtilis* L-form (cell wall-deficient)	(107)	BHI + 70 mg/ml penicillin + 50 mg/ml sucrose + 30 mg/ml yeast extract

Mutant strains derived from *B. subtilis* 168 CA/ED were provided at the Centre of Bacterial Cell Biology (CBCB), Newcastle University, UK. Further information on the synthesis and genetic background can be found at Strahl, *et al.* (108), Salzberg and Helmann (109) and Dominguez-Cuevas, *et al.* (110).

Mutant strains	**Deficiency**	**Genotype**	**Culture medium**
B. subtilis SDB206 (111)	Cardiolipin (all three CL synthases)	*ywiE2::neo ywjE::spc clsA::pMutin4 (ery)*	LB
B. subtilis HB5343	Phosphatidyl-ethanolamine (PE)	*ery* Δ*psd*	LB
B. subtilis HB5134	Lipid desaturase	*spc* Δ*des*	LB
B. subtilis HB5337	Lysylphosphatidylglycerol (LPG) synthase	*kan* Δ*mprF*	LB
B. subtilis 3728	MreB	*Ωneo3427* Δ*mreB*	LB + 20 mM $MgSO_4$
B. subtilis 4261	Mbl	*cat* Δ*mbl*	LB + 20 mM $MgSO_4$
B. subtilis 4262	MreBH	*ery* Δ*mreBH*	LB + 20 mM $MgSO_4$
B. subtilis PDC660	Mbl, MreBH (expresses MreB only)	Δ*mbl ΔmreBH* Δ*mreB::neo amyE*::*PspacHY-mreB cat*	LB + 5 µM IPTG
B. subtilis YK1119	MreB, MreBH (expresses Mbl only)	Δ*mbl* Δ*mreBH ΔmreB::neo amyE*::*PspacHY-mbl cat*	LB + 50 µM IPTG
B. subtilis PDC643	MreB, Mbl (expresses MreBH only)	Δ*mbl* Δ*mreBH* Δ*mreB::neo amyE*::*PspacHY-mreBH cat*	LB + 50 µM IPTG
B. subtilis 4277	MreBH, Mbl, MreBH	*Ωneo3427* Δ*mreB* Δ*mbl::cat* Δ*mreBH::erm Ω(neo::spc)*Δ*rsgI*	LB + 20 mM $MgSO_4$
B. subtilis 3481	MreC	*Ωneo3427 ΔmreC*	LB + 20 mM $MgSO_4$
B. subtilis PDC464	LytE	Δ*lytE::cat*	LB
B. subtilis PDC463	CwlO	Δ*cwlO::spc*	LB
B. subtilis AG723-1 (A. Guyet, CBCB; unpublished) *	LytF	Δ*lytF::spc*	LB
B. subtilis AG724-1 (A. Guyet, CBCB; unpublished) *	LytABC	Δ*lytABC::neo*	LB
B. subtilis HS70 (H. Strahl, CBCB; unpublished) °	Bkd (fatty acid synthesis)	Δ*bkd::ery*	LB + lipid precursors

* Transformation of *B. subtilis* 168 CA with DNA from *B. subtilis* 1A792 (*lytABC::neo lytD::tet lytE::cam lytF::spc*) (112).

° Transformation of *B. subtilis* 168 CA with DNA from *B. subtilis* RM113 (*amyE::tet xylR, spoVD::cat Pxyl-murE, sepFT11M, bkd::erm sup*) (113).

All strains expressing GFP- or YFP-labelled proteins were cultivated at 30 °C.

Mutant strains	Fluorescent protein	Genotype	Induction
B. subtilis 2566	MreB	*amyE::spc Pxyl-gfp-mreB*	0.3% xylose
B. subtilis 3751	Mbl	*amyE::spc Pxyl-gfp-mbl*	0.3% xylose
B. subtilis 3750	MreBH	*amyE::spc Pxyl-yfp-mreBH*	0.3% xylose
B. subtilis 3417*	MreC	*cat mreC::Pxyl-gfp-mreC*	0.3% xylose
B. subtilis 2020	FtsZ	*amyE::spc Pxyl-gfp-ftsZ*	0.1% xylose
B. subtilis PG62	FtsA	*aprE::spc Pspac-yfp-ftsA*	0.1 mM IPTG
B. subtilis 4181	SepF	*amyE::spc pxyl-sepF-gfp*	0.1% xylose
B. subtilis 3122*	Pbp2B	*pbp2B::cat pxyl-pbp2B-GFP*	0.5% xylose
B. subtilis LH131	MinD	*amyE::spc pxyl-gfp-minD*	0.5% xylose
B. subtilis 1988	MinC	*amyE::spc Pxyl-gfp-minC*	0.5% xylose
B. subtilis HS63°	DivIVA	*amyE::spc Pxyl-divIVA-msfGFP*	0.3% xylose
B. subtilis JWV042	Hbs	*cat amyE::Phbs-hbs-gfp*	-
B. subtilis HM4	Spo0J	*neo spo0J-gfp*	-
B. subtilis MS104	DnaN	*cat PdnaN-gfp-dnaN*	-
B. subtilis BS23*	FoF1 ATP synthase	*cat 'atpA–gfp Pxyl-atpA'*	0.5% xylose
B. subtilis HS401	MinDah (amphipathic helix)	*spc amyE::Pxyl-gfp-junLZ-minDah*	1% xylose

* Addition of supplements is mandatory for cell growth.

° Reference: Jahn N, Brantl S, Strahl H (2015) Against the mainstream: The membrane-associated type I toxin BsrG from Bacillus subtilis interferes with cell envelope biosynthesis without increasing membrane permeability.

Cell lines	Origin	Source
HeLa	Human cervical cancer	DSMZ (Braunschweig)
Erythrocytes	Human blood donation	Institute of Transfusion Medicine, Charité (Berlin)

5.2 Devices and software

Device	Model	Company
Plate reader	Safire^2	Tecan (Switzerland)
	Fluostar Optima	BMG Labtech (Ortenberg)
Flow cytometer	FACSCalibur™	BD Biosciences (Heidelberg)
Microscope slides	Multispot microscope slides (PTFE & specialised coating)	Hendley-Essex (UK)
Microscope	Axiovert 200M (Plan-Neofluar ×100/1.30 oil ph 3 objective)	Carl Zeiss (Jena)
	LSM 510 ConfoCor2 (plan-apochromat ×63, ×100/1.4 objective)	Carl Zeiss (Jena)
	Nikon Eclipse Ti (Plan Fluor ×100/1.30 oil ph3 DLL objective)	Nikon (Düsseldorf)
Centrifuge	Biofuge® primo R	Heraeus (Langenselbold)
	Eppendorf MiniSpin®	Eppendorf (Hamburg)
	Sigma 3K12	Sigma (Osterode am Harz)
Fluorescence spectrometer	LS-50B	Perkin Elmer (Rodgau)
HPLC, column	LC-2000 Plus, ProntoSil 300-5-C18-H column (250×4.6 mm, 5 µm)	Jasco (USA), Bischoff Chromatography (USA)
DLS	Zetasizer Nano ZS ZEN 3600	Malvern Instruments (UK)
ITC	MicroCal VP-ITC	Malvern Instruments (UK)
CD spectrometer	J-720	Jasco (USA)
Shaker	Eppendorf Thermomixer® comfort	Eppendorf (Hamburg)
Incubator (bacteria)	Multitron Pro (shaker)	Infors AG (Switzerland)
Incubator (cell culture)	Binder Series BD	Binder Inc. (USA)
Protein determination	BCA™ Protein Assay Kit	Thermo Scientific (Schwerte)
ATP detection	BacTiter-Glo™ Microbial Cell Viability Assay	Promega (USA)
Liposome extruder	LiposoFast mini extruder	Avestin (Switzerland)
Ultrasonication	Labsonic L ultrasonicator	B. Braun Biotech (Göttingen)
UPLC-MS, column	ACQUITY UPLC®, Ascentis® Express Peptide ES-C18 column (3×2.1 mm, 2.7 µm)	Waters (USA), Sigma (USA)

Software	Application	Source
ImageJ v.1.38	Image processing	Public domain (114)
CellQuest Pro™	Flow cytometry data acquisition	BD Biosciences
FCS Express V3	Flow cytometry data evaluation	De Novo Software
SigmaPlot12	Graph analysis	Systat Software GmbH
NITPIC	ITC data evaluation	Public domain (115)
Optima software (MARS)	Fluorescence spectroscopy	BMG Labtech
Decodon Delta 2D 4.1	2D-gel image analysis (proteomics)	Decodon

5.3 Peptide characterisation

5.3.1 Peptide synthesis

As reported previously, the parent peptide cWFW and the lysine-bearing analogues were prepared by multiple solid-phase synthesis using an Fmoc/tBu strategy according to SHEPPARD (70, 100, 116). Briefly, peptides were cleaved from the resin, followed by removal of protecting groups as described by Pearson, *et al.* (117) and manual cyclisation was achieved by HAPyU chemistry (118). Peptide purification and analysis were accomplished with high performance liquid chromatography (HPLC) on a Jasco LC-2000Plus (Japan) and Dionex UltiMate 3000 with ProntoSil 300-5-C18-H columns (250×4.6 mm, 5 μm) (Bischoff Chromatography, USA). Peptide mass was determined by UPLC-MS (ultra-performance liquid chromatography mass spectrometry) on an ACQUITY UPLC® System (Waters) using an Ascentis® Express Peptide ES-C18 column (3×2.1 mm, 2.7 μm) (Sigma-Aldrich). Final peptide purity was determined to be >95%.

The labelled peptide derivatives bearing the fluorescent groups 5(6)-carboxyfluorescein (Fluos), 3-N-(7-nitrobenz-2-oxa-1,3-diazole-4-yl)-2,3-diaminopropionic acid (Dap-NBD) and 7-methoxycoumarin (Cu) were purchased from Biosyntan GmbH, Berlin.

5.3.2 Bacterial growth conditions

E. coli and *B. subtilis* cells were inoculated from an overnight culture 1:100 and grown to mid-log phase (OD_{600} = 0.2-0.4) in the respective growth medium at 37 °C, 180 rpm in 100 ml conical flasks under aerobic conditions. Cultures from *B. subtilis* strains expressing fluorescent-labelled proteins were incubated for 30 minutes at 37 °C and transferred to 30 °C for the remaining cultivation.

Cell numbers were determined using a Petroff-Hausser counting chamber: OD_{600} = 1 corresponds to 2.8×10^8 CFU/ml *E. coli* and 8.8×10^7 CFU/ml *B. subtilis*.

Overnight cultures from L-form bacteria were diluted 1:10 and cultivated in BHI medium with the respective supplements, at 37 °C and vigorous shaking using flat bottom glass flasks. Cells were grown to late-log phase of OD_{550} ~0.8 and diluted for subsequent analysis to OD_{550} = 0.4.

Cell number was determined as described above: OD_{550} = 1 corresponds to 9.8×10^8 CFU/ml *E. coli* L-WF+ and 3.9×10^8 CFU/ml *B. subtilis* L-170.

5.3.3 Reversed-phase HPLC

5.3.3.1 Peptide hydrophobicity

Using reversed phase HPLC (high performance liquid chromatography) to detect the retention time t_R of the cyclic hexapeptides represent an efficient means to characterise the effective hydrophobicity of the molecules. The method is based on interaction of individual amino acid residues with the hydrophobic stationary phase of the HPLC column. Thus, increased retention times correlate directly with peptide hydrophobicity.

HPLC analysis was performed on a Jasco LC-2000Plus and a ProntoSil 300-5-C18-H column (250×4.6 mm, 5 µm). Peptide concentration was 1 mg/ml. The mobile phase A consisted of 0.1% TFA in deionised water, phase B was 0.1% TFA in 80% acetonitrile in deionised water. A linear gradient of 5% - 95% phase B was applied over 40 minutes, 22 °C for chromatographic analyses.

5.3.3.2 Cellular peptide uptake

In earlier studies, the cytoplasmic membrane of bacteria has been identified as the target of cWFW (101, 119). To investigate potential peptide uptake we used cell wall-deficient L-form strains derived from *E. coli* (LWF+) and *B. subtilis* (L-170) in order to reduce unknown interactions with the peptidoglycan layer and outer membrane components. The method is based on the irreversible chemical modification of extracellular peptides after addition of o-nitroaniline (Figure 10). As this highly reactive compound cannot cross cellular membranes, intracellular peptide moieties will not be modified. This allows for subsequent separation and quantification of modified and unmodified peptide moieties by HPLC according to their different retention behaviour at the hydrophobic column. The approach was originally developed by Oehlke, *et al.* (120) for the investigation of peptide uptake into eukaryotic cells. As the high reactivity of o-nitroaniline is restricted to free amino groups, the lysine-substituted hexapeptide cR2[NBD] was used which, in combination with NBD, allowed for fluorescence-based HPLC detection of peptide uptake into the cytoplasm.

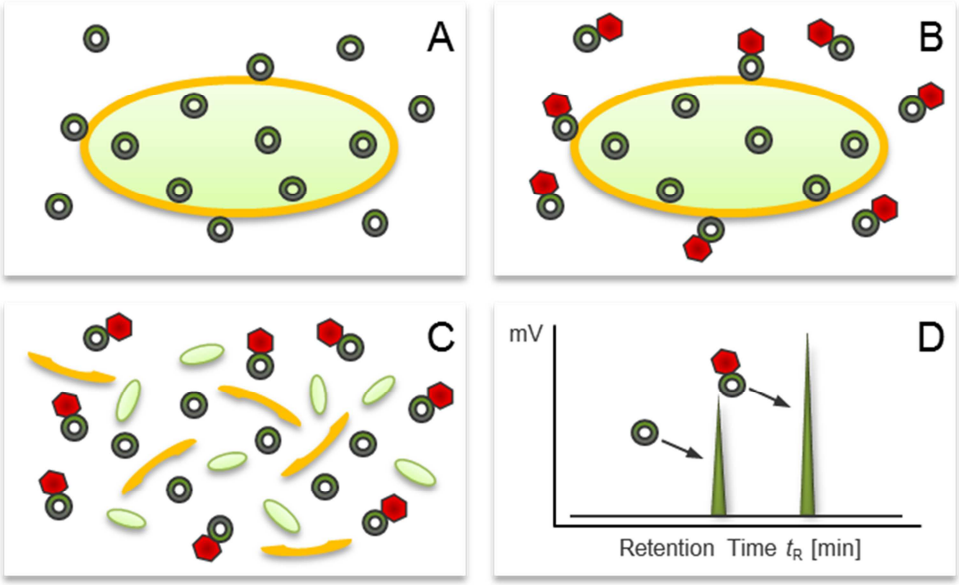

Figure 10 Investigation of cellular peptide uptake by HPLC. Schematic representation of the experimental procedure: (A) Cells are incubated with the peptide at the MIC; (B) addition of o-nitroaniline modifies all external and surface-bound peptides; (C) Peptides are separated from cell debris after cell fractionation; (D) Subsequent analysis with HPLC allows for quantification of modified (external) and unmodified (internal) peptide species.

L-form bacteria were cultivated to an OD_{550} ~0.8 in conical flasks as described above. Cells were harvested at 2000×g (Sigma 3K12) for 12 minutes and washed twice with DPBSG. 10^9 cells/ml phosphate buffer were incubated with 24 µM (24 nmol) Fluosbuforin II and cR2[NBD], respectively, for 30 min, 37 °C under gentle shaking (Eppendorf Thermomixer® comfort). After subsequent centrifugation at 1500×g, 4 minutes, 1°C (Biofuge® primo R, Heraeus®, Germany), the supernatant containing the peptide solution was removed and cells were washed twice with 0.5 ml ice-cold DPBS. 10 µl freshly diazotized o-nitroaniline solution was added to 0.5 ml cells in ice-cold DPBS and incubated for 10 minutes in an ice bath to modify cell surface-exposed peptide molecules. (Diazotized o-nitroaniline solution was prepared as follows: 35 mg o-nitroaniline were dissolved in 2 ml ethanol, followed by addition of 1 ml 0.25 M HCl. Meanwhile, 40 mg $NaNO_2$ were dissolved in 1 ml H_2O. The diazotized reagent solution was prepared by incubation of 400 µl o-nitroaniline solution with 50 µl $NaNO_2$ solution for 5 minutes at room temperature.) Cells were washed twice with ice-cold DPBS. Pellets were lysed with 0.5 ml 0.1% Triton X-100 (dissolved in 0.1% TFA) and stored at -20 °C until further HPLC analysis. To determine the total amount of cell-accumulated peptides, control samples were prepared under identical conditions, however, without o-nitroaniline treatment. Prior to HPLC analysis cell lysates were thawed to room temperature. The average protein content was determined with ~40 µg/10^9 cells using the BCA™ Protein Assay Kit (Thermo Scientific). Three independent experiments were performed in triplicates.

HPLC analysis was performed on a Jasco LC-2000 Plus using a ProntoSil 300-5-C18-H column (250×4.6 mm, 5 µm) and a precolumn with PolyenCap A300, 10 µm (119). Calibration curves for carboxyfluorescein (ex 445 nm, em 520 nm, gain 1000) and NBD fluorescence (ex 470 nm, em 520 nm, gain 1000) were recorded to enable quantification of the labelled peptides.

5.3.4 CD spectroscopy

The conformation of the cyclic hexapeptide was assessed using circular dichroism (CD) spectroscopy. This method is based on the differential absorption of left-handed and right-handed circular polarised light by optically active molecules (121). Analysis of CD signals in the UV range allows for the detection of structure elements in proteins and peptides, such as α-helices, β-turns and random coils, which are determined by the absorption of chiral C-atoms in peptide bonds of the molecule backbone. Furthermore, it provides information about aromatic systems within the molecule. The difference between the molecular absorption coefficients for left- and right-handed circular polarised light is described by the ellipticity (Θ) which is recorded as a function of wavelength in the CD spectrum.

For structure analysis in aqueous solution, 100 µM cyclic hexapeptides were dissolved in phosphate buffer (10 mM NaH_2PO_4/Na_2HPO_4, 154 mM NaF, pH 7.4). For investigation in membrane-mimicking environments, final concentrations of 25 mM SDS or 10 mM POPG SUVs (small unilamellar vesicles) were added to the peptide solution (see 5.5.2 for liposome preparation). CD spectroscopy was performed on a Jasco 720 spectrometer. Twenty scans were accumulated within the range of 260 and 190 nm using a 2 mm pathlength quartz cell. CD signals are presented as mean residue molar ellipticity Θ_{mr}. In the case of measurements with POPG SUVs, spectra were only recorded down to 205 nm due to light scattering of the liposomes.

5.3.5 Fluorescence absorption

In order to investigate the fluorescent properties of the chromophores coumarin and NBD, absorption spectra were recorded for the different hexapeptide derivatives. The emission spectra of coumarin (ex 328 nm) and NBD (ex 470 nm) were monitored between 340-500 nm and 480-600 nm, respectively, using a fluorescence spectrometer LS-50B (Perkin Elmer). Peptide concentration was 100 µM in DPBSG.

5.3.6 Antimicrobial activity

The antimicrobial activity of a substance can be assessed by determination of the minimal inhibitory concentration (MIC) which is defined as the lowest concentration able to inhibit growth of a microorganism *in vitro* (12). To investigate the antimicrobial activity of the cyclic hexapeptides we applied a microdilution technique in 96 well microtiter plates as described before (122). Bacteria were grown to mid-log phase and diluted in growth medium to give a final cell number of 5×10^5 cells/well. L-form bacteria were used at OD = 0.4/well, as lower cell densities were observed to exhibit a non-exponential growth behaviour. Small volumes of peptide solutions were added in a serial dilution ranging from 100 to 0.05 µM. Cells were cultivated for 18 hours, 37 °C, 180 rpm, followed by photometrical detection of the optical density using a microplate reader (Tecan). Peptide concentrations were tested in triplicates in three independent experiments.

5.3.7 Haemolysis

The haemolytic activity of the cyclic hexapeptides was determined with fresh erythrocytes from a human blood donation (Charité, Berlin). 2 ml cells were washed five times in Tris buffer (10 mM Tris, 150 mM NaCl, pH 7.4) at 4 °C, 2000×g, 5 minutes resulting in a clear supernatant. Cells were adjusted to 2.5×10^8 cells/ml and incubated with the peptide solutions at a final concentration of 100 µM in Tris buffer: 5 minutes on ice, 30 minutes at 37 °C, 5 minutes on ice. To give 100% haemoglobin release ($A_{100\%}$) 200 µl of the cell suspension were mixed with 2.3 ml NH_4OH to induce cell lysis. Haemoglobin absorption was detected at 540 nm in duplicates (in three biological repeats). Peptide-induced haemolysis ($A_{Peptide}$) was determined after centrifugation of the remaining cell suspension and mixing 200 µl of the supernatant with 2.3 ml NH_4OH. Cell suspensions without peptide incubation served as negative control ($A_{0\%}$). The following equation was used to calculate the haemoglobin release (R) from erythrocytes:

$$R\,[\%] = 100 \times \frac{A_{Peptide} - A_{0\%}}{A_{100\%} - A_{0\%}} \qquad \textbf{(Equation 1)}$$

5.3.8 Cytotoxicity

In order to investigate the specificity of the cyclic hexapeptides for bacteria species, we determined the viability of eukaryotic HeLa cells in the presence of different peptide concentrations. Cytotoxicity testing was performed with the well-established MTT-assay which allows for quantification of actively metabolising cells (123, 124). In contrast to descriptions found in the early literature, the exact molecular mechanism of the MTT reduction remains to be elucidated (125). However, it was reported that in the presence of cellular NADH and similar reducing molecules, the water-soluble MTT is converted to an insoluble formazan salt. Solubilisation of the precipitated salt is accompanied by a colour change from yellow to violet which can be detected photometrically.

HeLa cells were cultivated in DMEM and transferred to 96 well microtiter plates at 5×10^5 cells/well 24 hours before viability testing. Cells were incubated for 1 hour with different peptide concentrations solved in 200 µl DPBSG. Peptide solutions were removed and HeLa cells were incubated with 20 µl MTT reagent (5mg/ml) in 200 µl DMEM for 2 hours, 37 °C. After removal of the MTT solution, 100 µl DMSO were added to each well to dissolve the generated formazan and absorption was measured at 550 nm. Control cells without peptide incubation served as control for 100% viability.

5.4 Fluorescence microscopy

Confocal laser scanning microscopy (CLSM) was applied for fluorescence analysis. Obtained images were processed with ImageJ v.1.38. Data evaluation was achieved manually on the basis of at least three independent experiments performed in duplicates.

5.4.1 Peptide translocation

Bacteria from an overnight culture were diluted 1:100 in fresh medium and grown to mid-log phase. LB-agarose pads were prepared by adding 1.5% agarose to LB medium and heated until the agarose was completely dissolved. The solution was slightly cooled down before peptides were added at a final concentration of 12 µM. 100 µl LB-agarose were applied in a thin layer on a cover slip and stored at 8 °C in the dark for ~30 minutes. For fluorescence imaging, the agarose layer was lifted carefully and placed to cover 10 µl cell culture (OD_{600} 0.4). Live cell imaging was performed for up to 100 minutes in a heat controlled chamber to avoid desiccation using a CLSM 510 ConfoCor2 (plan-apochromat ×63, ×100/1.4 oil objective).

5.4.2 Cardiolipin staining

Specific staining of cardiolipin with NAO has been reported before and is neither influenced by fixation nor depolarisation of the membrane (126, 127). The dye also interacts with other anionic lipids. However, an emission shift from green to red fluorescence (525 to 640 nm) is only observed after binding of NAO to the cardiolipin head group which is suggested to be caused by narrower stacking of dye molecules.

B. subtilis 168 was grown to mid-log phase and adjusted to OD_{600} 0.2. Cells were incubated with 500 nM NAO for 60 minutes in the dark, at room temperature and 600 rpm to ensure sufficient aeration. Afterwards, cWFW was added at a final concentration of 12 µM and co-incubated with the dye for another 30 minutes under the same conditions. Images were captured using a Zeiss Axiovert M200 inverted fluorescence microscope (Zeiss plan-Neofluar ×100/1.30 oil ph3 objective).

5.4.3 Phase separation

Peptide-induced separation of lipid domains in the bacterial membrane was visualised with the membrane dye Nile Red. The hydrophobic dye emits almost no fluorescence in polar solvents. However, upon integration into phospholipid bilayers Nile Red fluorescence is strongly increased (ex/em ~552/636 nm). The fluorescence intensity is considered to be independent of the interaction with certain lipid head groups but is affected by the degree of membrane fluidity (108, 128).

B. subtilis 168 wild type cells were grown at 37 °C to mid-log phase and adjusted to OD 0.2 in growth medium. cWFW was added at a final concentration of 12 µM and incubated with the cells for 30 minutes, 37 °C, shaking. Meanwhile microscope slides were covered with a thin layer of 1.2% agarose in H_2O and stored at 8 °C (adjusted to room temperature prior to use). Immediately before imaging, 2 µl Nile Red (1 µg/ml) were added to the cells and fluorescence microscopy was performed using Zeiss Axiovert M200 (Zeiss Plan-Neofluar ×100/1.30 oil ph3objective).

5.4.4 Protein localisation

Peptide-induced delocalisation of membrane-associated proteins was investigated with *B. subtilis* strains expressing fluorescent fusion-proteins. Cells were cultivated at 30 °C to mid-log phase and protein expression was induced with respective supplements (see page 31). Cells were adjusted to OD 0.2 (200 µl) in 2 ml Eppendorf tubes in growth medium and incubated with 12 µM cWFW for 30 minutes at 30 °C, shaking. Analogous to investigations on phase separation, 0.5 µl cells were fixed on freshly prepared 1.2% agarose microscope slides and imaged immediately using a Nikon Eclipse Ti (Nikon Plan Fluor ×100/1.30 oil ph3 DLL objective). GFP/YFP fluorescence was detected at 525 nm.

5.5 Peptide-membrane interaction

5.5.1 Membrane permeabilisation (FACS)

Peptide-induced permeabilisation of the bacterial membrane was investigated with flow cytometry. This technology enables sorting of different cell populations with regard to various biophysical parameters, such as size, morphology and fluorescent properties. To quantify disruption of the lipid bilayer, propidium iodide (PI) has been widely employed in antibiotic-related studies on membrane condition (129-131). The small fluorescent dye intercalates into nucleic acids which results in an emission blue-shift of ~15 nm accompanied with a strong increase in fluorescence intensity. As the dye is membrane impermeable, it is excluded from vital cells. Hence, fluorescence detection is only possible in those cells with disintegrated membranes.

Cells were grown to mid-log phase, adjusted to 5×10^5 cells/ml in growth medium and mixed with 10 µg/ml PI. Peptides were added at respective MICs and PI fluorescence was monitored at different time points over 90 minutes. In between sample acquisition, cell suspensions were kept at 37 °C, shaking, in the dark. Cell sorting was performed on a FACSCalibur™ flow cytometer (Becton-Dickinson) equipped with a 488 nm argon laser and PI fluorescence was detected with a 585/42 nm band-pass filter (channel F2). All detectors were used with logarithmic amplification. At least 10.000 events were recorded per sample. Data were acquired and evaluated with BD CellQuest Pro™ (BD Biosciences) and FCS Express 3 (De Novo Software), respectively.

5.5.2 Liposome preparation

Small unilamellar vesicles (SUVs) were used to determine peptide conformation in membrane-mimicking environments with CD spectroscopy. Dried POPG lipids were resuspended in phosphate buffer (containing 154 mM NaF as used for subsequent CD analysis) by thorough vortexing at a final concentration of 20-40 mM. Lipid suspensions were sonicated under nitrogen on ice for 20 minutes using a titanium tip ultrasonicator (Labsonic L ultrasonicator). Formed titanium debris was removed by

centrifugation. Vesicle size was determined with differential light scattering (DLS) and confirmed the existence of a main population (> 95%) with a mean diameter of 30 nm.

Large unilamellar vesicles (LUVs) were prepared for peptide analysis with isothermal titration calorimetry (ITC). Lipids were dissolved in chloroform to obtain the desired molar ratios (POPE/CL and POPC/CL at 87.5/12.5%, POPC/POPG and POPE/POPG at 75/25%). To generate liposomes with identical surface charge, cardiolipin, which potentially carries two negative charges, was applied at half POPG concentrations (132). In order to obtain dried lipid films, the solvent was evaporated under nitrogen and lipid samples were exposed to high vacuum overnight. Subsequent resuspension of the lipids in phosphate buffer was facilitated by warming the solution to 40 °C for 2-3 times and thorough vortexing. For preparation of POPE and POPC LUVs, lipid solutions were extruded 35-fold through two stacked polycarbonate membranes with 100 nm pore size using a mini extruder (Avestin). Vesicles with a diameter of 90-120 nm were produced as determined with dynamic light scattering (DLS).

The lipid concentration of liposomes from *E. coli* extract was determined by gravimetric analysis from dried lipid films which were then resuspended in phosphate buffer and sonicated under nitrogen on ice for 25 minutes. Titanium debris from the tip was removed by centrifugation. The diameter of *E. coli* extract LUVs was 90 nm as determined with DLS.

5.5.3 Isothermal titration calorimetry (ITC)

To investigate peptide binding to different phospholipids of bacterial membranes we performed high-sensitivity isothermal titration calorimetry (ITC) using model bilayer systems. The thermodynamic characterisation of peptide-lipid interactions provides useful information on specific binding parameters, such as the hydrophobic partition coefficient (K_0), enthalpy ($\Delta H°$) and entropy changes ($-T\Delta S°$) (133).

Biological and chemical reactions are accompanied by changes in enthalpy where heat is either released (exothermic) or taken up (endothermic) from the environment. A titration calorimeter consists of two heated cells, for reference and sample analysis,

respectively, which are maintained at identical temperatures. Using a syringe, small volumes of the binding partner (i.e. lipids) are added step-wise to the sample solution (containing the peptide). This leads to changes in the heat of the system and results in a temperature difference compared to the reference cell. In order to keep both cells at a constant temperature the electrical power of the system is adjusted. The differential heating power necessary to compensate for this difference is monitored over time. The area under the curve is integrated and plotted as function of increasing lipid/peptide ratios which allows for calculation of the binding parameters.

To consider electrostatic interactions between peptides and liposomes in the calculation of the partition coefficient K_0, a surface partition model in combination with the Gouy-Chapman theory was applied as described before by Keller, *et al.* (134). Simulations were based on the assumption that peptide adsorption is related in a linear way to the peptide concentration immediately above the membrane surface. This concentration depends on the bulk concentration of peptide, peptide charge and membrane surface potential. As the cationic peptides are attracted by the negatively charged lipid head groups, peptide concentration at the surface will be higher than in the surrounding solution. In contrast, peptide absorption to neutral lipid bilayers will increase the positive charge of the membrane and result in electrostatic repulsion of further peptide molecules.

Further thermodynamic description of the interaction between peptides and model membrane systems was derived from calculation of the Gibbs free energy $\Delta G°$:

$$\Delta G° = -RT \ln(55.5\ \mathrm{M} \times K_0) \qquad \textbf{(Equation 2)},$$

where 55.5 M is the molar concentration of water in the aqueous phase. The entropic contribution ($-T\Delta S°$) of peptide partitioning into lipid bilayers, was further obtained applying the Gibbs-Helmholtz equation:

$$\Delta G° = \Delta H° - T\Delta S° \qquad \textbf{(Equation 3)}$$

ITC experiments were carried out at 25 °C on a VP-ITC instrument (MicroCal). Prior to use, peptide and buffer solutions were gently degassed under vacuum. 10 µl aliquots of 5 to 10 mM lipid vesicles were titrated into a 40 µM peptide solution inside the calorimeter cell (1.4 ml) under continuous stirring at 307 rpm. To allow for the heat signal to return to baseline level, time intervals between injections were adjusted to 10 minutes. Automated baseline adjustment and peak integration were accomplished with the public domain software NITPIC (115). Nonlinear least-squares data fitting was performed with Excel 2010 (Microsoft) using the Solver add-in (Frontline Systems) (135). Results obtained from titration of lipid vesicles into buffer solution without peptides served as control. Experiments were performed in three independent repeats.

5.5.4 Membrane depolarisation

Peptide-induced changes in membrane potential were measured using the small potential sensitive fluorophore $DiSC_3(5)$. In aqueous solution the dye emits strong fluorescence (ex/em ~544/660) which is quenched upon integration into hydrophobic lipid bilayers. When the membrane becomes depolarised, $DiSC_3(5)$ is released from the bilayer which results in an emission increase. The fluorescence intensity directly correlates with membrane potential which allows for detection of peptide-induced depolarisation.

B. subtilis 168 was grown at 37 °C to mid-log phase and diluted in LB medium to OD_{600} 0.2. After centrifugation for 1 minute, 16.500 rpm in conical tubes (Eppendorf MiniSpin®), the supernatant was removed and cells carefully resuspended in 1 ml pre-warmed LB containing 0.1 mg/ml BSA. Subsequently, 140 µl of the cell suspension were transferred into a 96 well microtiter plate and allowed to settle. Then, 10 µl of 15 µM $DiSC_3(5)$ in LB/15% DMSO were quickly added to the wells to give a final $DiSC_3(5)$ concentration of 1 µM. Incorporation of $DiSC_3(5)$ into the membrane was reflected by fluorescence quenching and followed until the signal had returned to base line level (Fluostar Optima, BMG Labtech). The peptide was added at desired concentrations at 5 µl/well and changes in $DiSC_3(5)$ fluorescence were monitored for at least 20 minutes. Solutions, plates and instruments were warmed to 37 °C prior to use.

5.5.5 Determination of cellular ATP

ATP is produced by metabolically active cells and reduction of the intracellular ATP concentration accounts for deficiencies in energy metabolism. The BacTiter-Glo™ Microbial Cell Viability Assay Kit (Promega) was used to investigate the influence of the antimicrobial peptide on bacterial ATP production. The method is based on the enzymatic conversion of luciferin to oxyluciferin which is accompanied by luminescence emission that can be detected photometrically (Figure 11). The reaction is catalysed by a thermostable luciferase from firefly which requires Mg^{2+}, ATP and molecular oxygen as cofactors. The intensity of the luminescence signal is directly proportional to the ATP molecules used which enables quantification of the intracellular ATP amount.

B. subtilis DSM 347 cells were grown to mid-log phase and diluted in growth medium to 5×10^5 cells/150 µl in a 96 well microtiter plate. 50 µl peptide solutions were added at desired concentrations and incubated with the cells for 30 minutes at 37 °C. Subsequently, the cell suspensions were mixed 1:1 with BacTiter-Glo™ reagent provided with the kit and incubated for 5 minutes in the dark. Luminescence detection was performed in opaque microtiter plates using a Safire^2 plate reader (Tecan). According to manufacturer's instructions an ATP standard curve was generated to allow for quantification of bacterial ATP.

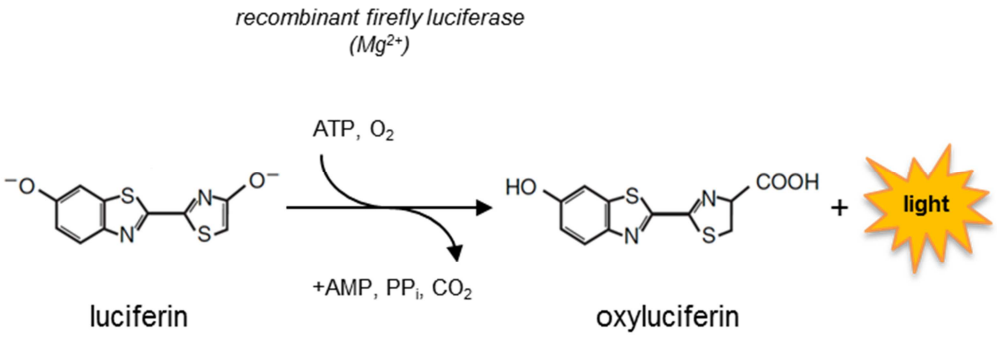

Figure 11 Chemical reaction catalysed by luciferase. Conversion of luciferin to oxyluciferin in the presence of ATP and molecular oxygen leads to elimination of carbon dioxide under luminescence development (modified from: BacTiter-Glo™ Microbial Cell Viability Assay, technical bulletin, revised 12/12).

5.5.6 Membrane fluidity

For investigations on bacterial membrane fluidity Laurdan generalised polarisation (GP) measurements were applied. The small hydrophobic probe integrates into cellular membranes and is used to detect changes related to the lipid packing in the bilayer (136, 137). Depending on the polarity of the environment, Laurdan interaction with surrounding water molecules results in a fluorescence shift which can be detected spectroscopically or with fluorescence microscopy (Figure 12).

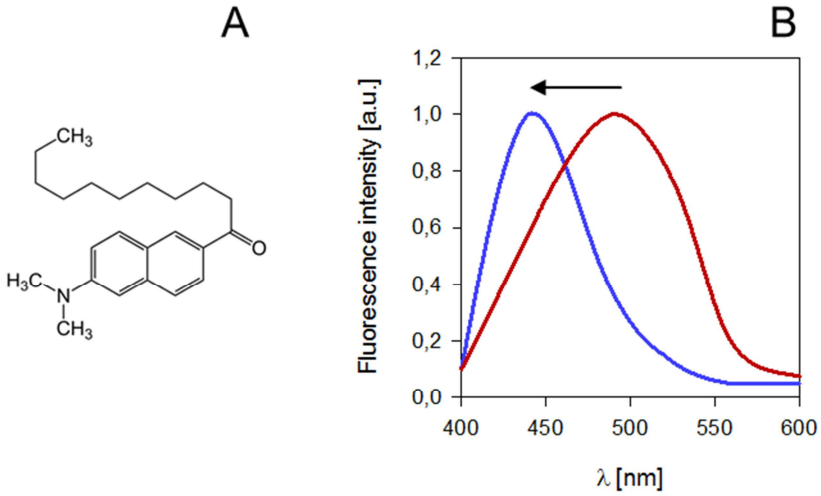

Figure 12 Properties of Laurdan. (A) Chemical structure of Laurdan (6-dodecanoyl-2-dimethylaminonaphthalene); (B) Schematic representation of the fluorescence blue-shift induced upon reduced polarity of the environment (modified from Sanchez et al. 2012 (137)).

Within a phospholipid bilayer the emission maximum is located at 490 nm when the lipids are in a disordered phase and is blue-shifted to ~ 440 nm upon tighter lipid packing. A mathematical quantification of the emission shift is achieved by calculation of the Laurdan GP (generalised polarisation) (Equation 4).

$$\mathrm{GP} = (I_{435} - I_{490})/(I_{435} + I_{490}) \qquad \textbf{(Equation 4)}$$

B. subtilis 168 cells were grown to OD_{600} ~0.5 at 37 °C in LB/0.1% glucose and incubated with 10 µM Laurdan for 5 minutes, shaking in the dark. Subsequently, cells were washed 4 times, 1 minute, 16.500 rpm in PBS/0.1% glucose and triplicates of 150 µl cell suspension were transferred to a 96 well microtiter plate. The peptide was added at the desired final concentration at a maximum volume of 3 µl/well. The supernatant which was removed from the cells after the last washing step served as background for Laurdan fluorescence. The solvent benzyl alcohol (BA) has a fluidising effect on lipid bilayers and was used as positive control (50 mM). All samples were shaken briefly before fluorescence was detected simultaneously at 435±5 nm and 490±5 nm with excitation at 350±10 nm using a plate reader (Fluostar Optima, BMG Labtech). Laurdan fluorescence was monitored for at least 20 minutes. Peptide influence on membrane fluidity was investigated in three independent experiments.

Further studies of peptide-induced changes in membrane fluidity were performed using a *B. subtilis* mutant strain which is deficient in membrane lipid synthesis. Branched chain fatty acids (BCFAs) are the main constituents in the *B. subtilis* membrane and were reported to be essential for bacterial growth (138). They are built from three different precursor molecules: isobutyrate (IB), isovalerate (IV) and 2-methylbutyrate (MB) which in turn are synthesised from the branched amino acids valine, leucine and isoleucine, respectively (Figure 13). The constructed mutation, termed Δ*bkd*, leads to the disruption of the enzyme complex BCKAD which catalyses the synthesis of the BCFA precursors (113). The resulting phenotype was observed to be lethal. However, supplementation of the growth medium with IV, IB or MB reconstitutes cell viability. Based on the chemical structure of the precursors, only distinct fatty acid chains can be synthesised which differ in length and position of branching (Figure 13). This is used to artificially influence the membrane fluidity of the mutant bacteria by selective addition of either one precursor or a mixture.

B. subtilis Δ*bkd* cells were cultivated at 37 °C in supplemented minimal medium with addition of the desired BCFA precursor at a final concentration of 100 µM. Subsequent analysis of membrane fluidity was performed according to Laurdan GP measurement described above.

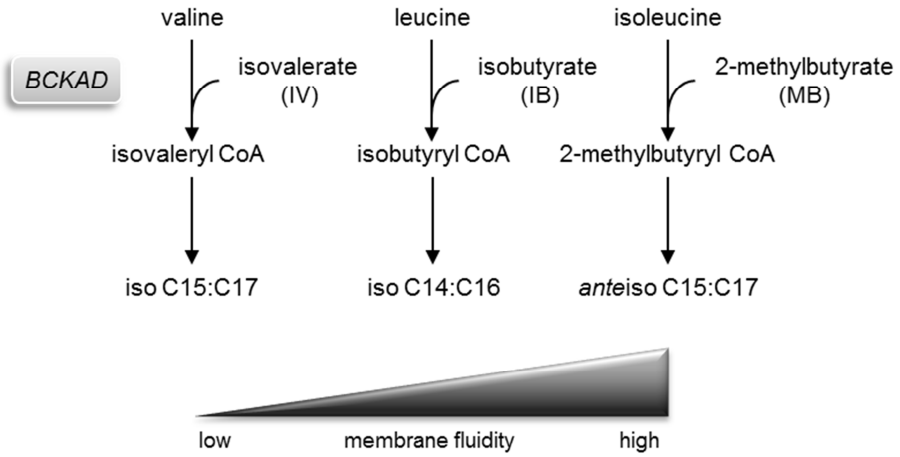

Figure 13 Branched chain fatty acid (BCFA) synthesis in *B. subtilis*. Schematic representation of the BCFA synthesis pathway. Membrane fluidity can be deduced from the fatty acid type synthesised from the precursors isovalerate (IV), isobutyrate (IB) and 2-methylbutyrate (MB) (modified from Mercier et al., 2012 (113)).

5.6 Proteomic profiling

Proteomics related data were generated during a collaboration project with the group of Prof. Dr. Julia Bandow at the Ruhr University, Bochum (Germany). Experiments were performed by Dr. Michaela Wenzel. Publication of the results within the scope of the present study was approved by the collaboration partners.

Peptide-induced protein expression in *B. subtilis* cells was investigated using a proteomics-based approach. The protein induction pattern has been described to respond to a particular antibiotic treatment in a specific manner (139). Hence, with reference to known substances the obtained protein profiles can be correlated with distinct antimicrobial mechanisms of action.

In order to identify specific responder proteins, growing cells are stressed with an antibiotic agent. The subsequent incubation with radioactive amino acids results in selective labelling of newly synthesised proteins which can be further analysed with mass spectrometry (136).

B. subtilis 168 cells were grown in BMM at 37 °C to early log phase and treated for 15 minutes with 8 µM cWFW which was determined as MIC under the respective growth conditions. Subsequently, cells were pulse-labelled with L-[^{35}S]methionine for 5 minutes followed by preparation of the cytoplasmic protein fraction as described by Wenzel, *et al.* (140). For separation of the proteome two-dimensional polyacrylamide gel electrophoresis (2D-PAGE) was performed and gel images were analysed with Decodon Delta 2D 4.1 image analysis software (Decodon) (141). Proteins were excised from the gel and identified using MALDI/TOF (4800 MALDI TOF/TOF analyser; Applied Biosystems, USA) as reported before (129). Marker proteins were designated by at least two-fold induction upon peptide treatment. Experiments were performed in triplicates in three independent biological repeats.

6 Results

6.1 Peptide characterisation

6.1.1 Structure and activity

To get insight into the mechanism of antimicrobial action of cWFW, different methods were applied which required chemical modification of the cyclic hexapeptide. Potential translocation across the membrane was investigated with microscopy and HPLC. For this purpose, fluorescent reporter groups were introduced to facilitate real-time peptide imaging in live bacteria cells (Figure 14). The successful application of carboxyfluorescein (Fluos)-labelled peptides in uptake studies is well documented (142-144). It has been demonstrated before that substitution of phenylalanine with hydrophobic amino acids had only minor impact on the antimicrobial activity of cWFW (103). Therefore, the fluorophores coumarin (Cu) and nitrobenzoxadiazole (NBD) were chosen due to their hydrophobic nature and structural similarity to tryptophan and coupled at position 5 in the peptide ring (Figure 14).

The HPLC approach to investigate peptide uptake into the cytoplasm is based on covalent chemical modification of extracellular and surface-bound peptides with diazotized o-nitroaniline (145). This reaction is restricted to free amino groups. Hence, to be applicable for analysis of cWFW action, arginine residues were substituted with lysine at different positions in the peptide ring. An overview of the antimicrobial peptides synthesised for this study is given in Table 1. In order to test the applicability of the newly synthesised peptide derivatives as tools in further investigations, all molecules were characterised and compared to the parent peptide cWFW regarding structure, biophysical properties and biological activity.

Considering their antimicrobial effect, nearly all peptides were more active against Gram positive *B. subtilis* than Gram negative *E. coli* cells which is consistent with the activity profile described for this class of peptides (70, 71, 100). However, all modifications applied to cWFW led to a general reduction in biological activity (Table

1). By far the lowest antimicrobial activity was observed for the Fluos-labelled peptide derivatives cW_2[Fluos] and cW_3[Fluos]. Carboxyfluorescein was introduced via a lysine linker into the hydrophobic and polar domain, respectively, which leads to an overall loss in positive net charge compared to the parent peptide. Both, the bulky structure of the fluorophore as well as the change in hydrophobicity and amphipathicity might be responsible for the pronounced loss of antimicrobial activity to a level which was not observed for any of the other peptide derivatives. Also, coumarin and NBD, which were introduced in the middle of the hydrophobic cluster in an attempt to maintain the overall amphipathic character of the molecule, reduced the antimicrobial activity. Moreover, the haemolytic activity was increased (Table 1).

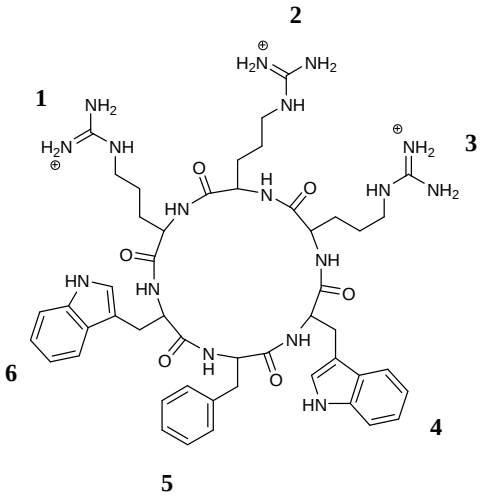

cWFW

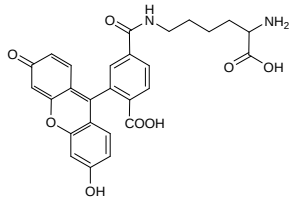

carboxyfluorescein
(lysine)

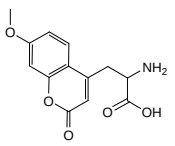

methoxycoumarin
(alanine)

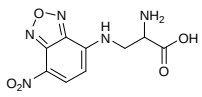

NBD
(diaminopropionic acid)

Figure 14 Chemical structures of the fluorescent reporter groups incorporated into cWFW. Fluorophores are represented coupled to the respective amino acid (given in brackets) used for introduction into the peptide ring.

Table 1 Cyclic hexapeptides derivatives and model peptides used in permeabilisation and translocation studies. The antimicrobial activity was determined as minimal inhibitory peptide concentration (MIC) where no bacterial growth is visible.

Peptide	Sequence	Activity (MIC) [µM]		Haemolysis at 100 µM [%]
		E. coli DH5α	*B. subtilis* DSM 347	
Parent peptide				
cWFW	c-RRRWFW	3	3	4
Fluorescence labelling				
cW_2[Fluos]	c-RRRWWK[Fluos]	>100	>100	9
cW_3[Fluos]	c-RRWWWK[Fluos]	>100	>100	2
cW[Cu]W	c-RRRW[Ala-Cu]W	25	6	23
cW[NBD]W	c-RRRW[Dap-NBD]W	50	25	76
Lysine substitution				
cRKR	c-RKRWFW	50	12	4
cRKK	c-RKKWFW	50	25	56
cKRK	c-KRKWFW	12	25	2
cKKR	c-KKRWFW	100	25	3
cKKK	c-KKKWFW	100	50	8
Fluorescence labelling/ lysine substitution				
cR2[Cu]	c-KRKW[Ala-Cu]W	50	6	4
cR2[NBD]	c-KRKW[Dap-NBD]W	50	12	26
Model peptides				
KLA-1	KLALKLALKAWKAALKLA-NH_2	1.5	1.5	n.d.
Polymyxin B (103)	cyclic decapeptide with variable acyl chain	0.8	6	n.d.
Fluos-buforin	Fluos-TRSSR AGLQF PVGRV HRLLR K-NH_2	50	50	n.d.
Fluos-penetratin	Fluos-RQIKI WFQNR RMKWK K-NH_2	25	3	n.d.

Cu-coumarin; Dap-diaminopropionic acid; Fluos-carboxyfluorescein; NBD-nitrobenzoxadiazole.

Most MIC values found for lysine substituted hexapeptides were slightly higher compared to the fluorescent labelled peptides (except Fluos-labelling). Here, the best antimicrobial activity was observed for cKRK suggesting that the arginine residue in the middle position of the cationic sequence motif is important for optimal peptide interaction with bacterial membranes.

The peptides cR2[Cu] and cR2[NBD] were synthesized to create a highly active lysine substituted fluorescent peptide based on cKRK. The introduction of both modifications led to similar antimicrobial activities and the undesired haemolytic effect was even reduced compared to single-modified fluorescent peptides (Table 1). Further investigations were focussed on elucidating the structural determinants for antimicrobial activity of the peptide analogues compared to cWFW (119).

6.1.2 Peptide hydrophobicity and conformation

The high antimicrobial activity of cWFW is based on the optimal distribution of polar and hydrophobic amino acid residues which renders this molecule extremely amphipathic. The cationic charge drives accumulation of the peptide at the negative surface of bacterial cells while the aromatic side chains facilitate interactions with the hydrophobic core of the lipid matrix (146).

In order to investigate the impact of fluorophore coupling and substitution of arginine for lysine on the hydrophobicity/amphipathicity of the cyclic hexapeptide, the retention time t_R was determined by reversed phase HPLC (Figure 15). t_R-measurements have successfully been applied to characterise amphipathic helices, β-structured peptides and different sets of small cyclic R-, W-rich peptides (50, 70, 146-148). Compounds are retained from the hydrophobic stationary phase according to their ability to form interactions with the HPLC matrix. Thus, differences in t_R reflect differences in the effective hydrophobicity of the molecule which is related to the intrinsic hydrophobicity of individual residues and their relative position. In amphipathic structures, polar and hydrophobic side chains align at opposite sides of the molecule. Hence, any change applied to the primary structure of the parent peptide is expected to influence its amphipathicity.

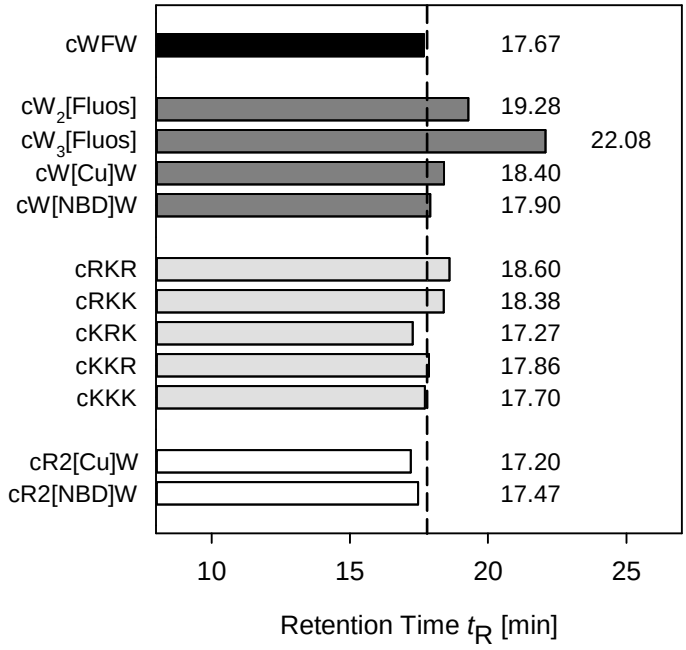

Figure 15 Retention times t_R of the cyclic hexapeptide derivatives. The impact of chemical modification on peptide hydrophobicity was determined with HPLC. Black: cWFW; dark grey: fluorescent labels; light grey: lysine substitution; white: double modifications.

Insertion of fluorophores into the peptide ring led to an increase in retention time (Figure 15). This can be related to an enlargement of the aromatic ring system compared to the phenylalanine side chain which leads to enhanced interaction with the stationary phase. The highest retention time was observed for the carboxyfluorescein-labelled peptides cW_2[Fluos] and cW_3[Fluos]. Moreover, in both cases fluorophore-coupling was accompanied with a loss in positive net charge. These changes impair the amphipathic nature of the molecule which is likely to account for the reduced antimicrobial activity (Table 1, Figure 15).

The retention time determined for lysine substituted peptides was dependent on the site of introduction. Although the hydrophobicity of lysine is reported to be slightly lower compared to arginine, cWFW and cKKK show basically identical t_R values (149). Also, the retention time determined for the other lysine-bearing peptides differed only

marginally from that of the parent structure cWFW. In all cases, interactions with the stationary phase of the column are determined by the same aromatic residues. Interestingly, cKRK, the only lysine-bearing peptide which showed pronounced antimicrobial activity, was found to have a retention time lower than that of the parent peptide. The strong impact of these particular lysine substitutions on the peptide's properties was also reflected in cR2[Cu] and cR2[NBD] which also showed lower retention times compared to cWFW. Apparently, the effective peptide hydrophobicity is rather affected by the side chains adjacent to the hydrophobic cluster and their contribution to peptide conformation than from the fluorophores in the middle position.

As the carboxyfluorescein-labelled peptides cW_2[Fluos] and cW_3[Fluos] did not show a significant antimicrobial activity compared to the parent peptide cWFW they were not considered suitable tools for translocation studies and excluded from all subsequent investigations. All other cyclic hexapeptide derivatives were further analysed regarding their conformation in different solvent systems using circular dichroism (CD) spectroscopy (Figure 16).

For the parent peptide cWFW dissolved in buffer a negative ellipticity minimum at 202 nm and a shoulder at 220 nm was observed (Figure 16A, solid line). The signal in the UV range next to 200 nm results from peptide bonds of the backbone while contributions of both, peptide bonds and aromatic side chains, superimpose in the 220-230 nm region. The spectrum of cWFW is comparable to that of cyclo-RRWWRF (cRW) which has been described in previous studies and is characterised by two β-turns in the backbone and rather flexible side chains (100, 150). The introduction of coumarin had only minor effects on the CD signal of the cyclic hexapeptide (Figure 16A, dotted line). However, the contribution of the NBD-fluorophore in cW[NBD]W and cR2[NBD] resulted in reduced negative ellipticity values (Figure 16A, short and long dashed lines). The intensity of the CD signal was decreased, however, ellipticity bands and shoulder positions were conserved which points to changes in backbone flexibility. Concerning the lysine substituted peptides, cKRK showed the strongest deviation from the cWFW spectrum. The high positive ellipticity below 200 nm is also related to pronounced changes in backbone conformation (Figure 16B) and might be decisive for the change in amphipathicity as reflected by the reduced retention time (see Figure 15).

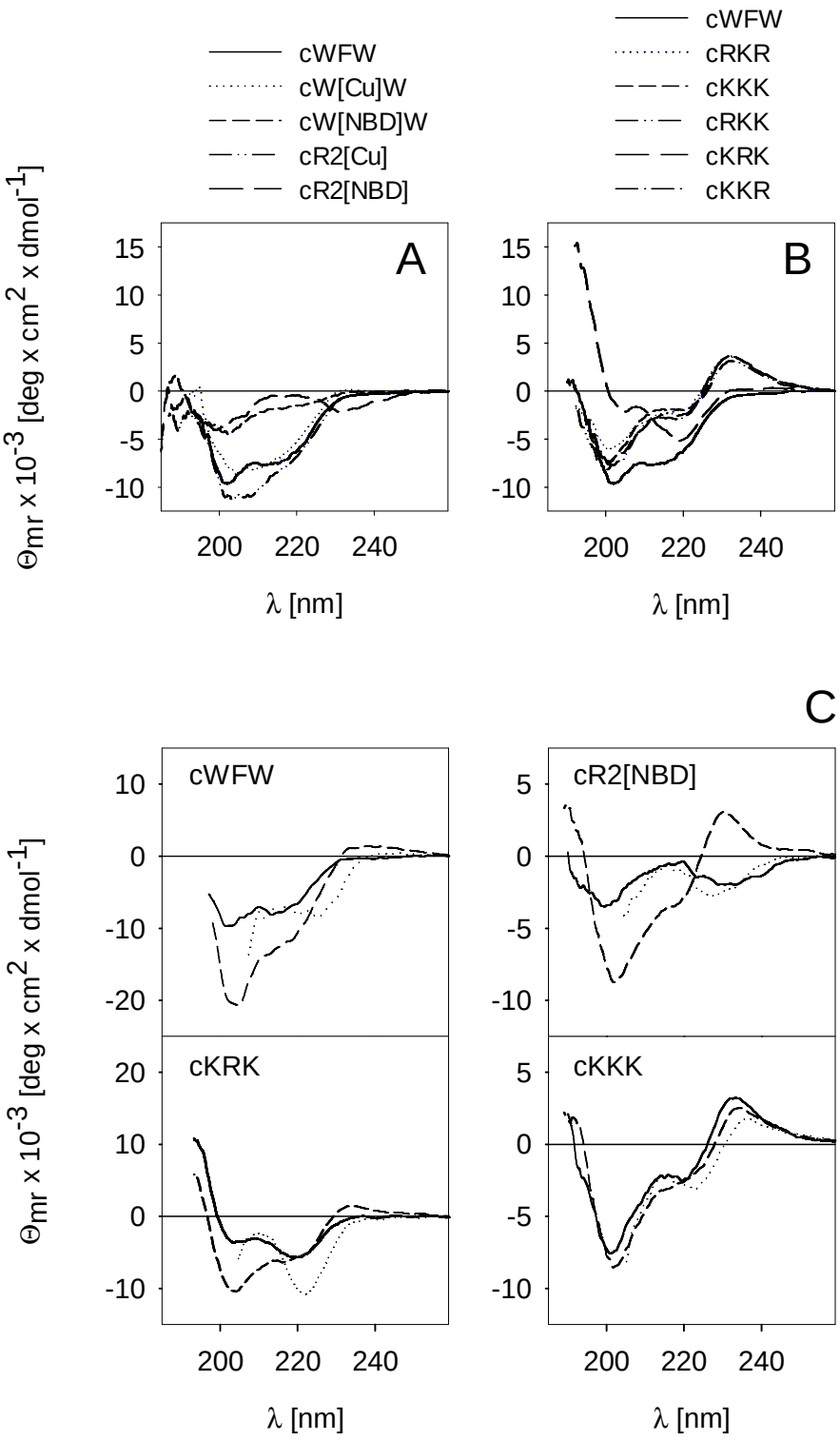

Figure 16 Effect of chemical modifications on peptide structure. CD spectra of fluorescent-labelled peptides (A) and lysine-substituted peptides (B) compared to cWFW in phosphate buffer. The effect of membrane-mimicking additives on the structure of selected lysine peptides is shown in (C): phosphate buffer (solid lines), 25 mM SDS (dashed lines) and 10 mM POPG-SUVs (dotted lines). Peptide concentration was 100 µM.

For all other K-peptides a positive ellipticity maximum at 230 nm could be observed with only minor spectral changes in the far UV wavelength range compared to cWFW.

To mimic the anisotropic nature of the lipid matrix of cell membranes, changes in peptide conformation were studied in the presence of detergent micelles and liposomes (Figure 16C). As reported before, the cyclic hexapeptide cWFW adopts an amphipathic structure with two β-turns when bound to micelles (102). The aromatic side chains point to the same direction establishing the hydrophobic part while the arginine residues are positioned to interact with the polar head groups on the micellar or liposomal surface. Partitioning of the antimicrobial peptide from the aqueous solution into SDS micelles and POPG liposomes led to an increase in ellipticity at 202 nm and a red shift of the shoulder from 220 nm to 225 nm. This indicates enhanced backbone rigidity and favourable changes in the orientation of the aromatic residues. The cyclic peptide derivatives presented in Figure 3C differ in their biological activity compared to the parent peptide cWFW (Table 1). Although the peptides showed variations in their spectra obtained in phosphate buffer (Figure 16A, B), very similar CD signals were observed when bound to membrane-mimicking POPG liposomes or SDS micelles (Figure 16, dotted and dashed lines, respectively). This indicates the high potential of the cyclic peptides to adopt amphipathic structures in interaction with the lipid matrix of bacterial membranes.

6.1.3 Fluorescence properties

The peptide derivatives were further analysed regarding the fluorescent properties of coumarin and NBD (Figure 17). The emission maximum of the two coumarin-bearing peptides was found at 400 nm and 520 nm in the case of both NBD-peptide analogues. This indicates that introduction of the two lysine residues in cR2[Cu] and cR2[NBD] did not shift the spectrum of the chromophores. However, we observed differences in fluorescence intensity which accounts for the strong environment sensitivity reported for both fluorophores (151, 152).

In general, the choice of these fluorophores bears potential disadvantages. While NBD was found to exhibit very low quantum yields, the excitation of coumarin in the UV range might interfere with the intrinsic cellular fluorescence. Hence, the selection of the most suitable peptide derivative for subsequent translocation studies was based on the property to retain the non-permeabilising mechanism of action of the parent peptide cWFW.

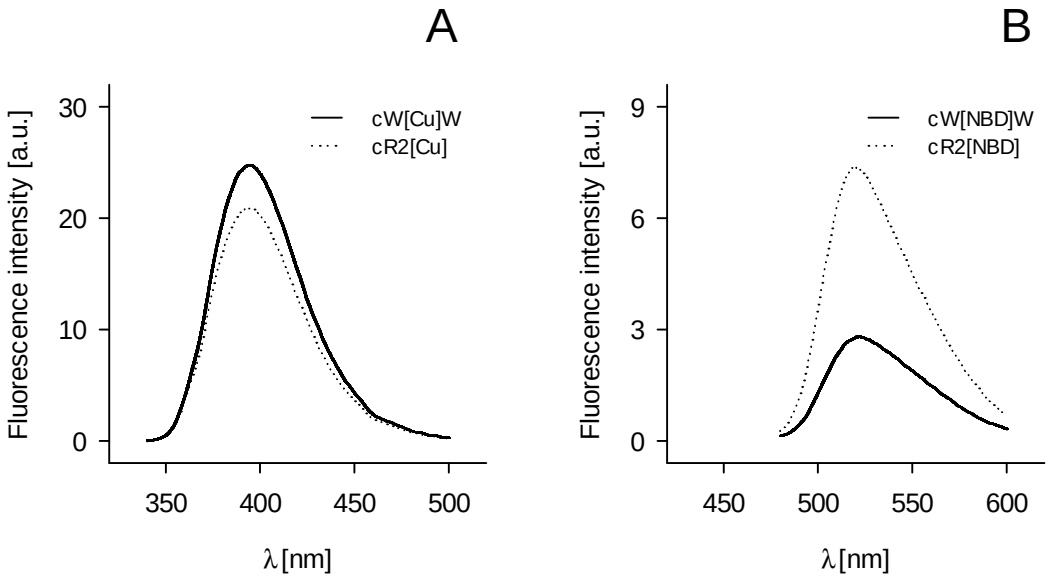

Figure 17 Fluorescence spectra of cyclic hexapeptide derivatives. (A) Coumarin and (B) NBD fluorophores were excited at 328 nm and 470 nm, respectively, as determined with absorption measurement (data not shown). Spectra were recorded in DPBSG, peptide concentration was 100 µM.

6.2 Mechanism of antimicrobial action

6.2.1 Membrane permeabilisation

Among the different mechanism of action described for antimicrobial peptides, membrane permeabilisation is the most common way of killing. Interaction with and integration into bacterial membranes is facilitated by the peptides' high amphipathicity. Although cWFW fulfils all the structural prerequisites it was demonstrated before that the antimicrobial action of the cyclic hexapeptide is not based on membrane permeabilisation (71, 119).

Application of the newly synthesized peptide derivatives in further studies requires a high degree of congruence with cWFW properties. Therefore, the coumarin- and NBD-labelled peptides based on cWFW and cKRK, respectively, were tested regarding the potential to retain the non-permeabilising mechanism of action (Figure 18).

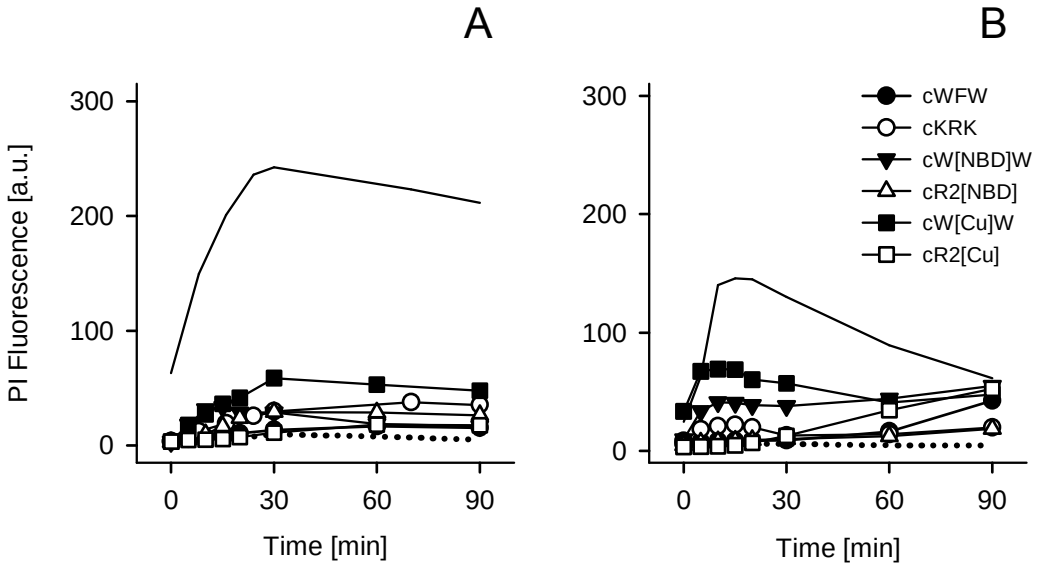

Figure 18 Bacterial membrane permeabilisation determined with propidium iodide (PI). PI fluorescence was measured after treatment with cyclic hexapeptide derivatives in *B. subtilis* DSM 347 (A) and *E. coli* DH5α (B). Peptide concentrations correspond to MICs (see Table 1). The helical model peptide KLA-1 (5 µM) and the antibiotic polymyxin B (5 µM) were reported to exhibit a high membrane permeabilising potential and served as positive control in Gram positive and Gram negative cells, respectively (solid lines) (144, 153). Preparations without peptide were used as negative control (dotted lines).

Disintegration of the cytoplasmic membrane leads to influx of propidium iodide (PI) and binding to DNA. Subsequent increase in PI fluorescence was detected with flow cytometry and could be observed for the control peptides polymyxin B and KLA-1 confirming strong membrane permeabilisation in *E. coli* and *B. subtilis*, respectively. (147, 154). However, PI signals detected for the newly synthesised hexapeptide derivatives were comparably low. Although slightly elevated values were found within 30 minutes treatment with cW[Cu]W and cW[NBD]W, lysine substituted peptides induced PI fluorescence similar to the parent peptide cWFW (Figure 5). Furthermore, PI signals in cells treated with the hexapeptide derivatives did not significantly change over time which would account for a non-lytic killing mechanism. Although the changes applied to cWFW had an impact on peptide properties, the derivatives, like the parent peptide, did not permeabilise the bacterial membrane. The derivatives cW[NBD]W and cR2[NBD] were considered reliable tools for the application in subsequent translocation studies since the integrity of the cytoplasmic membrane, especially in *B. subtilis*, appeared to be unaffected (119).

6.2.2 Peptide translocation into the cytoplasm

As membrane permeabilisation could be ruled out as mechanism of action of the antimicrobial peptide cWFW, further investigations focussed on potential peptide translocation into the cytoplasm, where it might interfere with protein synthesis and DNA replication (39). To circumvent the mild membrane permeabilising effect observed for in cW[NBD]W *E. coli* cells, the peptide was applied at sub-MIC concentrations.

6.2.2.1 Peptide localisation with fluorescence microscopy

In order to identify the target location of the antimicrobial peptide, live *E. coli* and *B. subtilis* cells were incubated with cW[NBD] (Figure 19). The peptide buforin II served as positive control for peptide uptake into the cytoplasm. Its antimicrobial mechanism of action was reported to be based on interaction with DNA after translocation over the membrane (88, 155).

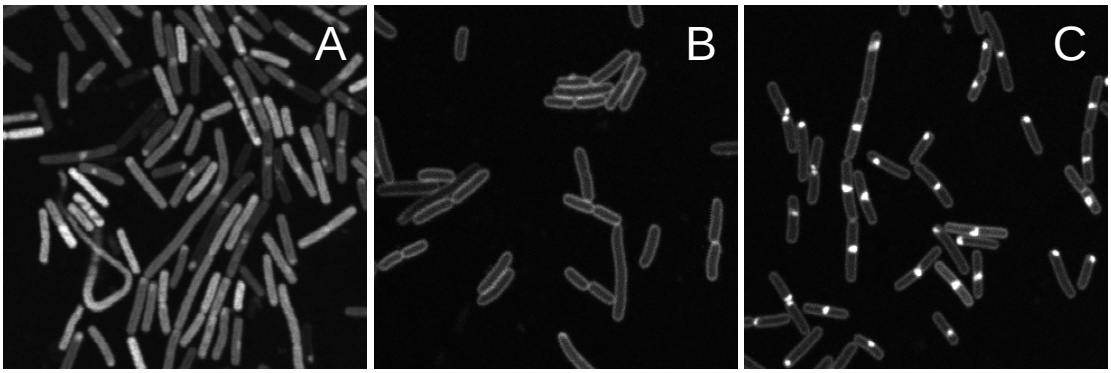

Figure 19 Localisation of antimicrobial peptides in *E. coli* and *B. subtilis*. Live cells were incubated with 12 µM peptide for 30 minutes and investigated with confocal laser scanning microscopy. (A) Fluos-labelled buforin II in *B. subtilis* which served as control for cytoplasmic peptide localisation, (B) cW[NBD]W in *E. coli* and (C) in *B. subtilis*. While buforin II was internalised into the cytoplasm, the cyclic hexapeptide bound to the membrane of Gram positive and Gram negative bacteria (156). Representative images from at least three independent experiments are shown.

Treatment of *B. subtilis* confirmed rapid internalisation of fluorescein-labelled buforin II into the cytoplasm (Figure 19A). On the contrary, cW[NBD]W fluorescence was found to be limited to the membrane in both *E. coli* and *B. subtilis* cells (Figure 19B, C). The peptide did not translocate over the cytoplasmic membrane even after 90 minutes (data not shown). Furthermore, prominent peptide accumulation was observed at distinct sites in Gram positive *B. subtilis* (Figure 19C). Here, the antimicrobial peptide was enriched mostly at the poles and division septa while some cells also showed membrane-associated sub-polar peptide localisation. Similar accumulation patterns of cW[NBD]W were also observed in *E. coli*, however, only after longer incubation time.

6.2.2.2 Peptide uptake studies with HPLC

Peptide localisation was further investigated with an HPLC-based approach where chemical modification with o-nitroaniline was applied to distinguish between external and internalised peptides (Figure 20), (156). The highly reactive compound covalently binds to the ε-amino group of the lysine side chains of cR2[NBD] which served as

substitute for cWFW in HPLC studies. Peptide moieties adsorbed to the cell surface are modified while deep insertion into or translocation across the membrane shields peptides from the reaction with o-nitroaniline. Hence, fluorescence-based HPLC monitoring allows for the quantification of unmodified and modified peptide species. As the cytoplasmic membrane of bacteria has been identified as the crucial barrier of cyclic R-,W-rich hexapeptides, cell wall-deficient L-form bacteria derived from *E. coli* (L-WF+) and *B. subtilis* (L-170) where used in the uptake studies. In control experiments without cells, unmodified peptides (t_R 13.6 min) could clearly be separated from modified species which were characterised by higher retention times (Figure 20A, bottom). Here, the large number of peaks after o-nitroaniline addition results from peptide moieties modified to a different extent. Investigation of peptide localisation in L-WF+ and L-170 cells is shown in Figure 20B and represents the amount of unmodified peptide that was not accessible for the o-nitroaniline reaction.

The results obtained for the cyclic hexapeptide were compared to internalisation of Fluos-buforin II. Here, similar amounts of unmodified peptide were found in control preparations without and after o-nitroaniline treatment. Fluos-buforin II was not exposed to the modification reaction which confirms our findings from microscopy studies where the control peptide did not accumulate in the membrane but translocated into the cytoplasm (Figure 20B, Figure 19A). By contrast, after 30 minutes treatment of L-form bacteria with cR2[NBD] most of the cyclic peptides had reacted with o-nitroaniline. This observation accounts for peptide localisation on the cell surface. The fraction of unmodified cR2[NBD] (inaccessible for chemical modification) amounts to about 20% and 30% of total cell-bound peptides in *E. coli* L-WF+ and *B. subtilis* L-170, respectively (Figure 20B). As we could not detect any peptide-fluorescence inside the cell with microscopy, we would suggest the unmodified species to be inserted deeply into the lipid matrix of the bacterial membrane (Figure 19B, C).

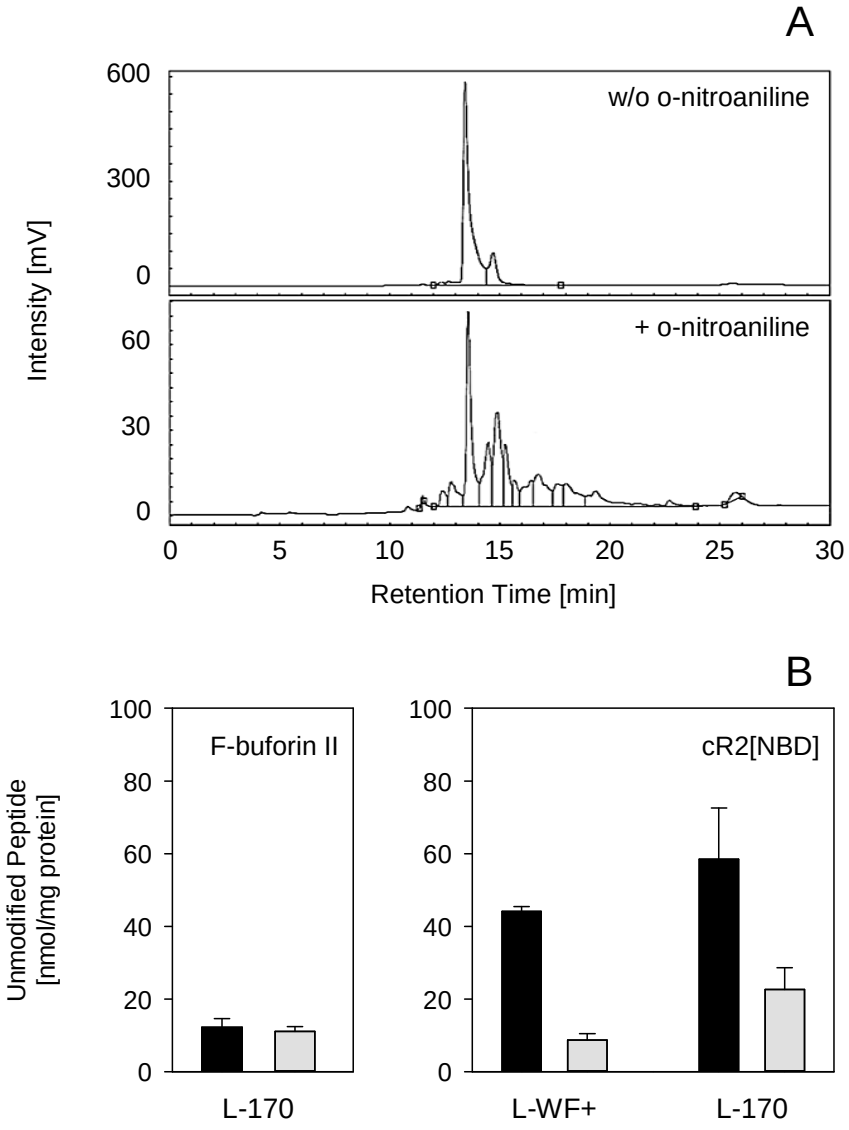

Figure 20 Antimicrobial peptide uptake into cell wall-deficient L-form bacteria. (A) Representative HPLC spectra of cR2[NBD] in *B. subtilis* L-170 cells without and after o-nitroaniline treatment revealed different retention times for modified and unmodified peptide species. Calibration experiments in TFA without cells showed identical retention profiles like untreated peptides in uptake studies (data not shown); (B) Quantification of unmodified peptides: Fluos-buforin II (left) and cR2[NBD] (right) after 30 minutes incubation time. Black bars: without o-nitroaniline (total amount of cell-associated peptides), grey bars: after o-nitroaniline treatment (amount of peptides not accessible for modification). Peptide concentration was 50 µM which was reported before as MIC for Fluos-buforin II and cR2[NBD] (156).

6.2.2.3 Peptide uptake in eukaryotic cells

The high specificity of R-,W-rich antimicrobial peptides for microorganism is based on electrostatic interactions with the negatively charged membrane (99, 157). The membrane of eukaryotic cells is mainly composed of neutral lipids, however, extracellular matrix components, such as heparan sulfate proteoglycan (HSPG), also confer negative charge upon the surface (158, 159). Furthermore, the cyclic hexapeptides obtain structural characteristics of so-called cell penetrating peptides (CPPs) which are also rich in arginine and often amphipathic (160-162). Putative translocation of the antimicrobial peptide was analysed in HeLa cells using fluorescence microscopy. The viability of the population was tested in the presence of cWFW, cW[NBD]W and cR2[NBD], respectively (Figure 21). We could demonstrate that even at high concentrations none of the cyclic hexapeptides had a toxic effect on HeLa cells.

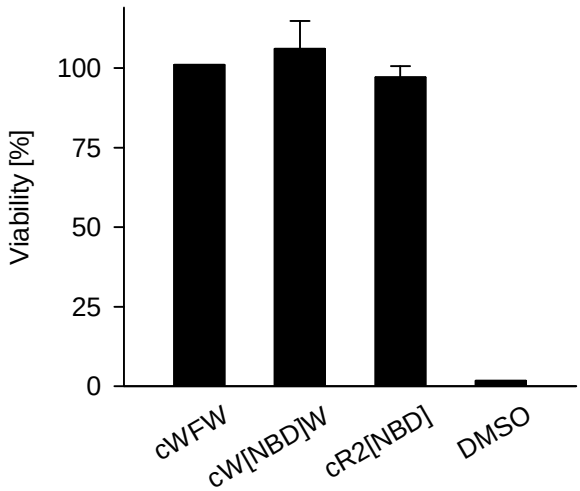

Figure 21 Viability of HeLa cells after antimicrobial peptide treatment. Cell viability was determined using an MTT assay after incubation with the cyclic hexapeptide derivatives at 50 µM for 30 minutes, 37 °C. 50% DMSO served as negative control. Two independent experiments were performed in triplicates. (The viability of HeLa cells in the presence of cWFW has been reported before (103).)

Analogous to CLSM experiments with *E. coli* and *B. subtilis*, peptide localisation in HeLa cells was investigated with cW[NBD]W. The well-characterised cell penetrating peptide (CPP) penetratin was reported to be taken up into eukaryotic cells by macropinocytosis and served as positive control (163, 164). Following peptide incubation for one hour we could detect Fluos-penetratin throughout the cells showing a preference for nuclear accumulation (Figure 22). Interestingly, treatment with the cyclic hexapeptide also led to peptide uptake, which appeared, however, to be restricted to the cytoplasm. The slightly spotty distribution of NBD-fluorescence points to an accumulation of the peptide inside vesicular structures. Furthermore, membrane integrity was verified with trypan blue staining indicating that the cyclic hexapeptide translocates into HeLa cells by a non-permeabilising mechanism. Hence, the uptake of the antimicrobial peptide into eukaryotic cells is comparable to other arginine-rich cell penetrating peptides and is also suggested to be based on endocytotic mechanisms.

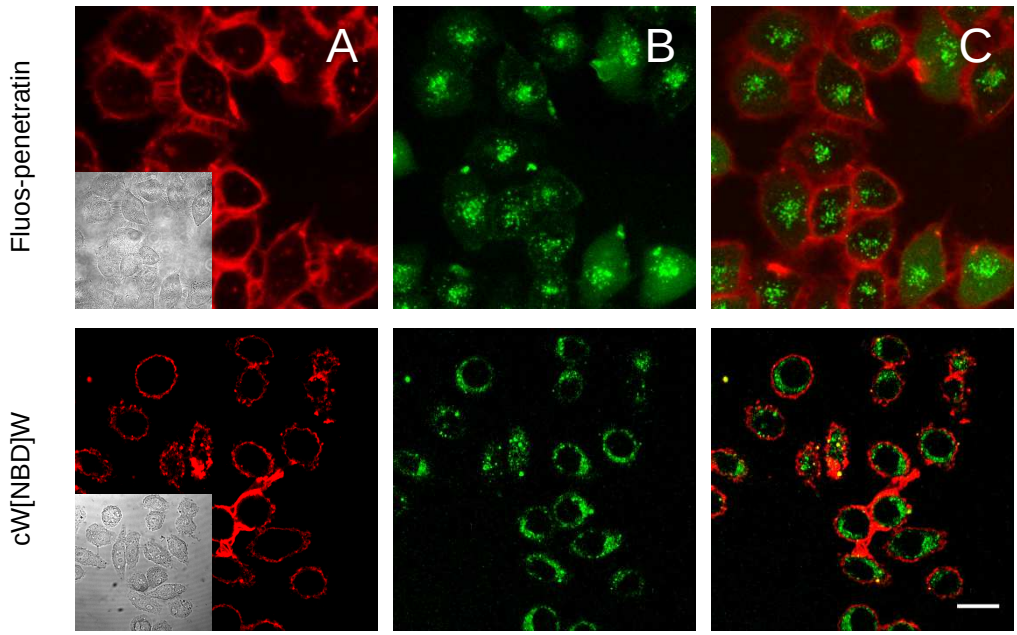

Figure 22 Peptide translocation into HeLa cells. Live adherent cells were incubated for one hour at 37 °C with 5 µM Fluos-penetratin (top row) and 40 µM cW[NBD]W (bottom row), respectively. (A) Trypan blue staining (red) was applied to visualise membrane integrity of intact cells, (B) peptide fluorescence and (C) merge. Scale bar represents 20 µm.

6.2.3 Peptide-membrane interaction

High membrane activity has been described for R-,W-rich antimicrobial peptides and is consistent with previous studies on cWFW interaction with model membrane systems which showed deep insertion of the hydrophobic cluster into the lipid bilayer (71, 150). Also, investigations on peptide uptake into bacteria cells confirmed the cytoplasmic membrane as target structure but revealed that the antimicrobial mechanism of action is not based on translocation into the cytoplasm (Figure 19). Hence, we suggest cWFW exerts its antimicrobial action by direct interaction with certain membrane components. As we could detect distinct peptide accumulation at the septum and poles of *B. subtilis*, further studies on the mechanism of action were focussed on specific peptide interaction with the lipid bilayer. The negatively charged phospholipid cardiolipin (CL) is found in the membrane of nearly all bacteria (165). Due to its conical shape it has been shown to accumulate in membrane regions with high curvature strain, i.e. cell septa and poles, and has been attributed a role in cell division processes (111, 166). Based on these observations we reasoned that potential interactions of cWFW with cardiolipin might contribute to peptide activity (156).

6.2.3.1 Peptide-cardiolipin interaction *in vitro*

Peptide-lipid interaction was first studied on model membrane systems. Isothermal titration calorimetry (ITC) was used to determine the affinity of cWFW to different bilayers mimicking the lipid composition of bacterial membranes (Figure 23). LUVs based on POPE (phosphatidylethanolamine) were doped with 25% POPG (phosphatidylglycerol) and 12.5% CL (net charge -2), respectively, to generate liposomes with identical surface charge. In addition, peptide binding was assessed to LUVs made from *E. coli* lipid extract. Vesicles from POPC, the predominant lipid in eukaryotic membranes, served as control. For appropriate fitting of the experimental data, a lipid accessibility factor of γ=0.5 was applied for POPE/POPG and POPC/CL liposomes assuming that only lipids in the outer leaflet of the bilayer are involved in peptide binding (134).

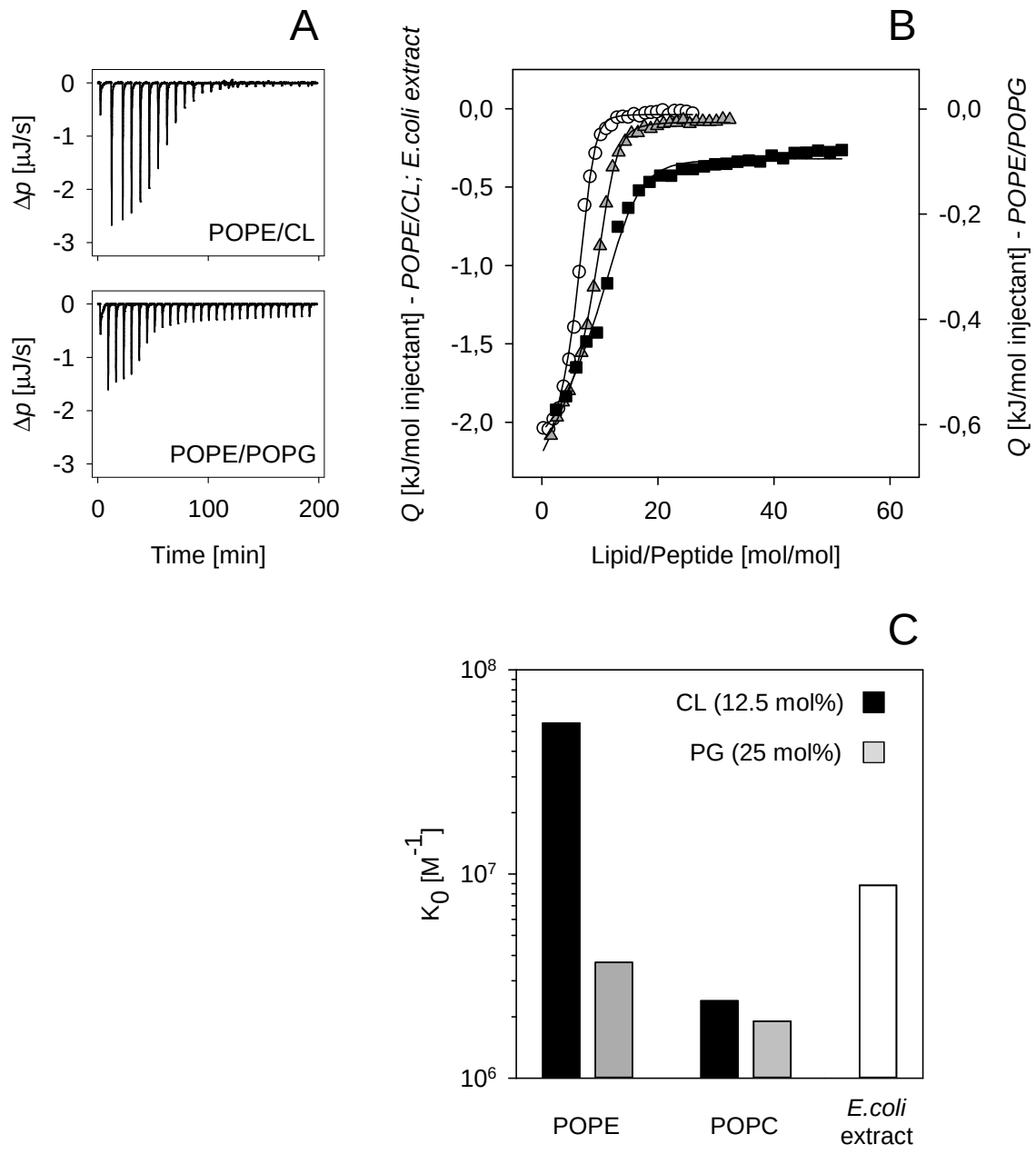

Figure 23 Thermodynamic characterisation of cWFW binding to model membranes of different lipid compositions. LUVs (5 mM POPE/CL, 10 mM POPE/POPG and *E. coli* lipid extract) were titrated into 40 µM cWFW solution at 25 °C. (A) Representative thermograms of the corresponding ITC titration experiments: differential heating power, Δ*p*, versus time, POPE/CL (87.5/12.5 mol%) (top) and POPE/POPG (75/25 mol%) (bottom). (B) Isotherms of peptide adsorption to negatively charged POPE-based liposomes: integrated and normalised heat of reaction *Q* versus lipid/peptide molar ratio, POPE/CL (circles, left ordinate), *E. coli* extract (triangles, left ordinate) and POPE/POPG (squares, right ordinate). Solid lines represent best fits to experimental data in terms of a surface partition equilibrium modulated by electrostatic effects (134).

However, cWFW adsorption to POPE/CL systems could not be characterised with this accessibility parameter. Good curve fitting was only achieved with γ=1 (with fit goodness given as sum of squared deviations: $\Sigma\Delta^2 Q$ (J/mol) = 3.84×10^{-2} for γ=1, compared to $\Sigma\Delta^2 Q$ (J/mol) = 1.37×10^{-1} for γ=0.5) suggesting that lipids from both sides of the bilayer contribute to the interaction with cWFW.

The thermodynamic parameters for peptide adsorption to the different lipid systems are presented in Table 2. Binding of cWFW to all investigated bilayers resulted in an exothermic reaction which is characteristic for membrane partitioning of amphipathic organic molecules and small cyclic peptides (167, 168). In general, detected binding constants in the range of 10^6 M^{-1} reflect strong peptide interactions with the lipid matrix. However, with $K_0 = 5.5\times10^7$ M^{-1} partitioning of cWFW into CL-containing POPE vesicles was more than 10- to 50-fold higher compared to the POPE/POPG system and also POPC-based liposomes. Peptide adsorption to *E. coli* lipid extract was slightly reduced compared to POPE/CL vesicles (Figure 23C).

Table 2 Thermodynamic parameters for cWFW interaction with different model membrane systems derived from ITC experiments. Hydrophobic partition coefficient (K_0), Gibbs free energy ($\Delta G°$), enthalpy ($\Delta H°$), entropic contribution to membrane partitioning ($-T\Delta S°$).

Lipid composition	K_0 ***[M^{-1}]***	$\Delta G°$ ***[kJ/mol]***	$\Delta H°$ ***[kJ/mol]***	$-T\Delta S°$ ***[kJ/mol]***
POPE/CL (87.5/12.5 mol%)	5.5×10^7	-54.1	-12.0	-42.1
POPE/POPG (75/25 mol%)	3.7×10^6	-47.4	-5.1	-42.3
E. coli extract	8.8×10^6	-49.6	-16.7	-32.9
POPC/CL (87.5/12.5 mol%)	1.4×10^6	-45.0	-24.3	-20.7

The high affinity of cWFW to the bacterial model membranes is related to a highly negative Gibbs free energy, $\Delta G°$, which is the result of both, favourable enthalpy and entropy changes, i.e. heat release and entropy increase (Table 2). Nonetheless, the entropic impact ($-T\Delta S°$) for cWFW adsorption to POPE and *E. coli* extract vesicles was found to be considerably higher than the enthalpic one ($\Delta H°$). Thus, cWFW partitioning into the investigated lipid systems is an entropy-driven process based on the hydrophobic effect which is determined by the release of water molecules from the hydrophobic side chains of the peptide (169). Considering $\Delta H°$ values, the negative enthalpy change was more pronounced for all CL-containing vesicles compared to the POPE/PG system. Taken together, the high affinity of cWFW towards the POPE/CL matrix is based on a pronounced entropic contribution of peptide binding to the POPE systems and a favourable change in enthalpy for CL interaction (Table 2).

6.2.3.2 Peptide-cardiolipin interaction *in vivo*

Further investigations on specific interaction between cWFW and cardiolipin in live cells were based on fluorescence microscopy. Detection of CL microdomains in the membrane of *B. subtilis* was achieved with NAO staining (Figure 24). The fluorescent probe emits at 525 nm upon binding to negatively charged phospholipids in general, while a red shift towards 640 nm is induced only upon specific interaction with CL due to tighter stacking of NAO molecules (126, 127).

In untreated cells CL domains could be observed at the poles and septa (Figure 24C, top row). However, incubation of *B. subtilis* with the antimicrobial hexapeptide cWFW resulted in a significant decrease in NAO fluorescence intensity when analysed with identical intensity settings. Even after appropriate image processing there was hardly any CL staining detectable at 640 nm (Figure 24C, bottom row). As the fluorescence signal at 525 nm was also strongly reduced, NAO binding to other negatively charged lipids was also affected. This suggests that cWFW severely interferes with the organisation of the lipid matrix *in vivo*.

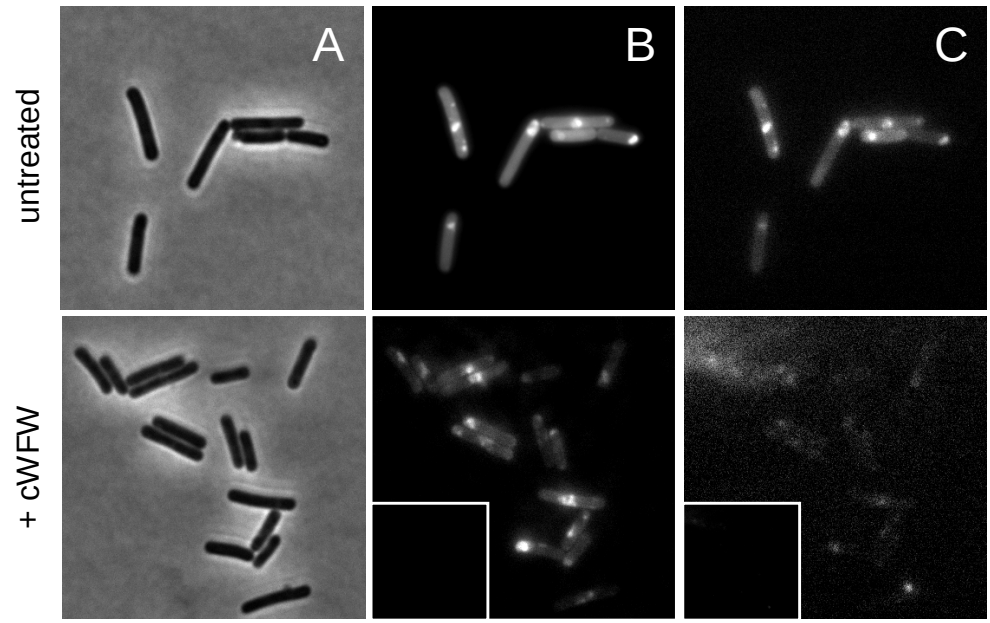

Figure 24 Influence of cWFW on cardiolipin distribution. Cardiolipin-specific staining in *B. subtilis* 168 membranes was performed with NAO in untreated control cells (top) and after peptide incubation with 12 µM cWFW (bottom). (A) Bright-field, (B) NAO fluorescence at 525 nm (corresponds to binding to negatively charged lipids) and (C) NAO fluorescence at 640 nm (corresponds to specific interaction with CL). Untreated cells show distinct staining of cardiolipin at the septum and polar regions of the cells. A strong decrease in fluorescence intensity was observed in the presence of the antimicrobial peptide cWFW in both fluorescence channels (insets showing pictures processed with identical intensity settings as applied for control cells). CL staining was performed in duplicates, representative images of at least two independent experiments are shown.

6.2.3.3 Peptide activity against Bacillus mutants

In order to elucidate putative target structures of cWFW, we tested the antimicrobial activity of the cyclic hexapeptide against different mutant strains derived from *B. subtilis*. In this context, genetic depletions affecting membrane lipids, cytoskeleton proteins, peptidoglycan synthesis (autolysins) and cell division were investigated. An overview of the mutant strains with a description of their phenotype and respective MIC values observed for cWFW treatment are given in Table 3.

With respect to the antimicrobial activity detected for *B. subtilis* DMS 347, the same MICs were also observed for the other wild type strains *B. subtilis* 168 and *B. subtilis* 168 ED. The latter holds the genetic background used for the generation of the cytoskeleton mutants. However, in the presence of 20 mM $MgSO_4$ in the growth medium peptide activity against *B. subtilis* 168 was reduced.

Regarding the lipid mutant strains, the depletion of cardiolipin or PE in the bacterial membrane did not result in increased resistance towards cWFW. Also, lack of MprF which normally catalyses the synthesis of positively charged lysosyl-phosphatidylglycerol (LPG), leading to reduced surface charged, did not alter sensitivity to cWFW (109). These observations indicate that, although peptide adsorption to the membrane surface is based on initial electrostatic interactions, the high antimicrobial activity of cWFW appears to be independent of the presence of specific lipid head groups.

The bacterial actin-homologues MreB, Mbl and MreBH are required for cell elongation and peptidoglycan synthesis (110, 170). As the corresponding cytoskeleton mutants are genetically based on *B. subtilis* 168 ED they require addition of 20 mM $MgSO_4$ to the growth medium. Single mutations (Δ*mreB* (1), Δ*mbl* (1) and Δ*mreBH* (1)) did not affect peptide activity, however, deletion of two or all three MreB isologues led to increased sensitivity. The highest peptide activity was observed for the MreC-mutant. The peripheral membrane protein MreC was suggested to bridge intracellular MreB molecules to extracellular peptidoglycan synthesis (171). Mutants lacking MreC have lost control over cell shape which results in a spheroidal phenotype (108, 172). The different MICs observed for the cytoskeleton mutant strains indicate that the presence of $MgSO_4$ in the growth medium reduces the effective peptide concentration which is caused by chelating sulfate ions that interact with the arginine side chains rather than shielding of the negative bacterial surface with positive magnesium ions.

Table 3 Antimicrobial activity of cWFW against mutant strains derived from *B. subtilis*. Peptide activity (MIC) was tested in triplicates in three independent experiments.

Strain	Description	MIC [µM]
Wild type		
B. subtilis 168	wt	6
B. subtilis 168 (Mg)	wt grown in the presence of 20 mM $MgSO_4$	25
B. subtilis 168 ED	wt (requires 20 mM $MgSO_4$)	25
Lipid mutants		
B. subtilis ΔCL (3)	cardiolipin deficient, normal growth	6
B. subtilis ΔPE	PE deficient, normal growth	6
B. subtilis Δ*des*	slower adaptation of fluidity upon cold shock	6
B. subtilis Δ*mprF*	increased negative surface charge	6
*Cytoskeleton mutants**		
B. subtilis Δ*mreB* (1)	impaired lateral cell wall synthesis	25
B. subtilis Δ*mbl* (1)	impaired lateral cell wall synthesis, relies on LytE system	25
B. subtilis Δ*mreBH* (1)	impaired lateral cell wall synthesis	25
B. subtilis mreB (only)	impaired lateral cell wall synthesis	12
B. subtilis mbl (only)	impaired lateral cell wall synthesis	12
B. subtilis mreBH (only)	impaired lateral cell wall synthesis	12
B. subtilis Δ*mreB*(3)	no lateral cell wall synthesis, spheroidal cells with increased membrane fluidity	12
B. subtilis Δ*mreC*	no lateral cell wall synthesis, spheroidal cells with normal membrane fluidity	6
Autolysin mutants		
B. subtilis Δ*lytE*	normal growth, narrow cells	6
B. subtilis Δ*cwlO*	disordered growth, uncontrolled cell width	12
B. subtilis Δ*lytF*	normal growth	12
B. subtilis Δ*lytABC*	normal growth	12

**Based on genetic background of B. subtilis 168 ED: require 20 mM $MgSO_4$ in growth medium.*

Next, peptide effect on cell wall turnover was tested in Bacillus autolysin mutants (Table 3). The endopeptidase activity of the major autolysins LytE and CwlO along the lateral cell wall was reported to be crucial for cell elongation (173). Like the antimicrobial peptide cWFW, LytF is localised at the septa and poles in *B. subtilis* and is involved in separation of daughter cells (174). The protein complex composed of LytA, LytB and LytC was attributed a role in cell motility (175, 176). While the MIC found for *B. subtilis* Δ*lytE* was unchanged compared to wild type cells, deletion of CwlO resulted in a slightly more resistant phenotype which was also observed in mutants lacking LytF and LytABC, respectively. These data suggest that cWFW affects the cell wall machinery in *B. subtilis*.

6.2.3.4 Peptide-induced protein expression

As sensitivity testing in mutant strains did not reveal putative peptide interaction with specific target structures, further investigations concentrated on evaluating bacterial stress mechanisms after treatment with cWFW. The physiological response of *B. subtilis* towards antibiotic stress can be deduced from the proteome and was recently reported to correlate with the antimicrobial mechanism of action (177, 178). Therefore, a collaboration project with the group of Julia Bandow at the Ruhr University, Bochum (Department of Biology of Microorganisms) was established which was aimed at elucidating cWFW-induced stress signals by proteomic profiling.

Proteins induced at least two-fold in response to cWFW treatment are designated marker proteins (Figure 25). An overview of the 30 most strongly upregulated proteins is given in Table 4. The functions of these proteins could be classified into the following categories: cell envelope, cell wall, membrane, energy limitation and oxidative as well as general stress (177). Upregulation of phage shock protein A (PspA) and NAD synthase (NadE), specific markers for membrane damage (136), points to the membrane lipid bilayer as target of cWFW which is consistent with our previous findings from uptake studies (Figure 19, Figure 20). Interference with cell wall synthesis is reflected by induction of LiaH. Although its exact function is unknown, protein expression was reported to respond to cell wall-specific antibiotics, such as

daptomycin, which interfere with the membrane-bound steps of peptidoglycan synthesis (179, 180). However, as other significant marker proteins for membrane-bound cell wall synthesis were not upregulated in the presence of cWFW, a direct influence of the cyclic hexapeptide on the bacterial cell wall is proposed to be unlikely.

In addition to NadE, further proteins involved in energy metabolism were induced in response to cWFW. Citrate synthase (CitZ) catalyses the first step in the citric acid cycle which delivers reduction equivalents to the respiratory chain, while NfrA and YwrO are stress-induced oxidoreductases involved in electron transport. Upregulation of these proteins point to peptide-induced energy limitation in *B. subtilis* which might be caused by impairment of cell respiration. In accordance with these observations, also elevated levels of proteins induced upon oxidative stress were found, such as YdbD and thiol peroxidase (Tpx).

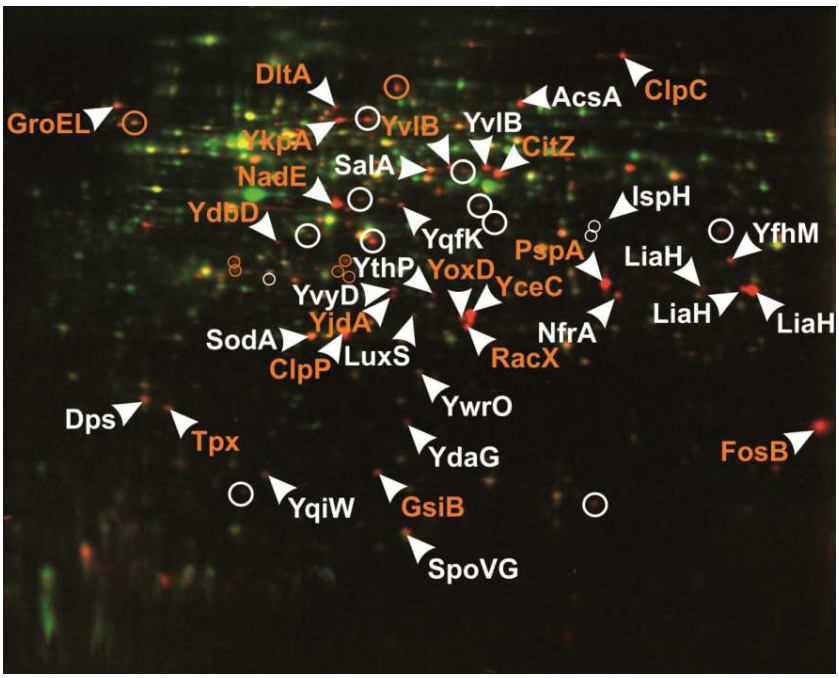

Figure 25 Cytosolic proteome analysis of *B. subtilis* 168 in response to cWFW treatment. Overlay of protein synthesis profiles obtained from 2D-PAGE after antibiotic treatment (false-coloured red) and untreated control preparation (false-coloured green): upregulated proteins appear red, downregulated proteins appear green, proteins with unchanged expression levels appear yellow. Peptide concentration was 8 µM. Representative data from three independent replicate experiments are shown. Gel evaluation was accomplished with Decodon Delta 2D 4.1. (136).

Table 4 Marker proteins identified in *B. subtilis* 168 stress response to cWFW treatment. Protein functions are derived from *Subti*Wiki (181).

Protein	***Induction factor***	***Protein function***	***Functional category***
YdbD	19.4	similar to manganese-containing catalase	oxidative stress
IspH	19.0	4-hydroxy-3-methylbut-2-enyl diphosphate reductase; part of MEP pathway of isoprenoid biosynthesis	membrane
LiaH	16.6	similar to phage shock protein	cell wall
RacX	12.0	amino acid racemase, involved in biofilm formation	cell wall, biofilm
NadE	11.0	NAD synthase	energy
YceC	9.9	similar to tellurium resistance protein	cell envelope, general stress
PspA	9.5	phage shock protein A homologue	membrane
YvlB	9.0	unknown	cell envelope
GsiB	8.4	general stress protein	general stress
FosB	8.3	bacillithiol-S-transferase, fosfomycin resistance	cell envelope
YqkF	7.7	similar to oxidoreductase	energy
YoxD	7.1	similar to 3-oxoacyl-acyl-carrier protein reductase	membrane
YvyD	6.2	general stress protein, required for ribosome dimerization in the stationary phase	general stress
YthP	5.9	similar to ABC transporter (ATP-binding protein)	cell envelope
YfhM	5.8	similar to epoxide hydrolase, general stress protein	cell envelope, general stress
NfrA	5.7	FMN-containing NADPH-linked nitro/flavin reductase	energy
YdaG	5.6	general stress protein	general stress
ClpC	5.4	ATPase subunit of the ATP-dependent ClpC-ClpP protease	general stress, heat shock
Dps	5.2	general stress protein, iron storage protein	general stress, iron metabolism
ClpP	4.8	ATP-dependent Clp protease proteolytic subunit (class III heat-shock protein)	general stress, heat shock

Protein	*Induction factor*	*Protein function*	*Functional category*
YwrO	4.3	similar to NAD(P)H oxidoreductase	energy
DltA	4.2	D-alanyl-D-alanine carrier protein ligase, antimicrobial peptide resistance	cell wall
Tpx	4.1	thiol peroxidase	oxidative stress
YpuA	4.0	unknown	cell wall
GroEL	3.9	chaperonin	chaperone, heat shock
AcsA	3.7	acetyl-CoA synthetase	membrane
CitZ	3.5	citrate synthase	energy
SalA	3.5	negative regulator of scoC expression, derepresses subtilisin	gene regulation, proteolysis
YjdA	3.4	similar to 3-oxoacyl-acyl-carrier protein reductase	membrane
LuxS	3.4	S-ribosylhomocysteine lyase, swarming, biofilm formation, methionine salvage	motility, biofilm

Proteome analysis further revealed bacterial adaptation strategies upon contact with antimicrobial agents. Firstly, the proteins IspH, acetyl-CoA synthetase (AcsA), YjdA and YoxD were found upregulated which play an important role in fatty acid biosynthesis. These findings are of particular importance as they indicate that cWFW induces changes in the lipid composition of the bilayer, a resistance mechanism that has been described before for antimicrobial peptide treatment (182).

Also, adaptation to antibiotics can be achieved by modification of the bacterial cell wall. This was observed by upregulation of DltA and RacX which leads to enhanced production of lipoteichoic acid and D-alanylation of the cell wall. Both mechanisms have also been reported in the development of bacterial resistance to daptomycin, vancomycin and telavancin (183-185). Furthermore, RacX is also involved in biofilm formation, a survival strategy which is frequently employed by Bacillus species to spatially evade stress conditions.

Subsequently, the cWFW-induced proteome response in *B. subtilis* 168 cells was compared to protein upregulation observed after treatment with well-characterised antibiotic compounds (Table 5). As a large number of marker proteins have previously been identified to be specific for certain mechanisms of action, mutual expression patterns could be indicative of the putative antimicrobial mechanism of the cyclic hexapeptide cWFW (177). Most matches in protein profiles were found for gramicidin S, gallidermin and valinomycin. All three antibiotics are highly membrane active and although they act by different mechanisms of action, their antimicrobial activity is based on integration into the bilayer without pore-formation, such as observed for cWFW treatment (186-188).

Table 5 Comparison of cWFW-induced protein expression with proteomic response to membrane targeting antibiotics. Matches in proteomic profiling refer to the 10 proteins induced most upon cWFW response in *B. subtilis* 168.

Protein	***YdbD***	***IspH***	***LiaH***	***RacX***	***NadE***	***YceC***	***PspA***	***YvlB***	***GsiB***	***FosB***
cWFW	x	x	x	x	x	x	x	x	x	x
Gramicidin S	x		x	x	x	x	x	x	x	
Gallidermin			x		x	x	x	x		
Valinomycin				x	x		x	x	x	

6.2.3.5 Peptide influence on energy metabolism

From proteome analysis in response to cWFW treatment and comparison with protein profiles from conventional antibiotic compounds, we can deduce a cWFW-related influence on bacterial energy metabolism and membrane stress. Therefore, further studies focussed on peptide-induced energy depletion and changes in lipid bilayer composition.

First, membrane depolarisation was investigated with the potential-sensitive fluorophore $DiSC_3(5)$ (Figure 26A). After addition of the cyclic hexapeptide to the cells we observed a strong fluorescence signal indicating rapid dissipation of membrane potential which increased with higher peptide concentrations. Membrane depolarisation at 6 µM (MIC) cWFW appeared to be transient, although $DiSC_3(5)$ fluorescence did not return to baseline within 20 minutes.

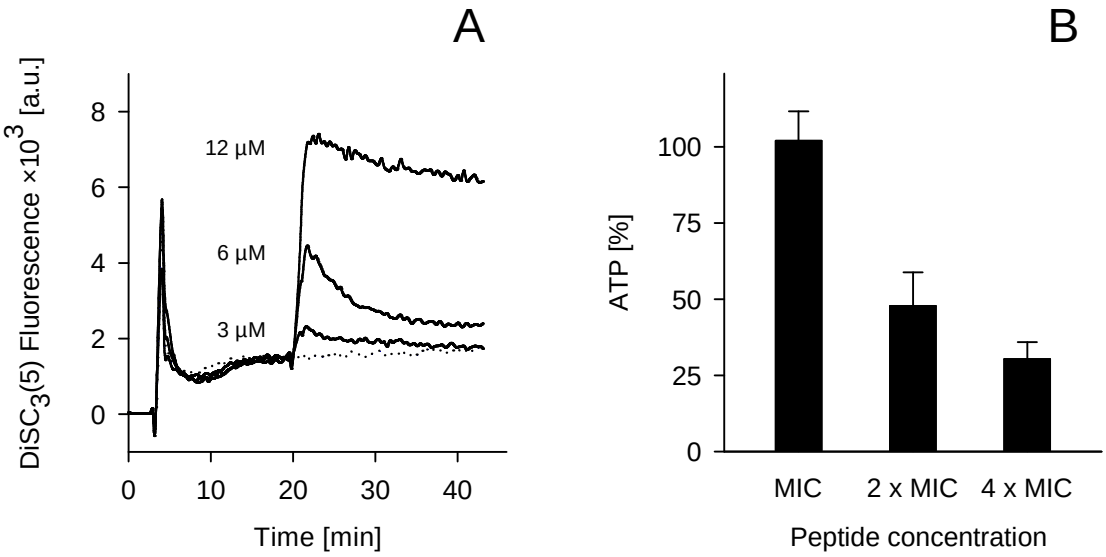

Figure 26 Peptide influence on energy metabolism in *B. subtilis*. (A) Concentration dependent dissipation of membrane potential determined with $DiSC_3(5)$. Untreated cells were used as control (dotted line); (B) Peptide-induced changes in intracellular ATP levels compared to untreated control cells (100% ATP); Depolarisation of membrane potential was dependent on peptide concentration and consistent with reduced ATP amounts.

Peptide treatment at 2 × MIC, however, resulted in a pronounced and continuing dissipation of membrane potential. In accordance with these observations, we could detect a concentration-dependent reduction in intracellular ATP levels (Figure 26B). Incubation with cWFW at 2 × MIC led to a decrease of 50% compared to untreated cells while peptide concentrations at the MIC did not affect ATP levels.

6.2.3.6 Peptide influence on membrane fluidity

Peptide influence on the composition of the lipid bilayer was investigated by measuring membrane fluidity (Figure 27). The small environment-sensitive probe Laurdan integrates into the bilayer and changes its fluorescence properties depending on polarity. Increased membrane fluidity is associated with higher lipid mobility and subsequent enhanced interaction with surrounding water molecules which enables indirect analysis of membrane composition. First, B. subtilis cells were treated with the solvent benzyl alcohol (BA) which highly increases membrane fluidity and served as positive control (Figure 27A) (189).

On the contrary, cWFW incubation at the MIC strongly reduced the fluidity of the lipid matrix. Furthermore, kinetic studies revealed that peptide-induced decrease in membrane fluidity proceeds very fast (within 2 minutes) and remains stable. Treatment with benzyl alcohol, however, led to changes in fluidity at a slower rate reaching maximum fluidity only after about 10 minutes (Figure 27B).

We were further interested to investigate the impact of cWFW on cells with different degrees of membrane fluidity (Figure 28). For this purpose we used the auxotrophic lipid strain *B. subtilis* Δ*bkd* which cannot synthesise branched fatty acid chains by itself but requires addition of particular lipid precursors to the growth medium in order to build up membrane lipids (190). Depending on the lipid precursor only distinct kinds of fatty acids can be produced which enables artificial modulation of the native membrane fluidity. For addition of isovalerate (IV), isobutyrate (IB), methylbutyrate (MB) and an equimolar mixture of all precursors, membrane fluidity can be postulated with regard to the chain properties of the corresponding fatty acids (Figure 13, page 51).

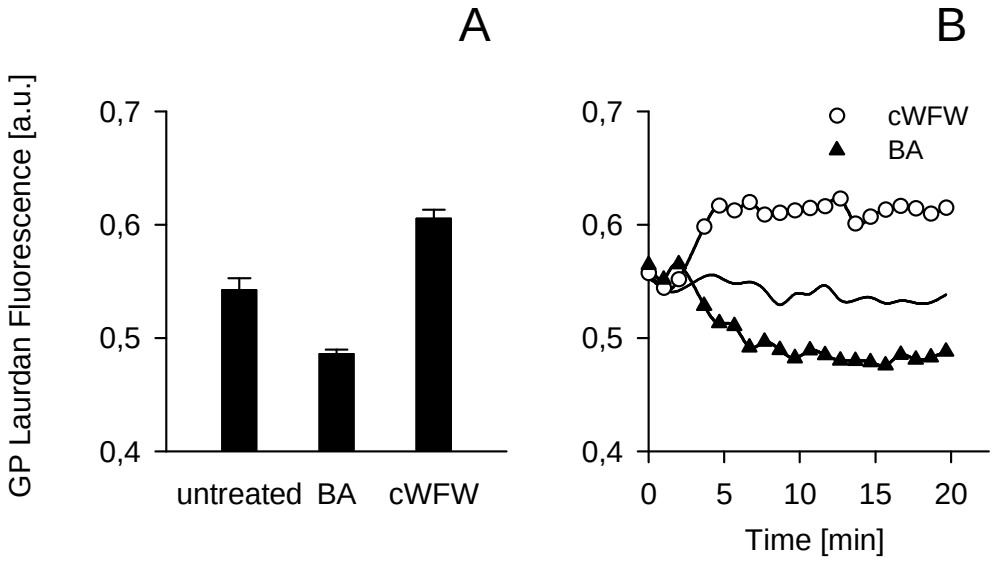

Figure 27 Peptide influence on membrane fluidity in wild type *B. subtilis*. GP values for Laurdan fluorescence were calculated as measure of membrane fluidity: high GP values represent low fluidity. (A) Membrane fluidity detected after 10 minutes in untreated cells compared to treatment with 50 mM benzyl alcohol (BA; positive control) and 6 µM cWFW, respectively; (B) Kinetic analysis of peptide-induced changes in Laurdan fluorescence.

IV and IB precursors lead to synthesis of acyl chains with odd and even numbers of carbon atoms, respectively, with branching at the last position (iso). In the case of MB, however, acyl chains are produced which are branched at the penultimate C-atom (ante) (138). According to Laurdan measurements with Bacillus wild type, fluidity of the different membrane compositions of *B. subtilis* Δ*bkd* was studied after peptide treatment (Figure 28). Membrane fluidity in untreated cells followed the order MB > mix > IB > IV which was consistent with our previous prediction based on length and branching position of the acyl chains (Figure 13). Addition of 6 µM cWFW to the mutant cells strongly reduced membrane fluidity as observed for wild type cells. However, independent of the initial lipid composition, the extent to which the fluidity was decreased was the same for all membrane systems. In fact, membrane fluidity of cells grown in the presence of MB was the same after peptide treatment compared to untreated wild type cells. These observations imply that the cells are challenged by the fast and strong change in fluidity.

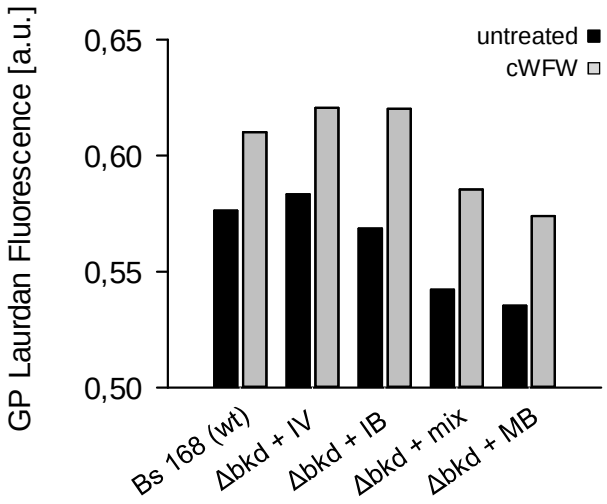

Figure 28 Peptide influence on *B. subtilis* Δ*bkd* mutants with altered membrane fluidity. Membrane fluidity derived from Laurdan fluorescence in untreated cells and after incubation with 6 µM cWFW for 10 minutes. *B. subtilis* Δ*bkd* cells were grown with isovalerate (IV), isobutyrate (IB), 2-methylbutyrate (MB) or an equimolar mixture of all lipid precursors (mix). Representative data from three independent experiments are shown.

Nevertheless, in the case of *B. subtilis* Δ*bkd* grown with isovalerate (IV) the antimicrobial activity of cWFW was increased (Table 6). The membrane of these cells was slightly less fluid in the native state compared to wild type. Hence, although the peptide-induced reduction in fluidity is the same, a more ordered lipid matrix might render the cells more sensitive in the first place. These data suggest that the level of membrane fluidity plays a role in antimicrobial peptide activity.

Table 6 Antimicrobial activity of cWFW in *B. subtilis* Δ*bkd* mutants with different degrees of membrane fluidity.

MIC [µM]	**Δ*bkd* + *IV***	**Δ*bkd* + *IB***	**Δ*bkd* + *MB***	**Δ*bkd* + *mix***
cWFW	1.5	6	6	6

6.2.3.7 Lipid demixing (phase separation)

Our studies on membrane fluidity in *B. subtilis* wild type cells as well as mutant strains confirm the severe impact of cWFW on the physical properties of the bacterial membrane. These data are also supported by the results obtained from investigation of peptide interaction cardiolipin (Figure 24). Arouri et al. have demonstrated before that treatment with R-,W-rich cyclic hexapeptides results in lipid demixing and enhances the phase transition temperature of PE/PG bilayers (90). This led to the assumption that cWFW induces the formation of distinct lipid domains also *in vivo*. In this context, we analysed the lipid arrangement in *B. subtilis* wild type cells after peptide incubation with the membrane dye Nile Red (Figure 29).

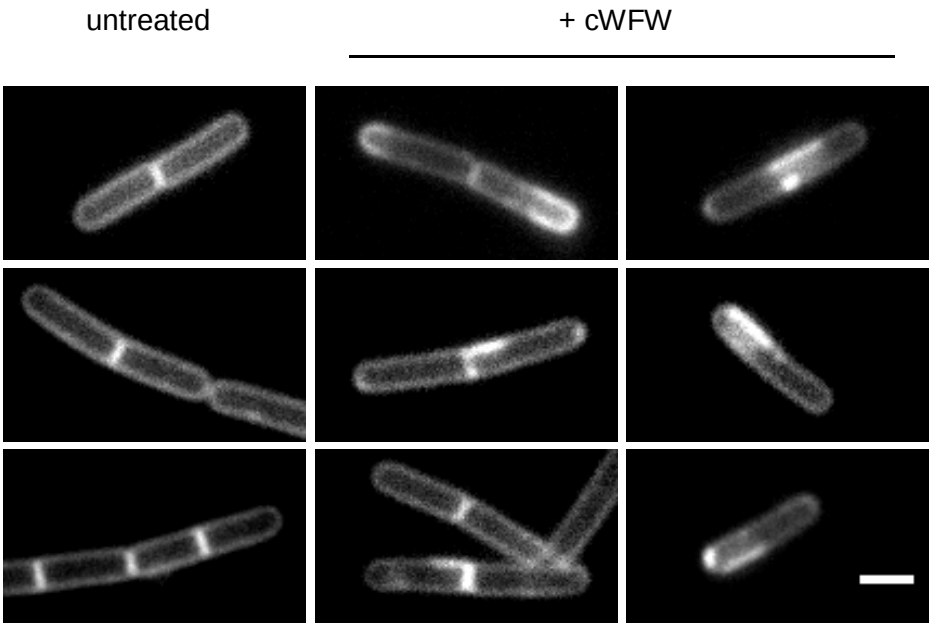

Figure 29 Peptide-induced phase separation in *B. subtilis* 168. Cells were incubated with 6 µM cWFW for 30 minutes followed by brief membrane staining with Nile Red. While untreated cells (left column) exhibited uniform distribution of the fluorescent probe, continuous membrane patches with enhanced Nile Red intensity were detected after peptide addition. Scale bar represents 2 µm.

Untreated cells displayed uniform membrane staining without obvious preference for certain lipid microdomains. However, in about 30% of all investigated cells, treatment with cWFW led to visible separation into membrane patches which differed in Nile Red intensity. Enhanced fluorescence was detected especially in regions close to the septum and at the poles. As reported by Strahl, *et al*. (108), strong accumulation of Nile Red is facilitated in membrane regions with higher fluidity which confirms our previous results from peptide-induced changes in Laurdan fluorescence.

6.2.3.8 Peptide influence on protein localisation

Peptide-induced energy depletion and severe lipid demixing suggests that cWFW interaction with the lipid bilayer interferes with the localisation and/or functionality of membrane-associated proteins (Figure 30-32).

To study the influence of the antimicrobial peptide on general membrane topology, we investigated peripheral and integral membrane proteins which are affected by membrane composition (Figure 30-1). The protein MinD depends on membrane fluidity and was shown to dissociate from the membrane with decreased membrane potential (191). Moreover, a fluorescent fusion construct of the membrane-bound amphipathic helix of MinD (GFP-MinDah) resides in regions with increased fluidity (RIFs) (108). Further studies involved localisation of AtpA which is the catalytic subunit of the enzyme ATP synthase. It is one of the most abundant proteins in *B. subtilis* and is found evenly distributed within in the cytoplasmic membrane (192). While the proton motive force is necessary to drive ATP synthesis across the membrane, localisation of the protein is independent of the membrane potential.

Incubation of *B. subtilis* cells with the antimicrobial peptide cWFW had a severe impact on the distribution of MinDah as well as AtpA (Figure 30-1). The amphipathic helix of MinD was found accumulated in distinct patches along the membrane while the fluorescence was lower in adjacent regions. Contrary effects were observed in the case of GFP-labelled AtpA. Here, addition of the peptide led to the formation of lateral membrane areas which were completely devoid of the protein.

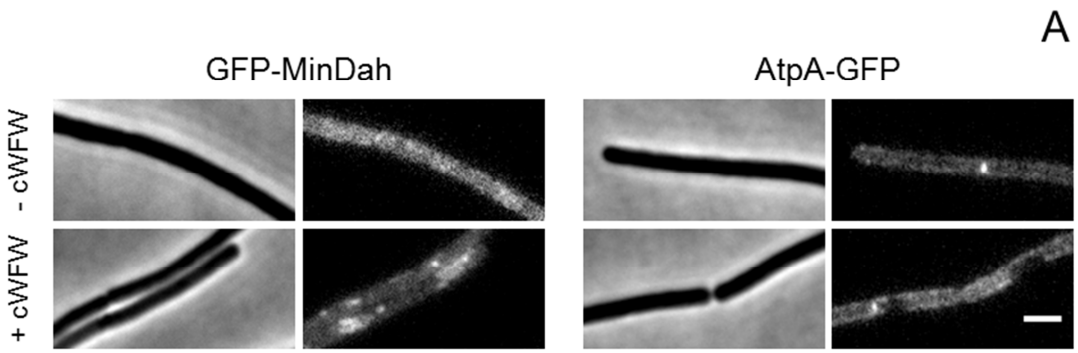

Figure 30-1 Influence of cWFW on protein localisation in *B. subtilis*. Distribution of fluorescent proteins after 30 minutes peptide incubation. (A) Peripheral (MinDah) and integral (AtpA) membrane proteins. Scale bar represents 2 µm.

We further investigated the cellular distribution of fluorescent fusion proteins which are associated with bacterial cell growth, division and chromosome segregation, respectively (Figures 30-2, 30-3). The bacterial cytoskeleton proteins MreB and Mbl appear in membrane-associated foci in untreated cells (Figure 30-2B). Incubation with the cyclic hexapeptide caused minor changes in protein patterns as GFP-MreB fluorescence was slightly decreased and more uniformly distributed inside the cells. GFP-Mbl, however, was found more pronounced inside the membrane compared to control preparations. By contrast, the cytoplasmic distribution of fluorescence fusion proteins MreBH and MreC was not altered upon peptide treatment.

The membrane-associated proteins FtsZ, FtsA, SepF and Pbp2B play an important role in bacterial cell division. FtsA and SepF were reported to tether FtsZ to the membrane which then polymerises and builds the scaffold for septum formation (193, 194). Pbp2B is part of the cell wall machinery which newly synthesizes peptidoglycan at the division plane. Treatment of the cells with cWFW resulted in delocalisation of all investigated division proteins to more or less extent (Figure 30-2C). The prominent accumulation at the division plane was shifted to a rather cytoplasmic distribution in the case of FtsZ, FtsA and Pbp2B. The most striking peptide-induced effects were observed for SepF. The native protein localisation at the septum was completely abolished and replaced by the appearance of bright foci irregularly spread over the membrane.

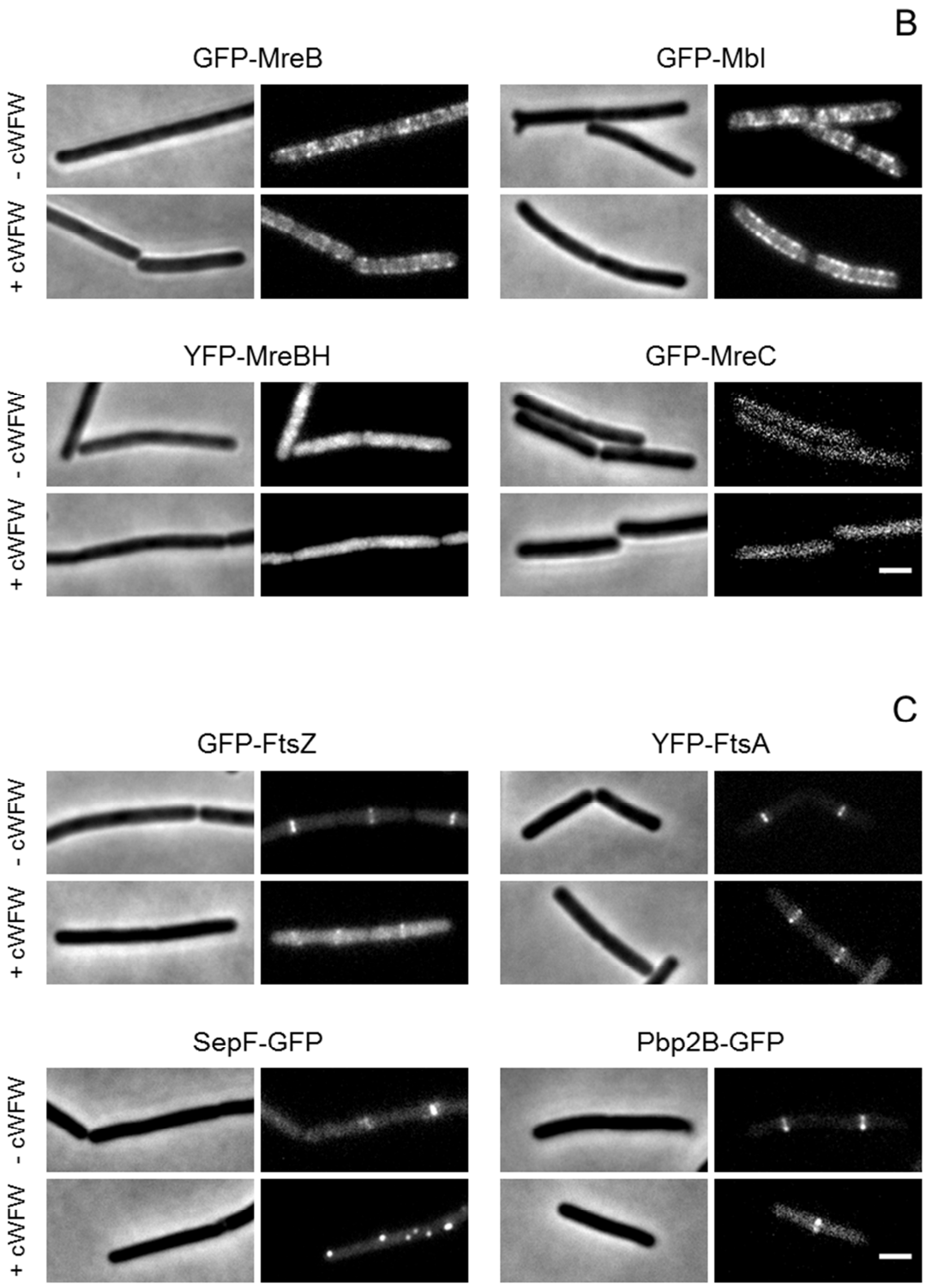

Figure 30-2 Influence of cWFW on protein localisation in *B. subtilis*. Distribution of fluorescent proteins after 30 minutes peptide incubation. (B) Elongasome proteins (involved in cell growth) and (C) divisome proteins (involved in cell division). Scale bar represents 2 µm.

The DNA binding proteins Hbs, Spo0J and DnaN are involved in DNA replication and chromosome segregation during cell division which guarantees equal distribution of genetic information among the two daughter cells (195-197). Treatment of the bacteria with the antimicrobial peptide did not change the localisation pattern of those proteins (Figure 30-3D). This suggests that DNA repair response is not directly involved in the activity of cWFW.

By contrast, the proteins of the Min-system (MinD, MinC and DivIVA) are usually restricted to the septum and poles and are responsible for correct positioning of the division plane in the middle of the bacterial cell (198, 199) (Figure 30-3E). Following peptide treatment, however, protein-associated fluorescence was enhanced throughout the cytoplasm. This points to reduced membrane interactions of MinD, MinC and DivIVA and is suggested to be related to peptide-induced rearrangement of lipid domains.

Altogether, we proposed that the strong phase separation in the cytoplasmic membrane and the severe reduction in membrane fluidity after treatment with cWFW lead to a significant delocalisation of membrane-associated proteins which eventually impairs their functionality.

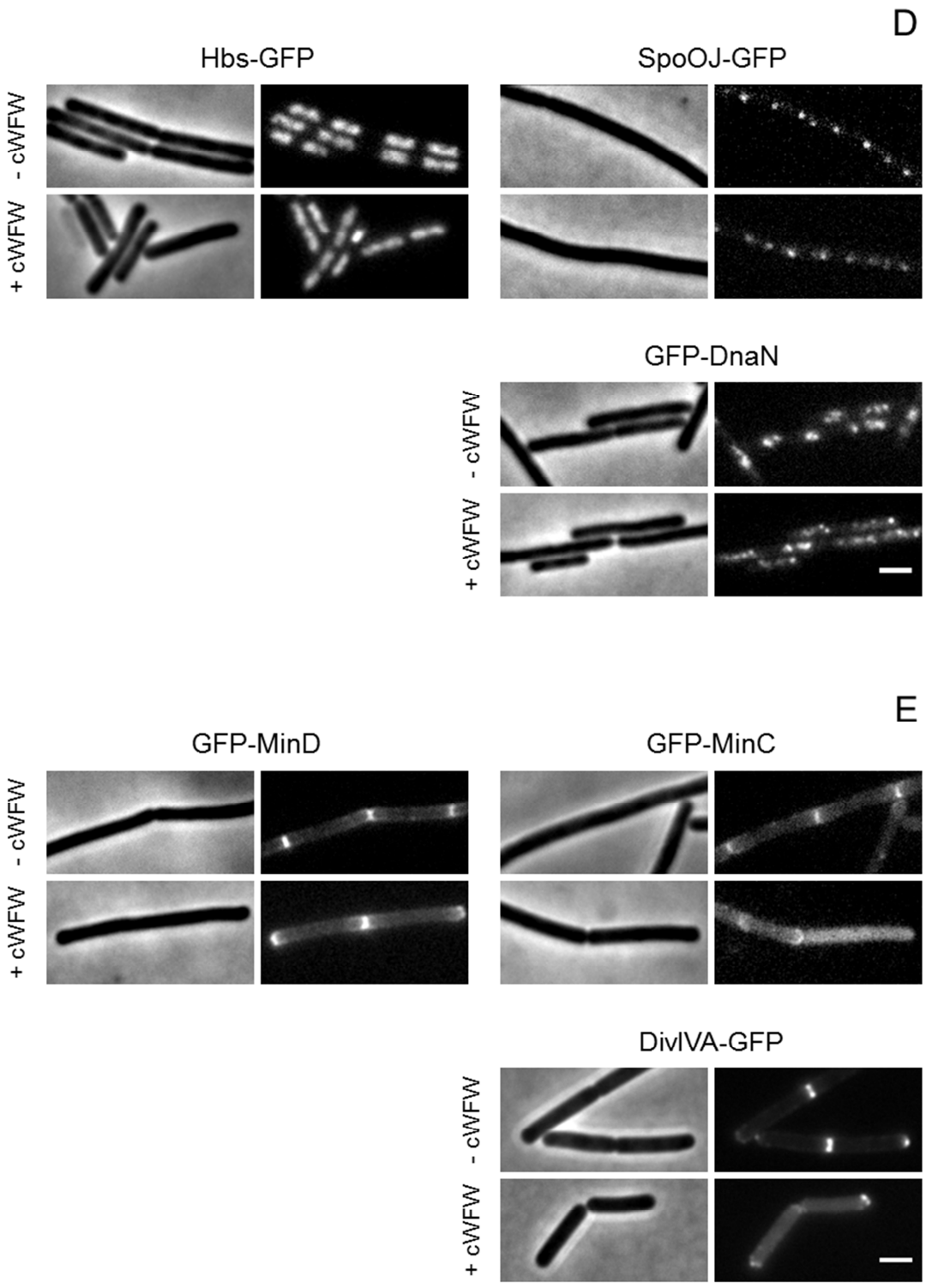

Figure 30-3 Influence of cWFW on protein localisation in *B. subtilis*. Distribution of fluorescent proteins after 30 minutes peptide incubation. (D) DNA binding proteins, (E) Min-system proteins (positioning of the division plane). Scale bar represents 2 µm.

7 Discussion

7.1 Structure and activity

The aim of this study was to shed light on the antimicrobial mechanism of action of the synthetic cyclic hexapeptide cWFW. Previous investigation revealed high selective activity against Gram positive and Gram negative cells and strong peptide interaction with lipid bilayers which is based on the amphipathic nature of the molecule. Furthermore, comparison of this class of hexapeptides and respective enantiomeric all-D-amino acid analogues showed nearly identical properties with regard to activity profile and membrane binding which rules out stereospecific, protein-mediated interactions (70). From these results we would have proposed a rather general killing mechanism, such as disruption of bacterial membranes, which is independent of the presence of specific components of the cell envelope. However, membrane permeabilisation, as most common mechanism of action of cationic antimicrobial peptides, could not be detected (119).

Investigation of linear K-/R- and W-rich peptides showed that the high abundance of these amino acid residues favours insertion into bacterial membranes and accumulation of several of these compounds in the cytoplasm (200). On the other hand, the conformationally restrained flexibility of the side chains in cyclic peptides was observed to increase the uptake efficiency of R-rich peptides into eukaryotic cells (201). Considering these observations, we were interested to investigate putative translocation of cWFW into the cytoplasm and interaction with phospholipids of the bilayer which were reported crucial steps in alternative mechanisms of antimicrobial action (80, 202). To this end, the cyclic hexapeptide had to be modified according to the technical requirements of the analytical methods.

In order to be applicable, the properties of the new peptide derivatives on cellular and model membrane level need to be as similar as possible compared to those of the parent structure cWFW. These include high antimicrobial activity, specificity for bacteria over eukaryotic cells and the non-permeabilising mechanism of action.

Earlier research on the cyclic hexapeptide had revealed a strong impact of certain structural modification on overall peptide characteristics (70, 101, 146). For example, introduction of the highly hydrophobic chromophore naphtylalanine into the aromatic cluster induced strong haemolysis of red blood cells, while insertion of the less hydrophobic tyrosine side chain reduced peptide activity. In addition, an increase in ring size led to permeabilisation of the membrane. All of these effects can be related to differences in the effective hydrophobicity and, hence, the amphipathic character of the molecule. Corresponding deviations from the parent peptide cWFW are reflected in changes in CD-spectra and retention behaviour determined with reversed phase HPLC.

Fluorescent analogues of cWFW were synthesised for application in confocal laser scanning microscopy to determine peptide localisation in live cells. Further uptake studies according to an HPLC-based approach established by Oehlke et al. (120) additionally required the substitution of arginine residues by lysine to enable modification of cell surface-bound peptides with o-nitroaniline. The new cyclic hexapeptide derivatives were compared to the parent peptide cWFW with regard to their biological activity and biophysical properties.

Introduction of carboxyfluorescein proved to be unsuitable as fluorescent marker as we observed strong reduction of antimicrobial activity which correlates with an increase in hydrophobicity/amphipathicity reflected by high retention times. This is in accordance with unpublished investigations on model membranes were carboxyfluorescein-bearing hexapeptides showed a tendency to induce membrane permeabilisation. Surprisingly, the haemolytic effect was low. Hence, opposite effects on cellular level and bilayer systems underline the complexity of peptide-membrane interaction *in vivo* and suggest that the lipid matrix is not the only determinant in peptide activity.

On the other hand, peptide properties were less affected after labelling with the fluorophores coumarin and NBD, respectively. Nevertheless, while the antimicrobial activity was conserved, we found a slight increase in undesired haemolytic activity. Although the overall hydrophobicity was similar to cWFW, CD spectroscopy revealed distinct changes in secondary structure in aqueous solution, especially after introduction of NBD. Interestingly, in interaction with membrane-mimicking POPG liposomes and SDS micelles, peptide conformations were highly similar which underlines the high

potential of the cyclic hexapeptides in the attempt to assume an amphipathic structure. With respect to investigation on the mechanism of antimicrobial action, the coumarin-labelled peptides induced slight permeabilisation of the bilayer in Gram positive and Gram negative cells while perturbation of membrane integrity was considered negligible for the NBD-containing peptides (Figure 18).

In the case of arginine-lysine exchange, peptide properties were determined by the site of substitution. Here, the best antimicrobial activity was obtained for cKRK which did not permeabilise the bacterial membrane. Although its structure in the lipid-bound state was identical to the parent peptide cWFW, lysine substitution reduced the effective hydrophobicity of the molecule which could account for reduced interactions with the bacterial membrane as reflected by higher MIC values.

Taken together, all chemical modifications applied to the hexapeptide ring reduced the antimicrobial activity (Table 1). However, NBD-labelling and double lysine substitution at the edge of the polar cluster were found to preserve the non-permeabilising mechanism of antimicrobial action which is considered the most important feature considering the suitability of a peptide derivative as tool for subsequent translocation studies. As the spectral characteristics of the NBD chromophore were reported to be sensitive to the environment (152, 203, 204), we compared the fluorescence properties of cW[NBD]W and cR2[NBD] (Figure 17). In general, the quantum yield of NBD is reported to be considerably low in aqueous solutions and further decreases with increased polarity of the environment (205). Detected fluorescence spectra revealed identical emission maxima for both peptides, however, in the case of cR2[NBD] the fluorescence intensity was slightly higher. This effect can be attributed to the impact of the lysine side chains which render the peptide overall less polar compared to a cluster of three arginine residues (206).

To conclude, with regard to antimicrobial activity, cell selectivity and mechanism of action, the cyclic hexapeptide analogues cW[NBD]W and cR2[NBD] showed the highest congruency with the parent structure and were chosen for subsequent investigations on the translocation ability of cWFW.

7.2 Peptide translocation

In order to investigate a putative translocation of the antimicrobial peptide into the cytoplasm of bacteria, we studied the localisation of the fluorescent-labelled derivative cW[NBD]W in live cells using confocal laser scanning microscopy (Figure 19). For the membrane-translocating antimicrobial peptide buforin II, which served as positive control, we could detect rapid uptake into the cytoplasm as reported before (155). No accumulation in the membrane was observed which was confirmed by our results from HPLC studies (Figure 20). These findings are consistent with earlier investigations of buforin II interaction with negative PG/PC and PG/PE model membranes which revealed low binding constants with about 2×10^5 M^{-1} (207). In contrast, the majority of the NBD-labelled peptide molecules strongly accumulated in the cell membrane which was reflected in the large difference between the amount of non-modified peptide moieties detected after o-nitroaniline modification compared to unmodified cR2[NBD] in control preparations without chemical modification (Figure 20B). Overall interaction of the cyclic hexapeptide with the bacterial membrane was 4- to 5-fold higher compared to buforin II. As we did not observe peptide translocation into the cytoplasm with fluorescence microscopy even after one hour incubation, the non-modified peptides detected in HPLC experiments after o-nitroaniline treatment are suggested to be membrane-bound. This in turn would account for deep insertion of the cyclic hexapeptide into the lipid bilayer.

As mentioned above, the biological activity of the fluorescent-labelled peptide derivative was reduced compared to cWFW which might be connected to slower initial adsorption to the bacterial surface. However, subsequent steps involved in the mechanism of antimicrobial killing are based on strong peptide interaction with the cytoplasmic membrane which could be confirmed as target structure of cW[NBD]W by microscopy and HPLC. The small cyclic antibiotic daptomycin has been shown to perturb bacterial membranes by formation of oligomeric structures that span the entire membrane (208). Furthermore, studies on the mechanism of action of lactoferricin-B peptides, R- and W-rich tritrpticin and indolicidin revealed interference with lipid bilayer structures in a way which might be sufficient for spontaneous peptide crossing (209).

To what extent the cyclic hexapeptide cWFW and its derivatives are able to integrate into the lipid matrix or even diffuse to the inner leaflet remains to be elucidated.

The differences found for peptide accumulation and uptake between both types of L-form cells are proposed to be related to membrane composition. While the cytoplasmic membrane of *B. subtilis* is highly negative, with about 70 mol% PG and only 20 mol% of neutral PE lipids, the opposite ratio of phospholipids is found in *E. coli* membranes (70mol% PE, 25 mol% PG). This would account for stronger electrostatic interaction of the cationic hexapeptide with the surface of Bacillus cells (7, 165). In addition, both types of bacteria contain about 5% negatively charged cardiolipin. Due to their conical structure, CL and also PE, induce negative curvature strain in the membrane, hence, they preferentially reside at the poles and the division septum (7, 92). The observed accumulation of the fluorescence-labelled peptide in exactly these regions might be indicative of facilitated integration into less densely packed lipid bilayer domains induced by curvature strain. In addition, specific interaction with cardiolipin microdomains might play a role which is discussed below in detail (111, 127, 208).

R- and W-rich antimicrobial peptides were shown to be highly specific for bacterial membranes based on the strong electrostatic attraction to the negative lipid head groups (99). However, recent studies elucidate the dual ability of many amphipathic structures to possess both, antimicrobial and cell penetrating properties (162, 210). These cell penetrating peptides are able to cross the membrane of eukaryotic cells which renders them highly useful tools for intracellular drug delivery approaches (211, 212). Translocation into eukaryotic cells has also recently been described for some other cyclic peptides (213). Therefore, we investigated the putative uptake of the antimicrobial hexapeptide cW[NBD]W into HeLa cells, in order to address membrane-related differences in peptide interaction with cellular surfaces. As reported before for cWFW, the fluorescent-labelled peptide derivatives did not influence cell viability even at high concentrations (Figure 21). Regarding peptide localisation, in contrast to *E. coli* and *B. subtilis*, where cW[NBD] strongly accumulated in the membrane, we now observed peptide translocation into the cytoplasm of HeLa cells (Figure 22).

The combination of antimicrobial and cell penetrating properties can be considered of great potential considering treatment of intracellular bacterial infections, such as described for *Listeria monocytogenes* (214). In this context, preliminary experiments were performed which confirmed reduction of bacterial load in mouse macrophages after incubation with the cyclic hexapeptide cWFW (unpublished data).

7.3 Peptide-membrane interaction

Based on the fact that we observed distinct peptide accumulation at the poles and septa of *B. subtilis* cells, we proposed a specific interaction of cWFW with the anionic phospholipid cardiolipin which is located in these regions (111, 215). Elevated levels of CL have been suggested to be involved in bacterial resistance towards the lipopeptide antibiotic daptomycin (208). Hence, a putative direct peptide-lipid interaction might be responsible for the high antimicrobial activity of cWFW. Binding studies based on ITC revealed preferred interaction of the cyclic hexapeptide with CL-doped POPE liposomes with binding constants over ten times higher than observed for all other lipid compositions tested (Figure 23C). This binding is not determined by electrostatic interactions with a particular lipid head group as we observed reduced peptide affinity in the presence of POPG. Moreover, peptide interaction with POPE-based systems and *E. coli* extract was accompanied by a highly favourable change in entropy reflecting a pronounced hydrophobic effect which accounts for deep and stable partitioning of cWFW into those bilayers (Table 2). In contrast to POPC and POPG which generate stable bilayers, a characteristic feature of the phospholipids POPE and CL is their tendency to induce negative curvature strain which appears to be essential for managing the lipid packing constraints at the septa and poles (215-217). Contribution of PE and CL to bacterial cell division has been illustrated in several studies and the formation of lipid domains seems to be involved in the recruitment of functional assembly of membrane proteins (for review see Matsumoto, *et al.* (92)). In fact, the binding affinity of the division plane regulators MinD and MinE to the *E. coli* membrane has been shown to be dependent on the anionic phospholipids CL and PG (218).

From these results we would deduce that peptide interaction with bacterial membranes and model bilayer systems is favoured in regions high negative curvature strain. These regions are characterised by distinct lipid and protein compositions and have been described in lipid raft models for eukaryotic as well as bacterial membranes (219).

In accordance with this assumption, we observed severe impact of cWFW on CL staining in live bacteria (Figure 24). In untreated *B. subtilis* cells, the specific dye NAO revealed polar and septal localisation of the phospholipid similar to what has been shown in previous publications (166). Addition of the antimicrobial hexapeptide, however, strongly reduced NAO fluorescence to an extent where it was hardly detectable anymore. Recently, Arouri et al. reported on cyclohexapeptide-induced lipid demixing which was accompanied by an increase of the main lipid phase transition temperature of PE/PG bilayers (90). Therefore, potential lipid separation by cWFW and subsequent rearrangement of pre-existing functional microdomains might lead to reduced NAO interaction with the bacterial membrane.

The hypothesis that the mechanism of action of cWFW is independent of interaction with certain phospholipid head groups was supported by our activity studies on *B. subtilis*-derived mutants with impaired membrane components (Table 3). Here, cells lacking PE or CL did not exhibit altered sensitivity towards the antimicrobial hexapeptide which indicates that their function in the bilayer can be taken over by other lipids (220). Furthermore, changes in surface charge, investigated with the mprF-deficient mutant strain, appeared to have no effect on peptide activity. Overall, studies on peptide activity against *B. subtilis* mutants did not reveal significant changes in MIC values which would have been indicative of cWFW interaction with specific membrane-associated target structures. Only the cytoskeleton mutant Δ*mreC* appeared to be more susceptible than the wild type strain *B. subtilis* 168 ED with a reduction in MIC from 25 µM to 6 µM. The bacterial cytoskeleton protein MreC was proposed to be involved in the spatial organisation of cell wall synthesis as it constitutes a scaffold for the assembly of peptidoglycan synthases (172). The protein is also referred to as “cell shape regulator” as MreC-deficient strains are characterised by a spheroidal phenotype. Again, the assembly of membrane lipids in these cells would be based on high curvature strain which might favour cWFW integration into the lipid matrix and facilitate subsequent steps in the antimicrobial mechanism of action.

In order to get more insight into potential cellular structures involved in cWFW action a proteomics-based approach was applied. As bacterial stress response mechanisms have been associated with treatment of certain antibiotic agents, changes in protein expression can be indicative of the underlying mechanism of action (139, 221). The proteins found upregulated in response to the cyclic hexapeptide can be classified into the functional categories of cell envelope/cell wall, cell membrane, oxidative and general stress as well as energy limitation (Figure 25, Table 4). These results confirm the high membrane activity of cWFW and are consistent with our previous findings from localisation studies. The highly upregulated protein LiaH is one of five specific marker proteins which indicate inhibition of membrane-bound peptidoglycan synthesis (221). However, as none of the other signature proteins was upregulated a direct interaction of cWFW with cell wall synthesis components is proposed to be unlikely. In fact, peptide perturbation of the cytoplasmic membrane organisation might subsequently lead to interference with membrane-associated lipid II synthesis as suggested by Wenzel, *et al.* (105). In accordance with this consideration, previous studies on cell wall-deficient L-form bacteria did not reveal significant differences of peptide activity compared to normal cells (156). Further evidence of the mechanism of action of the cyclic hexapeptide was deduced from the induction of proteins involved in fatty acid biosynthesis, as observed for IspH, YoxD, acetyl-CoA synthase (AcsA) and *YjdA* (Table 4). Strong upregulation especially of IspH, which is part of the MEP pathway for isoprenoid synthesis, indicates severe restructuring of the fatty acid composition of the bilayer upon cWFW binding to the membrane. Modification of the hydrophobic chains of the phospholipids leads to changes in membrane fluidity and thickness. This strategy is efficiently exploited in bacterial adaptation to cold shock and has also been reported to play a role in defence against certain antibiotic agents (19, 182, 222).

As the proteomic profile can provide information about the antimicrobial mechanism of action, we compared the bacterial response to treatment with cWFW and membrane active conventional antibiotics (Table 5). Most matches of protein upregulation were found for the cyclic decapeptide gramicidin S, the lantibiotic gallidermin and the K^+-selective ionophore valinomycin. These compounds act by different mechanism involving cell wall perturbation, binding to lipid II and pore formation. However, they

were all shown to integrate deeply into the lipid bilayer (83, 105, 188). The most striking feature the antibiotics have in common is their high ability to dissipate the membrane potential. This is reflected by upregulation of the marker proteins NadE and PspA which indicate interference with membrane integrity and, moreover, they are involved in the bacterial response to energy limitation (105). Both proteins were also strongly induced after treatment with the cyclic hexapeptide cWFW (Table 4). Accordingly, we also found YdbD upregulated which indicates severe oxidative stress. This in turn can be caused by interference with the respiratory chain due to interruption of electron transfer. Altogether, these findings prompted us to investigate the influence of cWFW on the energy metabolism of *B. subtilis* cells.

It has been demonstrated before that the membrane potential is necessary for cell division and also for localisation of membrane-associated proteins (191). Using the potential-sensitive fluorescent dye $DiSC_3(5)$ we observed depolarisation of the membrane in a concentration-dependent manner immediately after cWFW addition (Figure 26). Concordantly, intracellular ATP levels were reduced with increasing peptide concentration. These findings indicate significant impact of the cyclic hexapeptide on the bacterial energy metabolism. Strong depolarisation of the membrane potential has also been described for gramicidin S, however, already at sub-MIC concentrations which suggests that this effect does not necessarily lead to cell killing (223). Hence, as cWFW treatment at the MIC only led to a transient dissipation of the membrane potential, we would propose that depolarisation of the bacterial membrane is involved but is not the basis of the hexapeptide's antimicrobial activity.

Membrane depolarisation and energy limitation can result from cation leakage through small, transient pores in the bilayer or from interference with components of the electron transport chain. The involved protein complexes are integral or peripheral membrane proteins and were shown to be inhibited by certain antimicrobial peptides (224, 225). As previous studies on black lipid membranes did not reveal cWFW-induced ion flux (Oxana Krylova, FMP, unpublished data), we reasoned that the localisation and/or functionality of membrane proteins might be impaired by peptide-induced perturbation of the lipid order. Subsequent investigations showed a severe decrease in membrane fluidity in the presence of the cyclic hexapeptide (Figure 27).

Kinetic analysis further revealed a permanent effect which set in immediately after cWFW addition reaching the maximum within two minutes. Under physiological conditions, reduction of membrane fluidity as response to physical and biological stress conditions is a highly effective strategy to secure bacterial viability (226, 227). However, these adaptation mechanisms occur within a longer time range. Further studies on *B. subtilis* mutants (Δ*bkd*) with different degrees of membrane fluidity showed the same effect (Figure 28). Here, the extent to which fluidity was reduced was the same observed for wild type cells, regardless of the initial membrane state. These data suggest that the cells are not challenged by a crucial threshold of membrane fluidity but by the degree of change. Hence, considering the speed and the magnitude of rigidification of the bilayer, we propose reduction of membrane fluidity to be the basis of the antimicrobial mechanism of action of the cyclic hexapeptide cWFW. This would also account for the strong bactericidal effect.

Yet, the underlying principle of peptide-lipid interaction remained elusive. In eukaryotic cells, membrane-rigidifying cholesterol is incorporated in order to respond to environmental requirements (228). A comparable function of the antimicrobial hexapeptide would impair the movement of fatty acid chains and diffusion of phospholipids through the bilayer and lead to an overall reduced fluidity. As mentioned before, cationic antimicrobial peptides and cyclic hexapeptides were shown to cluster anionic lipids and induce lipid demixing (89, 90). Presumably, if cWFW induces lipid demixing also *in vivo*, this will lead to the formation of domains which differ in their individual fluidity.

In order to visualise potential lipid domains we stained live *B. subtilis* cells with the membrane dye Nile Red (Figure 29). The fluorescence intensity of the dye has been proposed to increase with membrane fluidity (108). In fact, after treatment with cWFW we observed small, continuous membrane regions with higher Nile Red fluorescence which account for more fluid domains. This, in turn, implies that the observed cWFW-induced reduction of membrane fluidity affects the majority of the bilayer.

To assess the functional aspects of lipid demixing and reduced bilayer fluidity, we analysed the localisation of fluorescence-labelled membrane-associated proteins in *B. subtilis* (Figure 30-1-3). The distribution of the peripheral amphipathic helix of MinD (MinDah) and the F1-subunit of the ATP synthase (AtpA), which constitutes the integral membrane domain of the respective protein, represents valuable information on membrane topology (Figure 30-1). Binding of the peripheral membrane protein MinD to the bilayer has been shown to be facilitated by high membrane fluidity (229). This would explain why, after cWFW treatment, the amphipathic helix was accumulated in few lateral membrane patches which were suggested above to bear a lower lipid order. In contrast, AtpA was found distributed evenly across the membrane except for distinct regions which were completely devoid of the protein. Consistent with our findings, the ATP synthase has previously been identified in bacterial rafts and was shown to be excluded from more fluid membrane domains (230). These observations confirm our hypothesis that cWFW-induced phase separation leads to broad, continuous membrane regions with decreased fluidity.

Furthermore, cWFW impact on phospholipid order was especially found to affect components of the cell division machinery. Although the native, septal localisation of the proteins FtsZ, FtsA and Pbp2B was not completely impaired, we observed increasing protein-related fluorescence in the cytoplasm (Figure 30-2). In contrast, SepF, which has been demonstrated to be responsible for alignment of FtsZ filaments to the mid-cell area, was found heavily delocalised, appearing in bright irregular foci along the membrane. SepF interaction with the bilayer is accomplished by an amphipathic α-helix which prefers positively curved membranes due to lower lipid density (193). Therefore, subsequent formation of the Z-ring involving FtsZ, FtsA and Pbp2B, is proposed to be disturbed by cWFW-induced local changes in membrane fluidity.

Proper cell division is further accomplished by the Min-system which is responsible for correct positioning of the cell division complex. Localisation of the inhibitory complex MinC/D is dependent on DivIVA. Treatment of the cells with the antimicrobial peptide resulted in detachment of DivIVA from the division plane and cytoplasmic distribution which in turn is suggested to be responsible for the complete delocalisation of MinC (Figure 30-3).

Multimeric DivIVA complexes are independent of certain lipid moieties, however, they were reported to target negatively curved membrane regions (231-233). Membrane binding, albeit indirectly, requires the presence of the translocon ATPase SecA (234). Taken into account that the bacterial secretion machinery has been shown to depend on anionic phospholipids (235), cWFW-induced lipid demixing would interfere not only with SecA functionality but also with the Min-system which elucidates a potential connection between phospholipid order and bacterial cell division.

8 Conclusion and outlook

The rationale behind the present study was to elucidate the mechanism of action of the antimicrobial peptide cWFW. We could demonstrate that the compound differs from other antimicrobial peptides in that the highly efficient mode of bacterial killing is neither based on membrane permeabilisation nor peptide translocation into the cytoplasm. However, we were able to confirm the cytoplasmic membrane as major target. Furthermore, the cyclic hexapeptide was found to exhibit severe impact on the architecture of the lipid bilayer leading to massive reduction in membrane fluidity. We reason that disturbance of the lipid organisation in the bilayer certainly impairs physiological microdomains (lipid rafts) which are enriched with a particular composition of lipids and proteins (236). Maintenance of membrane heterogeneity is considered vital for cellular processes involving signal transduction and secretion (219, 230). Consistently, we could demonstrate delocalisation of membrane proteins involved in cell elongation and division which accounts for the complete growth arrest observed within 30 minutes after peptide treatment. Therefore, we postulate peptide-induced lipid demixing and accompanying reduction in fluidity to be the basis of a highly effective, novel mechanism of antimicrobial action.

The obvious advantage of the cyclic hexapeptide cWFW is the high activity against Gram positive and Gram negative bacteria which is based on a rather unspecific mechanism. As proposed by Epand and Epand (6) the rapid rearrangement of phospholipids will not provide the bacteria with the opportunity to adapt as too many vital processes are impaired simultaneously. Therefore, the antimicrobial peptide is unlikely to provoke the development of bacterial resistance. Against the background of accelerated emergence of multi-resistant microorganisms there is a pressing need to explore novel approaches of antibiotic treatment. With regard to the dual ability of the peptide to also penetrate human cells without toxic side-effects, cWFW represents an eligible compound concerning an application in the treatment of intracellular bacterial infections. In this context, additional *in vitro* and *in vivo* studies are intended in order to investigate immune modulation and pharmacodynamic parameters. Furthermore, the compiled information on the relationship between physical and biological properties of cWFW is of high importance in the design of new antimicrobial peptides.

9 Bibliography

1. Winau F, Westphal O, & Winau R (2004) Paul Ehrlich - In search of the magic bullet. *Microbes Infect* 6(8):786-789.

2. Wright GD (2007) The antibiotic resistome: the nexus of chemical and genetic diversity. *Nat Rev Micro* 5(3):175-186.

3. Lewis K (2013) Platforms for antibiotic discovery. *Nat Rev Drug Discov* 12(5):371-387.

4. vfa - Die Forschenden Pharmaunternehmen (2015) Neue Antibiotika: Den Vorsprung gegenüber resistenten Bakterien wahren. Available from: http://www.vfa.de.

5. WHO - World Health Organization (2014) Antimicrobial Resistance - Global Report on Surveillance. Updated April 2015; Available from: http://www.who.int.

6. Epand RM & Epand RF (2011) Bacterial membrane lipids in the action of antimicrobial agents. *J Pept Sci* 17(5):298-305.

7. Epand RM & Epand RF (2009) Domains in bacterial membranes and the action of antimicrobial agents. *Mol Biosyst* 5(6):580-587.

8. Oliver PM, Crooks JA, Leidl M, Yoon EJ, Saghatelian A, & Weibel DB (2014) Localization of anionic phospholipids in Escherichia coli cells. *J Bacteriol* 196(19):3386-3398.

9. Blair JMA, Webber MA, Baylay AJ, Ogbolu DO, & Piddock LJV (2015) Molecular mechanisms of antibiotic resistance. *Nat Rev Micro* 13(1):42-51.

10. Straus SK & Hancock RE (2006) Mode of action of the new antibiotic for Gram-positive pathogens daptomycin: comparison with cationic antimicrobial peptides and lipopeptides. *Biochim Biophys Act* 1758(9):1215-1223.

11. Suerbaum S & Hahn H (2012) *Medizinische Mikrobiologie und Infektiologie* (Springer, Berlin [a.o.]) 7. revised Ed.

12. Ryan KJ & Sherris JC (2014) *Sherris Medical Microbiology* (Mc Graw-Hill, New York [a.o.]) 6. Ed.

13. WHO - World Health Organization (2015) Global Tuberculosis Report 2014. Available from: http://www.who.int/tb/publications/global_report/en/.

14. Fernández L & Hancock RE (2012) Adaptive and mutational resistance: role of porins and efflux pumps in drug resistance. *Clin Microbiol Rev* 25(4):661-681.

15. Cui L, Ma X, Sato K, Okuma K, Tenover FC, Mamizuka EM, Gemmell CG, Kim MN, Ploy MC, El-Solh N, Ferraz V, & Hiramatsu K (2003) Cell wall thickening is a common feature of vancomycin resistance in Staphylococcus aureus. *J Clin Microbiol* 41(1):5-14.

16. Kawai M, Yamada S, Ishidoshiro A, Oyamada Y, Ito H, & Yamagishi J (2009) Cell-wall thickness: possible mechanism of acriflavine resistance in meticillin-resistant Staphylococcus aureus. *J Med Microbiol* 58(Pt 3):331-336.

17. Bertsche U, Yang SJ, Kuehner D, Wanner S, Mishra NN, Roth T, Nega M, Schneider A, Mayer C, Grau T, Bayer AS, & Weidenmaier C (2013) Increased cell wall teichoic acid production and D-alanylation are common phenotypes among daptomycin-resistant methicillin-resistant Staphylococcus aureus (MRSA) clinical isolates. *PLoS One* 8(6):e67398.

18. Yang SJ, Mishra NN, Rubio A, & Bayer AS (2013) Causal role of single nucleotide polymorphisms within the mprF gene of Staphylococcus aureus in daptomycin resistance. *Antimicrob Agents Chemother* 57(11):5658-5664.

19. Mishra NN, Bayer AS, Tran TT, Shamoo Y, Mileykovskaya E, Dowhan W, Guan Z, & Arias CA (2012) Daptomycin resistance in enterococci is associated with distinct alterations of cell membrane phospholipid content. *PLoS One* 7(8):e43958.

20. Long KS, Poehlsgaard J, Kehrenberg C, Schwarz S, & Vester B (2006) The Cfr rRNA methyltransferase confers resistance to Phenicols, Lincosamides, Oxazolidinones, Pleuromutilins, and Streptogramin A antibiotics. *Antimicrob Agents Chemother* 50(7):2500-2505.

21. Wright GD (2005) Bacterial resistance to antibiotics: enzymatic degradation and modification. *Adv Drug Deliv Rev* 57(10):1451-1470.

22. Hancock RE (2001) Cationic peptides: effectors in innate immunity and novel antimicrobials. *Lancet Infect Dis* 1(3):156-164.

23. Baltzer SA & Brown MH (2011) Antimicrobial peptides: promising alternatives to conventional antibiotics. *J Mol Microbiol Biotechnol* 20(4):228-235.

24. Hancock RE & Diamond G (2000) The role of cationic antimicrobial peptides in innate host defences. *Trends Microbiol* 8(9):402-410.

25. Mansour SC, Pena OM, & Hancock RE (2014) Host defense peptides: front-line immunomodulators. *Trends Immunol* 35(9):443-450.

26. Brown KL & Hancock RE (2006) Cationic host defense (antimicrobial) peptides. *Curr Opin Immunol* 18(1):24-30.

27. Mookherjee N, Brown KL, Bowdish DM, Doria S, Falsafi R, Hokamp K, Roche FM, Mu R, Doho GH, Pistolic J, Powers JP, Bryan J, Brinkman FS, & Hancock RE (2006) Modulation of the TLR-mediated inflammatory response by the endogenous human host defense peptide LL-37. *J Immunol* 176(4):2455-2464.

28. Welling MM, Hiemstra PS, van den Barselaar MT, Paulusma-Annema A, Nibbering PH, Pauwels EK, & Calame W (1998) Antibacterial activity of human neutrophil defensins in experimental infections in mice is accompanied by increased leukocyte accumulation. *J Clin Invest* 102(8):1583-1590.

29. Nijnik A, Madera L, Ma S, Waldbrook M, Elliott MR, Easton DM, Mayer ML, Mullaly SC, Kindrachuk J, Jenssen H, & Hancock RE (2010) Synthetic cationic peptide IDR-1002 provides protection against bacterial infections through chemokine induction and enhanced leukocyte recruitment. *J Immunol* 184(5):2539-2550.

30. Durr M & Peschel A (2002) Chemokines meet defensins: the merging concepts of chemoattractants and antimicrobial peptides in host defense. *Infect Immun* 70(12):6515-6517.

31. Tjabringa GS, Ninaber DK, Drijfhout JW, Rabe KF, & Hiemstra PS (2006) Human cathelicidin LL-37 is a chemoattractant for eosinophils and neutrophils that acts via formyl-peptide receptors. *Int Arch Allergy Immunol* 140(2):103-112.

32. Davidson DJ, Currie AJ, Reid GS, Bowdish DM, MacDonald KL, Ma RC, Hancock RE, & Speert DP (2004) The cationic antimicrobial peptide LL-37 modulates dendritic cell differentiation and dendritic cell-induced T cell polarization. *J Immunol* 172(2):1146-1156.

33. Kin NW, Chen Y, Stefanov EK, Gallo RL, & Kearney JF (2011) Cathelin-related antimicrobial peptide differentially regulates T- and B-cell function. *Eur J Immunol* 41(10):3006-3016.

34. Kovacs-Nolan J, Mapletoft JW, Latimer L, Babiuk LA, & Hurk S (2009) CpG oligonucleotide, host defense peptide and polyphosphazene act synergistically, inducing long-lasting, balanced immune responses in cattle. *Vaccine* 27(14):2048-2054.

35. Hilchie AL, Wuerth K, & Hancock RE (2013) Immune modulation by multifaceted cationic host defense (antimicrobial) peptides. *Nat Chem Biol* 9(12):761-768.

36. Neumann A, Berends ET, Nerlich A, Molhoek EM, Gallo RL, Meerloo T, Nizet V, Naim HY, & von Kockritz-Blickwede M (2014) The antimicrobial peptide LL-37 facilitates the formation of neutrophil extracellular traps. *Biochem J* 464(1):3-11.

37. Overhage J, Campisano A, Bains M, Torfs EC, Rehm BH, & Hancock RE (2008) Human host defense peptide LL-37 prevents bacterial biofilm formation. *Infect Immun* 76(9):4176-4182.

38. Barlow PG, Beaumont PE, Cosseau C, Mackellar A, Wilkinson TS, Hancock RE, Haslett C, Govan JR, Simpson AJ, & Davidson DJ (2010) The human cathelicidin LL-37 preferentially promotes apoptosis of infected airway epithelium. *Am J Respir Cell Mol Biol* 43(6):692-702.

39. Brogden KA (2005) Antimicrobial peptides: pore formers or metabolic inhibitors in bacteria? *Nat Rev Microbiol* 3(3):238-250.

40. Peschel A & Sahl HG (2006) The co-evolution of host cationic antimicrobial peptides and microbial resistance. *Nat Rev Microbiol* 4(7):529-536.

41. Zasloff M (2002) Antimicrobial peptides of multicellular organisms. *Nature* 415(6870):389-395.

42. Yan H & Hancock RE (2001) Synergistic interactions between mammalian antimicrobial defense peptides. *Antimicrob Agents Chemother* 45(5):1558-1560.

43. Marr AK, Gooderham WJ, & Hancock RE (2006) Antibacterial peptides for therapeutic use: obstacles and realistic outlook. *Curr Opin Pharmacol* 6(5):468-472.

44. Fjell CD, Hiss JA, Hancock RE, & Schneider G (2012) Designing antimicrobial peptides: form follows function. *Nat Rev Drug Discov* 11(1):37-51.

45. Yount NY & Yeaman MR (2013) Peptide antimicrobials: cell wall as a bacterial target. *Ann N Y Acad Sci* 1277:127-138.

46. Bauer ME & Shafer WM (2015) On the in vivo significance of bacterial resistance to antimicrobial peptides. *Biochim Biophys Act* 1848(11 Pt B):3101-3111.

47. Nizet V (2006) Antimicrobial peptide resistance mechanisms of human bacterial pathogens. *Curr Issues Mol Biol* 8(1):11-26.

48. Maria-Neto S, de Almeida KC, Macedo ML, & Franco OL (2015) Understanding bacterial resistance to antimicrobial peptides: From the surface to deep inside. *Biochim Biophys Act* 1848(11 Pt B):3078-3088.

49. Koprivnjak T & Peschel A (2011) Bacterial resistance mechanisms against host defense peptides. *Cell Mol Life Sci* 68(13):2243-2254.

50. Kondejewski LH, Jelokhani-Niaraki M, Farmer SW, Lix B, Kay CM, Sykes BD, Hancock RE, & Hodges RS (1999) Dissociation of antimicrobial and hemolytic activities in cyclic peptide diastereomers by systematic alterations in amphipathicity. *J Biol Chem* 274(19):13181-13192.

51. Korting HC, Schollmann C, Stauss-Grabo M, & Schafer-Korting M (2012) Antimicrobial peptides and skin: a paradigm of translational medicine. *Skin Pharmacol Physiol* 25(6):323-334.

52. Delves-Broughton J, Blackburn P, Evans RJ, & Hugenholtz J (1996) Applications of the bacteriocin, nisin. *Antonie Van Leeuwenhoek* 69(2):193-202.

53. Steenbergen JN, Alder J, Thorne GM, & Tally FP (2005) Daptomycin: a lipopeptide antibiotic for the treatment of serious Gram-positive infections. *J Antimicrob Chemother* 55(3):283-288.

54. Cho JH, Sung BH, & Kim SC (2009) Buforins: histone H2A-derived antimicrobial peptides from toad stomach. *Biochim Biophys Act* 1788(8):1564-1569.

55. Gifford JL, Hunter HN, & Vogel HJ (2005) Lactoferricin: a lactoferrin-derived peptide with antimicrobial, antiviral, antitumor and immunological properties. *Cell Mol Life Sci* 62(22):2588-2598.

56. Wang G, Li X, & Wang Z (2009) APD2: the updated antimicrobial peptide database and its application in peptide design. *Nucleic Acids Res* 37(Database issue):D933-937.

57. Gennaro R & Zanetti M (2000) Structural features and biological activities of the cathelicidin-derived antimicrobial peptides. *Biopolymers* 55(1):31-49.

58. Bechinger B, Zasloff M, & Opella SJ (1993) Structure and orientation of the antibiotic peptide magainin in membranes by solid-state nuclear magnetic resonance spectroscopy. *Protein Sci* 2(12):2077-2084.

59. Gesell J, Zasloff M, & Opella SJ (1997) Two-dimensional 1H NMR experiments show that the 23-residue magainin antibiotic peptide is an alpha-helix in dodecylphosphocholine micelles, sodium dodecylsulfate micelles, and trifluoroethanol/water solution. *J Biomol NMR* 9(2):127-135.

60. Fahrner RL, Dieckmann T, Harwig SS, Lehrer RI, Eisenberg D, & Feigon J (1996) Solution structure of protegrin-1, a broad-spectrum antimicrobial peptide from porcine leukocytes. *Chem Biol* 3(7):543-550.

61. Hoover DM, Chertov O, & Lubkowski J (2001) The structure of human beta-defensin-1: new insights into structural properties of beta-defensins. *J Biol Chem* 276(42):39021-39026.

62. Rozek A, Friedrich CL, & Hancock RE (2000) Structure of the bovine antimicrobial peptide indolicidin bound to dodecylphosphocholine and sodium dodecyl sulfate micelles. *Biochemistry* 39(51):15765-15774.

63. Trabi M & Craik DJ (2002) Circular proteins--no end in sight. *Trends Biochem Sci* 27(3):132-138.

64. Brotz H & Sahl HG (2000) New insights into the mechanism of action of lantibiotics--diverse biological effects by binding to the same molecular target. *J Antimicrob Chemother* 46(1):1-6.

65. Simonsen SM, Sando L, Ireland DC, Colgrave ML, Bharathi R, Goransson U, & Craik DJ (2005) A continent of plant defense peptide diversity: cyclotides in Australian Hybanthus (Violaceae). *Plant Cell* 17(11):3176-3189.

66. Tang YQ, Yuan J, Osapay G, Osapay K, Tran D, Miller CJ, Ouellette AJ, & Selsted ME (1999) A cyclic antimicrobial peptide produced in primate leukocytes by the ligation of two truncated alpha-defensins. *Science* 286(5439):498-502.

67. Lehrer RI, Cole AM, & Selsted ME (2012) theta-Defensins: cyclic peptides with endless potential. *J Biol Chem* 287(32):27014-27019.

68. Craik DJ (2006) Chemistry. Seamless proteins tie up their loose ends. *Science* 311(5767):1563-1564.

69. Epand RM & Vogel HJ (1999) Diversity of antimicrobial peptides and their mechanisms of action. *Biochim Biophys Act* 1462(1-2):11-28.

70. Wessolowski A, Bienert M, & Dathe M (2004) Antimicrobial activity of arginine- and tryptophan-rich hexapeptides: the effects of aromatic clusters, D-amino acid substitution and cyclization. *J Pept Res* 64(4):159-169.

71. Junkes C, Wessolowski A, Farnaud S, Evans RW, Good L, Bienert M, & Dathe M (2008) The interaction of arginine- and tryptophan-rich cyclic hexapeptides with Escherichia coli membranes. *J Pept Sci* 14(4):535-543.

72. Chan DI, Prenner EJ, & Vogel HJ (2006) Tryptophan- and arginine-rich antimicrobial peptides: structures and mechanisms of action. *Biochim Biophys Act* 1758(9):1184-1202.

73. Strom MB, Rekdal O, & Svendsen JS (2002) Antimicrobial activity of short arginine- and tryptophan-rich peptides. *J Pept Sci* 8(8):431-437.

74. Yau WM, Wimley WC, Gawrisch K, & White SH (1998) The preference of tryptophan for membrane interfaces. *Biochemistry* 37(42):14713-14718.

75. Izadpanah A & Gallo RL (2005) Antimicrobial peptides. *J Am Acad Dermatol* 52(3 Pt 1):381-390; quiz 391-382.

76. Yang L, Harroun TA, Weiss TM, Ding L, & Huang HW (2001) Barrel-stave model or toroidal model? A case study on melittin pores. *Biophys J* 81(3):1475-1485.

77. Oren Z & Shai Y (1998) Mode of action of linear amphipathic alpha-helical antimicrobial peptides. *Biopolymers* 47(6):451-463.

78. Matsuzaki K, Murase O, Fujii N, & Miyajima K (1996) An antimicrobial peptide, magainin 2, induced rapid flip-flop of phospholipids coupled with pore formation and peptide translocation. *Biochemistry* 35(35):11361-11368.

79. Sengupta D, Leontiadou H, Mark AE, & Marrink SJ (2008) Toroidal pores formed by antimicrobial peptides show significant disorder. *Biochim Biophys Act* 1778(10):2308-2317.

80. Nguyen LT, Haney EF, & Vogel HJ (2011) The expanding scope of antimicrobial peptide structures and their modes of action. *Trends Biotechnol* 29(9):464-472.

81. Miteva M, Andersson M, Karshikoff A, & Otting G (1999) Molecular electroporation: a unifying concept for the description of membrane pore formation by antibacterial peptides, exemplified with NK-lysin. *FEBS Lett* 462(1-2):155-158.

82. Tieleman DP (2004) The molecular basis of electroporation. *BMC Biochem* 5:10.

83. Duax WL, Griffin JF, Langs DA, Smith GD, Grochulski P, Pletnev V, & Ivanov V (1996) Molecular structure and mechanisms of action of cyclic and linear ion transport antibiotics. *Biopolymers* 40(1):141-155.

84. Mogi T & Kita K (2009) Gramicidin S and polymyxins: the revival of cationic cyclic peptide antibiotics. *Cell Mol Life Sci* 66(23):3821-3826.

85. Rokitskaya TI, Kolodkin NI, Kotova EA, & Antonenko YN (2011) Indolicidin action on membrane permeability: carrier mechanism versus pore formation. *Biochim Biophys Act* 1808(1):91-97.

86. Mattila JP, Sabatini K, & Kinnunen PK (2008) Oxidized phospholipids as potential molecular targets for antimicrobial peptides. *Biochim Biophys Act* 1778(10):2041-2050.

87. Park CB, Yi KS, Matsuzaki K, Kim MS, & Kim SC (2000) Structure-activity analysis of buforin II, a histone H2A-derived antimicrobial peptide: the proline hinge is responsible for the cell-penetrating ability of buforin II. *Proc Natl Acad Sci U S A* 97(15):8245-8250.

88. Uyterhoeven ET, Butler CH, Ko D, & Elmore DE (2008) Investigating the nucleic acid interactions and antimicrobial mechanism of buforin II. *FEBS Lett* 582(12):1715-1718.

89. Wadhwani P, Epand RF, Heidenreich N, Burck J, Ulrich AS, & Epand RM (2012) Membrane-active peptides and the clustering of anionic lipids. *Biophys J* 103(2):265-274.

90. Arouri A, Dathe M, & Blume A (2009) Peptide induced demixing in PG/PE lipid mixtures: a mechanism for the specificity of antimicrobial peptides towards bacterial membranes? *Biochim Biophys Act* 1788(3):650-659.

91. Mileykovskaya E & Dowhan W (2005) Role of membrane lipids in bacterial division-site selection. *Curr Opin Microbiol* 8(2):135-142.

92. Matsumoto K, Kusaka J, Nishibori A, & Hara H (2006) Lipid domains in bacterial membranes. *Mol Microbiol* 61(5):1110-1117.

93. Bramkamp M & Lopez D (2015) Exploring the existence of lipid rafts in bacteria. *Microbiol Mol Biol Rev* 79(1):81-100.

94. Wieprecht T, Dathe M, Krause E, Beyermann M, Maloy WL, MacDonald DL, & Bienert M (1997) Modulation of membrane activity of amphipathic, antibacterial peptides by slight modifications of the hydrophobic moment. *FEBS Lett* 417(1):135-140.

95. Powers JP & Hancock RE (2003) The relationship between peptide structure and antibacterial activity. *Peptides* 24(11):1681-1691.

96. Blondelle SE, Perez-Paya E, & Houghten RA (1996) Synthetic combinatorial libraries: novel discovery strategy for identification of antimicrobial agents. *Antimicrob Agents Chemother* 40(5):1067-1071.

97. Blondelle SE & Lohner K (2010) Optimization and high-throughput screening of antimicrobial peptides. *Curr Pharm Design* 16(28):3204-3211.

98. Dathe M, Schumann M, Wieprecht T, Winkler A, Beyermann M, Krause E, Matsuzaki K, Murase O, & Bienert M (1996) Peptide helicity and membrane surface charge modulate the balance of electrostatic and hydrophobic interactions with lipid bilayers and biological membranes. *Biochemistry* 35(38):12612-12622.

99. Dathe M, Meyer J, Beyermann M, Maul B, Hoischen C, & Bienert M (2002) General aspects of peptide selectivity towards lipid bilayers and cell membranes studied by variation of the structural parameters of amphipathic helical model peptides. *Biochim Biophys Act* 1558(2):171-186.

100. Dathe M, Nikolenko H, Klose J, & Bienert M (2004) Cyclization increases the antimicrobial activity and selectivity of arginine- and tryptophan-containing hexapeptides. *Biochemistry* 43(28):9140-9150.

101. Junkes C, Harvey RD, Bruce KD, Dolling R, Bagheri M, & Dathe M (2011) Cyclic antimicrobial R-, W-rich peptides: the role of peptide structure and E. coli outer and inner membranes in activity and the mode of action. *Eur Biophys J* 40(4):515-528.

102. Appelt C, Wessolowski A, Dathe M, & Schmieder P (2008) Structures of cyclic, antimicrobial peptides in a membrane-mimicking environment define requirements for activity. *J Pept Sci* 14(4):524-527.

103. Junkes C (2011) Strukturelle Grundlagen der antimikrobiellen Aktivität und Selektivität kleiner cyclischer Peptide. Dr. rer. nat. Doctoral Thesis (Freie Universität Berlin).

104. Stulke J, Hanschke R, & Hecker M (1993) Temporal activation of beta-glucanase synthesis in Bacillus subtilis is mediated by the GTP pool. *J Gen Microbiol* 139(9):2041-2045.

105. Wenzel M, Kohl B, Munch D, Raatschen N, Albada HB, Hamoen L, Metzler-Nolte N, Sahl HG, & Bandow JE (2012) Proteomic response of Bacillus subtilis to lantibiotics reflects differences in interaction with the cytoplasmic membrane. *Antimicrob Agents Chemother* 56(11):5749-5757.

106. DSMZ - Leibniz Institute DSMZ - German Collection of Microorganisms and Cell Culture. Available from: https://www.dsmz.de.

107. Allan EJ, Hoischen C, & Gumpert J (2009) Bacterial L-forms. *Adv Appl Microbiol* 68:1-39.

108. Strahl H, Burmann F, & Hamoen LW (2014) The actin homologue MreB organizes the bacterial cell membrane. *Nat Commun* 5:3442.

109. Salzberg LI & Helmann JD (2008) Phenotypic and transcriptomic characterization of Bacillus subtilis mutants with grossly altered membrane composition. *J Bacteriol* 190(23):7797-7807.

110. Dominguez-Cuevas P, Porcelli I, Daniel RA, & Errington J (2013) Differentiated roles for MreB-actin isologues and autolytic enzymes in Bacillus subtilis morphogenesis. *Mol Microbiol* 89(6):1084-1098.

111. Kawai F, Shoda M, Harashima R, Sadaie Y, Hara H, & Matsumoto K (2004) Cardiolipin domains in Bacillus subtilis marburg membranes. *J Bacteriol* 186(5):1475-1483.

112. Margot P & Karamata D (1992) Identification of the structural genes for N-acetylmuramoyl-L-alanine amidase and its modifier in Bacillus subtilis 168: inactivation of these genes by insertional mutagenesis has no effect on growth or cell separation. *Mol Gen Genet* 232(3):359-366.

113. Mercier R, Domínguez-Cuevas P, & Errington J (2012) Crucial Role for Membrane Fluidity in Proliferation of Primitive Cells. *Cell Rep* 1(5):417-423.

114. ImageJ - NIH Image Processing and Analysis in Java. Updated 2004; Available from: http://imagej.nih.gov/ij/.

115. Keller S, Vargas C, Zhao H, Piszczek G, Brautigam CA, & Schuck P (2012) High-precision isothermal titration calorimetry with automated peak-shape analysis. *Anal Chem* 84(11):5066-5073.

116. Chan W & White P eds (1999) *Fmoc Solid Phase Peptide Synthesis - A Practical Approach* (Oxford University Press, Oxford), p 370.

117. Pearson DA, Blanchette M, Baker ML, & Guindon CA (1989) Trialkylsilanes as scavengers for the trifluoroacetic acid deblocking of protecting groups in peptide synthesis. *Tetrahedron Lett* 30(21):2739-2742.

118. Ehrlich A, Heyne HU, Winter R, Beyermann M, Haber H, Carpino LA, & Bienert M (1996) Cyclization of all-L-Pentapeptides by Means of 1-Hydroxy-7-azabenzotriazole-Derived Uronium and Phosphonium Reagents. *J Org Chem* 61(25):8831-8838.

119. Scheinpflug K, Nikolenko H, Komarov I, Rautenbach M, & Dathe M (2013) What Goes around Comes around-A Comparative Study of the Influence of Chemical Modifications on the Antimicrobial Properties of Small Cyclic Peptides. *Pharmaceuticals* 6(9):1130-1144.

120. Oehlke J, Scheller A, Wiesner B, Krause E, Beyermann M, Klauschenz E, Melzig M, & Bienert M (1998) Cellular uptake of an alpha-helical amphipathic model peptide with the potential to deliver polar compounds into the cell interior non-endocytically. *Biochim Biophys Act* 1414(1-2):127-139.

121. Lottspeich F, Zorbas H, & (editors) eds (1998) *Bioanalytik* (Spektrum, Akad. Verl., Heidelberg [a.o.]).

122. Wiegand I, Hilpert K, & Hancock RE (2008) Agar and broth dilution methods to determine the minimal inhibitory concentration (MIC) of antimicrobial substances. *Nat Protoc* 3(2):163-175.

123. Berridge MV & Tan AS (1993) Characterization of the cellular reduction of 3-(4,5-dimethylthiazol-2-yl)-2,5-diphenyltetrazolium bromide (MTT): subcellular localization, substrate dependence, and involvement of mitochondrial electron transport in MTT reduction. *Arch Biochem Biophys* 303(2):474-482.

124. Mosmann T (1983) Rapid colorimetric assay for cellular growth and survival: application to proliferation and cytotoxicity assays. *J Immunol Methods* 65(1-2):55-63.

125. Marshall NJ, Goodwin CJ, & Holt SJ (1995) A critical assessment of the use of microculture tetrazolium assays to measure cell growth and function. *Growth Regulat* 5(2):69-84.

126. Petit JM, Maftah A, Ratinaud MH, & Julien R (1992) 10N-nonyl acridine orange interacts with cardiolipin and allows the quantification of this phospholipid in isolated mitochondria. *Eur J Biochem* 209(1):267-273.

127. Mileykovskaya E, Dowhan W, Birke RL, Zheng D, Lutterodt L, & Haines TH (2001) Cardiolipin binds nonyl acridine orange by aggregating the dye at exposed hydrophobic domains on bilayer surfaces. *FEBS Lett* 507(2):187-190.

128. Kucherak OA, Oncul S, Darwich Z, Yushchenko DA, Arntz Y, Didier P, Mely Y, & Klymchenko AS (2010) Switchable nile red-based probe for cholesterol and lipid order at the outer leaflet of biomembranes. *J Am Chem Soc* 132(13):4907-4916.

129. Wenzel M, Senges CH, Zhang J, Suleman S, Nguyen M, Kumar P, Chiriac AI, Stepanek JJ, Raatschen N, May C, Kramer U, Sahl HG, Straus SK, & Bandow JE (2015) Antimicrobial Peptides from the Aurein Family Form Ion-Selective Pores in Bacillus subtilis. *Chembiochem* 16(7):1101-1108.

130. Troskie AM, de Beer A, Vosloo JA, Jacobs K, & Rautenbach M (2014) Inhibition of agronomically relevant fungal phytopathogens by tyrocidines, cyclic antimicrobial peptides isolated from Bacillus aneurinolyticus. *Microbiology* 160(9):2089-2101.

131. Choi H & Lee DG (2012) Antimicrobial peptide pleurocidin synergizes with antibiotics through hydroxyl radical formation and membrane damage, and exerts antibiofilm activity. *Biochim Biophys Act* 1820(12):1831-1838.

132. Olofsson G & Sparr E (2013) Ionization constants pKa of cardiolipin. *PLoS One* 8(9):e73040.

133. Seelig J (1997) Titration calorimetry of lipid-peptide interactions. *Biochim Biophys Act* 1331(1):103-116.

134. Keller S, Heerklotz H, & Blume A (2006) Monitoring lipid membrane translocation of sodium dodecyl sulfate by isothermal titration calorimetry. *J Am Chem Soc* 128(4):1279-1286.

135. Kemmer G & Keller S (2010) Nonlinear least-squares data fitting in Excel spreadsheets. *Nat Protoc* 5(2):267-281.

136. Harris FM, Best KB, & Bell JD (2002) Use of laurdan fluorescence intensity and polarization to distinguish between changes in membrane fluidity and phospholipid order. *Biochim Biophys Act* 1565(1):123-128.

137. Sanchez SA, Tricerri MA, & Gratton E (2012) Laurdan generalized polarization fluctuations measures membrane packing micro-heterogeneity in vivo. *Proc Natl Acad Sci U S A* 109(19):7314-7319.

138. Kaneda T (1991) Iso- and anteiso-fatty acids in bacteria: biosynthesis, function, and taxonomic significance. *Microbiol Rev* 55(2):288-302.

139. Bandow JE, Brotz H, Leichert LI, Labischinski H, & Hecker M (2003) Proteomic approach to understanding antibiotic action. *Antimicrob Agents Chemother* 47(3):948-955.

140. Wenzel M, Patra M, Albrecht D, Chen DY, Nicolaou KC, Metzler-Nolte N, & Bandow JE (2011) Proteomic signature of fatty acid biosynthesis inhibition available for in vivo mechanism-of-action studies. *Antimicrob Agents Chemother* 55(6):2590-2596.

141. Bandow JE (2005) Proteomic approaches to antibiotic drug discovery. in *Current Protocols in Microbiology*, p Unit 1F 2.

142. Wells S & Johnson I (1994) Fluorescent labels for confocal microscopy. *Three-Dimensional Confocal Microscopy: Volume Investigation of Biological Specimens*, (Academic Press, London), pp 101-129.

143. Madani F, Abdo R, Lindberg S, Hirose H, Futaki S, Langel U, & Graslund A (2013) Modeling the endosomal escape of cell-penetrating peptides using a transmembrane pH gradient. *Biochim Biophys Act* 1828(4):1198-1204.

144. Scheller A, Oehlke J, Wiesner B, Dathe M, Krause E, Beyermann M, Melzig M, & Bienert M (1999) Structural requirements for cellular uptake of alpha-helical amphipathic peptides. *J Pept Sci* 5(4):185-194.

145. Oehlke J, Savoly B, & Blasig IE (1994) Utilization of endothelial cell monolayers of low tightness for estimation of transcellular transport characteristics of hydrophilic compounds. *Eur J Pharm Sci* 2(5–6):365-372.

146. Bagheri M, Keller S, & Dathe M (2011) Interaction of W-substituted analogs of cyclo-RRRWFW with bacterial lipopolysaccharides: the role of the aromatic cluster in antimicrobial activity. *Antimicrob Agents Chemother* 55(2):788-797.

147. Dathe M & Wieprecht T (1999) Structural features of helical antimicrobial peptides: their potential to modulate activity on model membranes and biological cells. *Biochim Biophys Act* 1462(1-2):71-87.

148. Radchenko DS, Michurin OM, Grygorenko OO, Scheinpflug K, Dathe M, & Komarov IV (2013) Confining the χ space of basic natural amino acids: cyclobutane-derived χ1,χ2-constrained analogues of arginine, lysine and ornithine. *Tetrahedron* 69(2):505-511.

149. Wimley WC & White SH (1996) Experimentally determined hydrophobicity scale for proteins at membrane interfaces. *Nat Struct Biol* 3(10):842-848.

150. Appelt C, Wessolowski A, Soderhall JA, Dathe M, & Schmieder P (2005) Structure of the antimicrobial, cationic hexapeptide cyclo(RRWWRF) and its analogues in solution and bound to detergent micelles. *Chembiochem* 6(9):1654-1662.

151. Wagner BD (2009) The use of coumarins as environmentally-sensitive fluorescent probes of heterogeneous inclusion systems. *Molecules* 14(1):210-237.

152. Fery-Forgues S, Fayet J-P, & Lopez A (1993) Drastic changes in the fluorescence properties of NBD probes with the polarity of the medium: involvement of a TICT state? *J Photoch Photobio A* 70(3):229-243.

153. Schindler PR & Teuber M (1975) Action of polymyxin B on bacterial membranes: morphological changes in the cytoplasm and in the outer membrane of Salmonella typhimurium and Escherichia coli B. *Antimicrob Agents Chemother* 8(1):95-104.

154. Bush K (2012) Antimicrobial agents targeting bacterial cell walls and cell membranes. *Rev Sci Tech* 31(1):43-56.

155. Kobayashi S, Chikushi A, Tougu S, Imura Y, Nishida M, Yano Y, & Matsuzaki K (2004) Membrane translocation mechanism of the antimicrobial peptide buforin 2. *Biochemistry* 43(49):15610-15616.

156. Scheinpflug K, Krylova O, Nikolenko H, Thurm C, & Dathe M (2015) Evidence for a Novel Mechanism of Antimicrobial Action of a Cyclic R-,W-Rich Hexapeptide. *PLoS One* 10(4):e0125056.

157. Glukhov E, Stark M, Burrows LL, & Deber CM (2005) Basis for selectivity of cationic antimicrobial peptides for bacterial versus mammalian membranes. *J Biol Chem* 280(40):33960-33967.

158. Leupold E, Nikolenko H, Beyermann M, & Dathe M (2008) Insight into the role of HSPG in the cellular uptake of apolipoprotein E-derived peptide micelles and liposomes. *Biochim Biophys Act* 1778(12):2781-2789.

159. Sydow K, Torchilin VP, & Dathe M (2014) Lipopeptide-modified PEG-PE-based pharmaceutical nanocarriers for enhanced uptake in blood–brain barrier cells and improved cytotoxicity against glioma cells. *Eur J Lipid Sci Tech* 116(9):1174-1183.

160. Herce HD, Garcia AE, & Cardoso MC (2014) Fundamental molecular mechanism for the cellular uptake of guanidinium-rich molecules. *J Am Chem Soc* 136(50):17459-17467.

161. Mishra A, Lai GH, Schmidt NW, Sun VZ, Rodriguez AR, Tong R, Tang L, Cheng J, Deming TJ, Kamei DT, & Wong GC (2011) Translocation of HIV TAT peptide and analogues induced by multiplexed membrane and cytoskeletal interactions. *Proc Natl Acad Sci U S A* 108(41):16883-16888.

162. Zhu WL & Shin SY (2009) Antimicrobial and cytolytic activities and plausible mode of bactericidal action of the cell penetrating peptide penetratin and its lys-linked two-stranded peptide. *Chem Biol Drug Des* 73(2):209-215.

163. Schmidt N, Mishra A, Lai GH, & Wong GC (2010) Arginine-rich cell-penetrating peptides. *FEBS Lett* 584(9):1806-1813.

164. Amand HL, Fant K, Norden B, & Esbjorner EK (2008) Stimulated endocytosis in penetratin uptake: effect of arginine and lysine. *Biochem Biophys Res Commun* 371(4):621-625.

165. Epand RM & Epand RF (2009) Lipid domains in bacterial membranes and the action of antimicrobial agents. *BBA-Biomembranes* 1788(1):289-294.

166. Mileykovskaya E & Dowhan W (2009) Cardiolipin membrane domains in prokaryotes and eukaryotes. *BBA-Biomembranes* 1788(10):2084-2091.

167. Wang J, Mura M, Zhou Y, Pinna M, Zvelindovsky AV, Dennison SR, & Phoenix DA (2014) The cooperative behaviour of antimicrobial peptides in model membranes. *Biochim Biophys Act* 1838(11):2870-2881.

168. Wang Q, Hong G, Johnson GR, Pachter R, & Cheung MS (2010) Biophysical properties of membrane-active peptides based on micelle modeling: a case study of cell-penetrating and antimicrobial peptides. *J Phys Chem B* 114(43):13726-13735.

169. Reynolds JA, Gilbert DB, & Tanford C (1974) Empirical correlation between hydrophobic free energy and aqueous cavity surface area. *Proc Natl Acad Sci U S A* 71(8):2925-2927.

170. Ozyamak E, Kollman JM, & Komeili A (2013) Bacterial actins and their diversity. *Biochemistry* 52(40):6928-6939.

171. Defeu Soufo HJ & Graumann PL (2006) Dynamic localization and interaction with other Bacillus subtilis actin-like proteins are important for the function of MreB. *Mol Microbiol* 62(5):1340-1356.

172. Leaver M & Errington J (2005) Roles for MreC and MreD proteins in helical growth of the cylindrical cell wall in Bacillus subtilis. *Mol Microbiol* 57(5):1196-1209.

173. Hashimoto M, Ooiwa S, & Sekiguchi J (2012) Synthetic lethality of the lytE cwlO genotype in Bacillus subtilis is caused by lack of D,L-endopeptidase activity at the lateral cell wall. *J Bacteriol* 194(4):796-803.

174. Kiriyama Y, Yazawa K, Tanaka T, Yoshikawa R, Yamane H, Hashimoto M, Sekiguchi J, & Yamamoto H (2014) Localization and expression of the Bacillus subtilis DL-endopeptidase LytF are influenced by mutations in LTA synthases and glycolipid anchor synthetic enzymes. *Microbiology* 160(Pt 12):2639-2649.

175. Yamamoto H, Kurosawa S, & Sekiguchi J (2003) Localization of the vegetative cell wall hydrolases LytC, LytE, and LytF on the Bacillus subtilis cell surface and stability of these enzymes to cell wall-bound or extracellular proteases. *J Bacteriol* 185(22):6666-6677.

176. Chai Y, Norman T, Kolter R, & Losick R (2010) An epigenetic switch governing daughter cell separation in Bacillus subtilis. *Gene Dev* 24(8):754-765.

177. Kawai Y, Asai K, & Errington J (2009) Partial functional redundancy of MreB isoforms, MreB, Mbl and MreBH, in cell morphogenesis of Bacillus subtilis. *Mol Microbiol* 73(4):719-731.

178. Mansilla MC, Aguilar PS, Albanesi D, Cybulski LE, Altabe S, & de Mendoza D (2003) Regulation of fatty acid desaturation in Bacillus subtilis. *Prostaglandins Leukot Essent Fatty Acids* 68(2):187-190.

179. Hachmann AB, Angert ER, & Helmann JD (2009) Genetic analysis of factors affecting susceptibility of Bacillus subtilis to daptomycin. *Antimicrob Agents Chemother* 53(4):1598-1609.

180. Dominguez-Escobar J, Wolf D, Fritz G, Hofler C, Wedlich-Soldner R, & Mascher T (2014) Subcellular localization, interactions and dynamics of the phage-shock protein-like Lia response in Bacillus subtilis. *Mol Microbiol* 92(4):716-732.

181. Michna RH, Commichau FM, Todter D, Zschiedrich CP, & Stulke J (2014) SubtiWiki-a database for the model organism Bacillus subtilis that links pathway, interaction and expression information. *Nucleic Acids Res* 42(Database issue):D692-698.

182. Franzel B, Frese C, Penkova M, Metzler-Nolte N, Bandow JE, & Wolters DA (2010) Corynebacterium glutamicum exhibits a membrane-related response to a small ferrocene-conjugated antimicrobial peptide. *J Biol Ionorg Chem* 15(8):1293-1303.

183. Bertsche U, Weidenmaier C, Kuehner D, Yang SJ, Baur S, Wanner S, Francois P, Schrenzel J, Yeaman MR, & Bayer AS (2011) Correlation of daptomycin resistance in a clinical Staphylococcus aureus strain with increased cell wall teichoic acid production and D-alanylation. *Antimicrob Agents Chemother* 55(8):3922-3928.

184. Cafiso V, Bertuccio T, Spina D, Purrello S, Campanile F, Di Pietro C, Purrello M, & Stefani S (2012) Modulating activity of vancomycin and daptomycin on the expression of autolysis cell-wall turnover and membrane charge genes in hVISA and VISA strains. *PLoS One* 7(1):e29573.

185. Rose WE, Fallon M, Moran JJ, & Vanderloo JP (2012) Vancomycin tolerance in methicillin-resistant Staphylococcus aureus: influence of vancomycin, daptomycin, and

telavancin on differential resistance gene expression. *Antimicrob Agents Chemother* 56(8):4422-4427.

186. Katsu T, Kuroko M, Morikawa T, Sanchika K, Fujita Y, Yamamura H, & Uda M (1989) Mechanism of membrane damage induced by the amphipathic peptides gramicidin S and melittin. *Biochim Biophys Act* 983(2):135-141.

187. Berezin SK (2015) Valinomycin as a Classical Anionophore: Mechanism and Ion Selectivity. *J Membrane Biol* 248(4):713-726.

188. Christ K, Al-Kaddah S, Wiedemann I, Rattay B, Sahl HG, & Bendas G (2008) Membrane lipids determine the antibiotic activity of the lantibiotic gallidermin. *J Membr Biol* 226(1-3):9-16.

189. Konopasek I, Strzalka K, & Svobodova J (2000) Cold shock in Bacillus subtilis: different effects of benzyl alcohol and ethanol on the membrane organisation and cell adaptation. *Biochim Biophys Act* 1464(1):18-26.

190. Mercier R, Dominguez-Cuevas P, & Errington J (2012) Crucial role for membrane fluidity in proliferation of primitive cells. *Cell Rep* 1(5):417-423.

191. Strahl H & Hamoen LW (2010) Membrane potential is important for bacterial cell division. *Proc Natl Acad Sci U S A* 107(27):12281-12286.

192. Eymann C, Dreisbach A, Albrecht D, Bernhardt J, Becher D, Gentner S, Tam le T, Buttner K, Buurman G, Scharf C, Venz S, Volker U, & Hecker M (2004) A comprehensive proteome map of growing Bacillus subtilis cells. *Proteomics* 4(10):2849-2876.

193. Duman R, Ishikawa S, Celik I, Strahl H, Ogasawara N, Troc P, Lowe J, & Hamoen LW (2013) Structural and genetic analyses reveal the protein SepF as a new membrane anchor for the Z ring. *Proc Natl Acad Sci U S A* 110(48):E4601-4610.

194. Gamba P, Veening JW, Saunders NJ, Hamoen LW, & Daniel RA (2009) Two-step assembly dynamics of the Bacillus subtilis divisome. *J Bacteriol* 191(13):4186-4194.

195. Micka B & Marahiel MA (1992) The DNA-binding protein HBsu is essential for normal growth and development in Bacillus subtilis. *Biochimie* 74(7-8):641-650.

196. Scholefield G, Whiting R, Errington J, & Murray H (2011) Spo0J regulates the oligomeric state of Soj to trigger its switch from an activator to an inhibitor of DNA replication initiation. *Mol Microbiol* 79(4):1089-1100.

197. Lenhart JS, Sharma A, Hingorani MM, & Simmons LA (2013) DnaN clamp zones provide a platform for spatiotemporal coupling of mismatch detection to DNA replication. *Mol Microbiol* 87(3):553-568.

198. Bramkamp M & van Baarle S (2009) Division site selection in rod-shaped bacteria. *Curr Opin Microbiol* 12(6):683-688.

199. Rowlett VW & Margolin W (2013) The bacterial Min system. *Curr Biol* 23(13):R553-556.

200. Amand HL, Rydberg HA, Fornander LH, Lincoln P, Norden B, & Esbjorner EK (2012) Cell surface binding and uptake of arginine- and lysine-rich penetratin peptides in absence and presence of proteoglycans. *Biochim Biophys Act* 1818(11):2669-2678.

201. Lattig-Tunnemann G, Prinz M, Hoffmann D, Behlke J, Palm-Apergi C, Morano I, Herce HD, & Cardoso MC (2011) Backbone rigidity and static presentation of guanidinium groups increases cellular uptake of arginine-rich cell-penetrating peptides. *Nat Commun* 2:453.

202. Huang HW (2006) Molecular mechanism of antimicrobial peptides: The origin of cooperativity. *BBA-Biomembranes* 1758(9):1292-1302.

203. Pucadyil TJ, Mukherjee S, & Chattopadhyay A (2007) Organization and dynamics of NBD-labeled lipids in membranes analyzed by fluorescence recovery after photobleaching. *J Phys Chem B* 111(8):1975-1983.

204. Angeletti C & Nichols JW (1998) Dithionite quenching rate measurement of the inside-outside membrane bilayer distribution of 7-nitrobenz-2-oxa-1,3-diazol-4-yl-labeled phospholipids. *Biochemistry* 37(43):15114-15119.

205. Lin S & Struve WS (1991) Time-resolved fluorescence of nitrobenzoxadiazole-aminohexanoic acid: effect of intermolecular hydrogen-bonding on non-radiative decay. *Photochem Photobiol* 54(3):361-365.

206. Hristova K & Wimley WC (2011) A look at arginine in membranes. *J Membrane Biol* 239(1-2):49-56.

207. Fleming E, Maharaj NP, Chen JL, Nelson RB, & Elmore DE (2008) Effect of lipid composition on buforin II structure and membrane entry. *Proteins* 73(2):480-491.

208. Zhang T, Muraih JK, Tishbi N, Herskowitz J, Victor RL, Silverman J, Uwumarenogie S, Taylor SD, Palmer M, & Mintzer E (2014) Cardiolipin prevents membrane translocation and permeabilization by daptomycin. *J Biol Chem* 289(17):11584-11591.

209. Vogel HJ, Schibli DJ, Jing W, Lohmeier-Vogel EM, Epand RF, & Epand RM (2002) Towards a structure-function analysis of bovine lactoferricin and related tryptophan- and arginine-containing peptides. *Biochem Cell Biol* 80(1):49-63.

210. Henriques ST, Melo MN, & Castanho MA (2006) Cell-penetrating peptides and antimicrobial peptides: how different are they? *Biochem J* 399(1):1-7.

211. Boisguerin P, Deshayes S, Gait MJ, O'Donovan L, Godfrey C, Betts CA, Wood MJ, Lebleu B, Farkhani SM, Valizadeh A, Karami H, Mohammadi S, Sohrabi N, & Badrzadeh F (2015) Delivery of therapeutic oligonucleotides with cell penetrating peptides. *Adv Drug Deliv Rev* 57:78-94.

212. Farkhani SM, Valizadeh A, Karami H, Mohammadi S, Sohrabi N, & Badrzadeh F (2014) Cell penetrating peptides: efficient vectors for delivery of nanoparticles, nanocarriers, therapeutic and diagnostic molecules. *Peptides* 57:78-94.

213. Cascales L, Henriques ST, Kerr MC, Huang YH, Sweet MJ, Daly NL, & Craik DJ (2011) Identification and characterization of a new family of cell-penetrating peptides: cyclic cell-penetrating peptides. *J Biol Chem* 286(42):36932-36943.

214. Lebreton A, Stavru F, & Cossart P (2015) Organelle targeting during bacterial infection: insights from Listeria. *Trends Cell Biol* 25(6):330-338.

215. Renner LD & Weibel DB (2011) Cardiolipin microdomains localize to negatively curved regions of Escherichia coli membranes. *Proc Natl Acad Sci U S A* 108(15):6264-6269.

216. Dowhan W (1997) Molecular basis for membrane phospholipid diversity: why are there so many lipids? *Annu Rev Biochem* 66:199-232.

217. Bishop RE (2014) Emerging roles for anionic non-bilayer phospholipids in fortifying the outer membrane permeability barrier. *J Bacteriol* 196(18):3209-3213.

218. Renner LD & Weibel DB (2012) MinD and MinE Interact with Anionic Phospholipids and Regulate Division Plane Formation in Escherichia coli. *J Biol Chem* 287(46):38835-38844.

219. Lingwood D & Simons K (2010) Lipid rafts as a membrane-organizing principle. *Science* 327(5961):46-50.

220. Mileykovskaya E, Ryan AC, Mo X, Lin C-C, Khalaf KI, Dowhan W, & Garrett TA (2009) Phosphatidic Acid and N-Acylphosphatidylethanolamine Form Membrane Domains in Escherichia coli Mutant Lacking Cardiolipin and Phosphatidylglycerol. *J Biol Chem* 284(5):2990-3000.

221. Wenzel M & Bandow JE (2011) Proteomic signatures in antibiotic research. *Proteomics* 11(15):3256-3268.

222. de Mendoza D (2014) Temperature sensing by membranes. *Annu Rev Microbiol* 68:101-116.

223. Zhang L, Dhillon P, Yan H, Farmer S, & Hancock RE (2000) Interactions of bacterial cationic peptide antibiotics with outer and cytoplasmic membranes of Pseudomonas aeruginosa. *Antimicrob Agents Chemother* 44(12):3317-3321.

224. Mogi T, Ui H, Shiomi K, Omura S, & Kita K (2008) Gramicidin S identified as a potent inhibitor for cytochrome bd-type quinol oxidase. *FEBS Lett* 582(15):2299-2302.

225. Wenzel M, Chiriac AI, Otto A, Zweytick D, May C, Schumacher C, Gust R, Albada HB, Penkova M, Kramer U, Erdmann R, Metzler-Nolte N, Straus SK, Bremer E, Becher D, Brotz-Oesterhelt H, Sahl HG, & Bandow JE (2014) Small cationic antimicrobial peptides delocalize peripheral membrane proteins. *Proc Natl Acad Sci U S A* 111(14):E1409-1418.

226. Mykytczuk NC, Trevors JT, Leduc LG, & Ferroni GD (2007) Fluorescence polarization in studies of bacterial cytoplasmic membrane fluidity under environmental stress. *Prog Biophys Mol Bio* 95(1-3):60-82.

227. Mansilla MC, Cybulski LE, Albanesi D, & de Mendoza D (2004) Control of membrane lipid fluidity by molecular thermosensors. *J Bacteriol* 186(20):6681-6688.

228. Kaiser HJ, Surma MA, Mayer F, Levental I, Grzybek M, Klemm RW, Da Cruz S, Meisinger C, Muller V, Simons K, & Lingwood D (2011) Molecular convergence of bacterial and eukaryotic surface order. *J Biol Chem* 286(47):40631-40637.

229. Mazor S, Regev T, Mileykovskaya E, Margolin W, Dowhan W, & Fishov I (2008) Mutual effects of MinD-membrane interaction: I. Changes in the membrane properties induced by MinD binding. *Biochim Biophys Act* 1778(11):2496-2504.

230. Bach JN & Bramkamp M (2013) Flotillins functionally organize the bacterial membrane. *Mol Microbiol* 88(6):1205-1217.

231. Lenarcic R, Halbedel S, Visser L, Shaw M, Wu LJ, Errington J, Marenduzzo D, & Hamoen LW (2009) Localisation of DivIVA by targeting to negatively curved membranes. *EMBO J* 28(15):2272-2282.

232. Renner LD, Eswaramoorthy P, Ramamurthi KS, & Weibel DB (2013) Studying biomolecule localization by engineering bacterial cell wall curvature. *PLoS One* 8(12):e84143.

233. Bach JN, Albrecht N, & Bramkamp M (2014) Imaging DivIVA dynamics using photo-convertible and activatable fluorophores in Bacillus subtilis. *Front Microbiol* 5:59.

234. Halbedel S, Kawai M, Breitling R, & Hamoen LW (2014) SecA is required for membrane targeting of the cell division protein DivIVA in vivo. *Front Microbiol* 5:58.

235. Gold VA, Robson A, Bao H, Romantsov T, Duong F, & Collinson I (2010) The action of cardiolipin on the bacterial translocon. *Proc Natl Acad Sci U S A* 107(22):10044-10049.

236. Lopez D & Kolter R (2010) Functional microdomains in bacterial membranes. *Gene Dev* 24(17):1893-1902.

10 Appendix

10.1 List of figures

10.2 List of tables

10.3 Abbreviations

AMP	Antimicrobial peptide
ATP	Adenosine triphosphate
B. cereus	*Bacillus cereus*
B. subtilis	*Bacillus subtilis*
BA	Benzyl alcohol
BCFA	Branched chain fatty acid
BCKAD	Branched-chain keto acid dehydrogenase
BHI	Brain heart infusion
BSA	Bovine serum albumin
CD	Circular dichroism
CFU/ml	Colony forming units per ml
CL	Cardiolipin
CLSM	Confocal laser scanning microscopy
ddH2O	Double-distilled water
$DiSC_3(5)$	3,3'-dipropylthiadicarbocyanine iodide
DLS	Differential light scattering
DMSO	Dimethyl sulfoxide
E. coli	*Escherichia coli*
EDTA	Ethylenediaminetetraacetic acid
Ex/em	Excitation/emission wavelength
FACS	Fluorescence-activated cell sorting (flow cytometry)
FCS	Foetal calf serum
FDA	U.S. Food and Drug Administration
Fluos	Carboxyfluorescein
GFP	Green fluorescent protein

HPLC	High-performance liquid chromatography
HSPG	Heparan sulfate proteoglycan
IB	Isobutyrate
IV	Isovalerate
IPTG	Isopropyl-β-D-thiogalactopyranoside
LB	Lysogeny broth
LPG	Lysylphosphatidylglycerol
LPS	Lipopolysaccharides
LTA	Lipoteichoic acids
LUVs	Large unilamellar vesicles
MB	2-methylbutyrate
MIC	Minimal inhibitory concentration
MRSA	Methicillin-resistant *Staphylococcus aureus*
MTT	3-(4,5-Dimethylthiazol-2-yl)-2,5-diphenyl-tetrazoliumbromid
NADH	Nicotinamide adenine dinucleotide (reduced)
NAO	Nonyl acridine orange
NBD	Nitrobenzoxadiazole
P. aeruginosa	*Pseudomonas aeruginosa*
PDB	Protein data bank
PI	Propidium iodide
POPC	Phosphatidylcholine
POPE	Phosphatidylethanolamine
POPG	Phosphatidylglycerol
PP_i	Pyrophosphate
PTFE	Polytetrafluoroethylene
SDS	Sodium dodecyl sulfate
SUVs	Small unilamellar vesicles

TFA	Trifluoroacetic acid
TLR	Toll-like receptor
t_R	Retention time
Tris	Tris(hydroxymethyl)aminomethane
UPLC-MS	Ultra-performance liquid chromatography tandem mass-spectrometry
wt	Wild type
Y. kristensenii	*Yersinia kristensenii*
YFP	Yellow fluorescent protein
λ	Wavelength (*lambda*)

10.4 Publications

Scheinpflug K, Krylova O, Nikolenko H, Thurm C, & Dathe M (2015) Evidence for a Novel Mechanism of Antimicrobial Action of a Cyclic R-,W-Rich Hexapeptide. *PLoS One* 10(4):e0125056.

Scheinpflug K, Nikolenko H, Komarov I, Rautenbach M, & Dathe M (2013) What Goes around Comes around-A Comparative Study of the Influence of Chemical Modifications on the Antimicrobial Properties of Small Cyclic Peptides. *Pharmaceuticals* 6(9):1130-1144.

Radchenko DS, Michurin OM, Grygorenko OO, Scheinpflug K, Dathe M, & Komarov IV (2013) Confining the χ space of basic natural amino acids: cyclobutane-derived χ1,χ2-constrained analogues of arginine, lysine and ornithine. *Tetrahedron* 69(2):505-511.

10.5 Conference contributions and project presentations

May 2015	Gordon Research Conference/Seminar on Antimicrobial Peptides "Basic and Translational Aspects", Il Ciocco (Italy) *Oral Presentation & Poster* ("All Mixed up - A Novel Mechanism of Action based on Phase Separation and Membrane Fluidity") **Elected vice chair of GRS in 2017, GRS chair 2019**
December 2014	Centre for Bacterial Cell Biology (CBCB), Newcastle University, Newcastle (UK), Institute Superlab Seminar Series *Oral Presentation* ("Comedy of Errors… or how to find the mechanism of action of a small antimicrobial peptide")
October 2014	ICAR 2014 - "International Conference on Antimicrobial Research", Madrid (Spain) *Oral Presentation* ("The X marks the spot: Investigations on the site of action of a small cyclic antimicrobial peptide")
July 2014	AG Rolff - Evolutionsbiologie, FU Berlin, invited speaker *Oral Presentation* ("The X-marks the spot: Investigations on the site of action of a small cyclic antimicrobial peptide")
June 2014	AMP 2014 - "4th International Symposium on Antimicrobial Peptides", Lorient (France) *Oral Presentation* ("The X-marks the spot: Investigations on the site of action of a small cyclic antimicrobial peptide") *Poster* ("The best of both worlds: investigating cyclic antimicrobial peptides with cell penetrating properties")
November 2013	"Biomolecules and Synthetic Nanostructures in Cells and Model Systems: Experimental and Theoretical Studies", Kiev (Ukraine) *Oral Presentation* ("What Goes Around Comes Around - How Chemical Modifications Influence the Antimicrobial Activity of Small Cyclic Peptides")

October 2013	EMBO/EMBL Symposium “New Approaches and Concepts in Microbiology”, Heidelberg (Germany) *Poster* (“A Vicious Cycle …or How to Elucidate the Mode of Action of a Small Cyclic Peptide”)
July 2013	FEMS 2013 - 5th International Congress of European Microbiologists, Leipzig (Germany) *Poster* (“A Vicious Cycle …or How to Elucidate the Mode of Action of a Small Cyclic Peptide”)
February 2013	Gordon Research Conference/Seminar on Antimicrobial Peptides “Discovery, Function and Application”, Ventura, CA (USA) *Oral Presentation & Poster* (“A Vicious Cycle …or How to Elucidate the Mode of Action of a Small Cyclic Peptide”)
August 2012	IMAP - International Meeting on Antimicrobial Peptides “Antimicrobial peptides as lead compounds to combat multi-drug resistant pathogens”, Leipzig (Germany) *Poster* (“Lord of the Peptide Rings - A Small Cyclic Peptide and its Mode of Antimicrobial Action”)
June 2012	AMP 2012 - 3rd International Symposium on Antimicrobial Peptides - "Today knowledge and future applications", Lille (France) *Poster & Oral Presentation* (“Lord of the Peptide Rings - A Small Cyclic Peptide and its Mode of Antimicrobial Action”)
May 2012	Wissenschaftlicher Austausch der Arbeitsgruppen, FMP, Berlin (Germany) *Oral Presentation* (“Lord of the Peptide Rings - A Small Cyclic Peptide and its Mode of Antimicrobial Action”)

February 2012	BAMP 2012 - International Scientific Conference on Bacteriocins and Antimicrobial Peptides, Košice (Slovakia) *Oral Presentation* ("Lord of the Peptide Rings - A Small Cyclic Peptide and its Mode of Antimicrobial Action")
September 2011	13th MDC/FMP PhD Student Retreat, Liebenwalde (Germany) *Poster* ("Small Cyclic Antimicrobial Peptides - Elucidation of their Antibiotic Mode of Action")
May 2011	Campus Buch Symposium 2011, MDC, Berlin (Germany) *Poster* ("Small Cyclic Antimicrobial Peptides - Elucidation of their Antibiotic Mode of Action")
May 2011	Peptide Vectors and Delivery of Therapeutics, Tallinn (Estonia) *Poster* ("Small Cyclic Antimicrobial Peptides - Elucidation of their mode of action")

10.6 Awards

May 2015	*Speed Lecture Award* XIII. BIONNALE 2015, 3rd place, Berlin (Germany) "How to combat intracellular bacterial infections"
June 2012	*Poster Award* AMP 2012 - 3rd International Symposium on Antimicrobial Peptides - Lille (France) "Lord of the Peptide Rings - A Small Cyclic Peptide and its Mode of Antimicrobial Action"